Late and Early Transition Metal-Catalyzed Homo and Copolymerizations Studies of Olefins and Polar Monomers

By

Goran Stojcevic

A thesis submitted to the Department of Chemistry

in conformity with the requirements for

the degree of Doctor of Philosophy

Queen's University

Kingston, Ontario, Canada

February, 2008

ABSTRACT

The aims of this work were two-fold.

The first part of this thesis involves the synthesis of the Brookhart's diimine catalyst $[Pd(N\text{-}N)Me(Et_2O)]^+$ (**1**) (N-N = (2,6-(i-Pr)$_2$C$_6$H$_3$)-N=CH$_2$CH$_2$=N-(2,6-(i-Pr)$_2$C$_6$H$_3$)) and an investigation of its insertion behaviour with the polar monomer acrylonitrile (AN), as well as its copolymerization behaviour with ethylene. Acrylonitrile displaces the ethyl ether ligand of Brookhart's cationic complex $[Pd(N\text{-}N)Me(Et_2O)]^+$ (**1**) to form the N-bonded species $[Pd(N\text{-}N)Me(AN)]^+$ (**2**) which exists as two equilibrating rotamers (**2a** and **2b**). On heating, $[Pd(N\text{-}N)Me(AN)]^+$ which appears to undergo 2,1-insertion, presumably via an unobserved η^2 isomer, to give the new complex, $[Pd(N\text{-}N)(CH(CN)CH_2CH_3)(AN)]^+$ (**3**) which apparently undergoes subsequent β-hydrogen elimination to give a hydride which then reacts further with AN to give a cyanoethyl complex (**5**). Although $[Pd(N\text{-}N)Me(AN)]^+$ does behave as a typical Brookhart ethylene polymerization catalyst, it does not catalyze AN polymerization and added AN suppresses ethylene polymerization. $[Pd(N\text{-}N)Me(AN)]^+$ does not copolymerize ethylene and acrylonitrile.

The second part of this thesis involves utilizing the early metal catalyst *rac*-$Et(Ind)_2ZrCl_2$ (Ind = C_9H_7) /methylaluminoxane (MAO) to copolymerize propylene or ethylene and the compounds $CH_2=CH(CH_2)_7CH_2OR$ {R = Me, (**A**); $PhCH_2$, (**B**); Ph_3C, (**C**); Me_3Si, (**D**); Ph_3Si, (**E**)}, all ethers of 9-decen-1-ol. The results showed new copolymer materials of up to 2.0 mol % of incorporated polar monomer into polypropylene and 1.2 mol % for polyethylene. All materials were characterized by ^1H and ^{13}C NMR spectroscopy, differential scanning calorimetry and infrared spectroscopy.

It was found that the increasing bulkiness of protecting groups did not increase the amount of polar monomer within the copolymers obtained. As a control, propylene-1-hexene copolymerization results were found to be comparable to those results of the polar monomer copolymerization results (up to 2.9 mol % of 1-hexene incorporated).

Furthermore, ^{1}H NMR monitoring reactions of the homopolymerization of these vinyl and silyl ethers (**A - E)** were investigated with the zwitterionic compound **G** $[Cp_2ZrMe][MeB(C_6F_5)_3]$ (Cp = C_5H_5). It was found that the protecting groups were effective in protecting the functional group from poisoning the catalyst.

Finally, the "aging" of MAO by heating, removing trimethylaluminum (TMA) or adding water content all proved to contribute adversely in copolymerization results, whereas adding oxygen content proved to have little effect.

ACKNOWLEDGEMEMTS

First I would like to thank my mentor and friend, Professor Michael C. Baird, for the opportunity to work in his laboratory for my Ph. D. Your wisdom and guidance are invaluable and your “down to earth nature” is something I will never forget.

I would also like to thank all the faculty and staff members in the Department of Chemistry for all their help and making each work day an enjoyable one. Special recognition goes to Dr. Francoise Sauriol for all her help with NMR and Dr. Bernd Keller for his assistance with mass spectrometry.

I would like to thank all my friends and colleagues for the laughter and “crazy times” during my stay in Kingston. You all know who you are and I wish all the best for each of you in the future. To my beautiful girl Emily, thanks for movies, dinners, walks and being there when I needed you the most. You are truly a special person to me.

Last, but definitely not least, I would like to thank my mom, dad, sister and brother in- law. I am a lucky person to have such a great family. You all have supported me, both financially and mentally, throughout the many obstacles in my life to date. I am truly indebted to you all.

STATEMENT OF ORIGINALITY

The research discussed in this thesis was carried out by the author in the Department of Chemistry at Queen's University under the supervision of Dr. Michael C. Baird.

The work in Part 1 of this thesis reports the synthesis, characterization and homopolymerization behaviour of Brookhart's late metal catalyst $[Pd(N\text{-}N)Me(Et_2O)]^+$ (N-N = (2,6-(i-Pr)$_2$C$_6$H$_3$)-N=CH$_2$CH$_2$=N-(2,6-(i-Pr)$_2$C$_6$H$_3$)) with acrylonitrile and its copolymerization behaviour with ethylene. Dr. Ernest M. Prokopchuk was a collaborator for this work, performing some preliminary experiments.

The work in Part 2 of this thesis reports the synthesis and characterization of long chain polar monomers and their interaction with early metal metallocene coordination catalysts. Furthermore, their copolymerization behaviour with olefins, such as ethylene and propylene, was investigated to generate new polymeric materials with potential enhanced properties.

TABLE OF CONTENTS

Page

LIST OF TABLES

LIST OF FIGURES

LIST OF SCHEMES

LIST OF SYMBOLS AND ABBREVIATIONS

Ar_f	3,5-bis(trifluoromethyl)phenyl
AN	acrylonitrile
br	broad
^{n}Bu	n-butyl
^{t}Bu	*tert*-butyl
Cp	cyclopentadienyl (η^5-$C_5H_5^-$)
Cp^*	pentamethylcyclopentadienyl anion (η^5-$C_5Me_5^-$)
Cp'	substituted cyclopentadienyl
d	doublet
Da	Daltons
ES	electrospray
ESMS	electrospray mass spectrometry
Et	ethyl
GPC	gel permeation chromatography
η	hapticity
HDPE	high density polyethylene
h	hour
IR	infrared spectroscopy
Ind	indenyl group
^{i}Pr	isopropyl group
J	coupling constant
kg	kilogram

L	litre
LDPE	low density polyethylene
LLDPE	linear low density polyethylene
mol	moles
m	multiplet (NMR), medium (ESMS)
m/z	mass over charge
MAO	methylaluminoxane
Me	methyl
mg	milligram
Mhz	megahertz
mL	milliliter
mmol	millimole
MS	mass spectrometry
M_n	number average molecular weight
M_w	weight average molecular weight
MW	molecular weight
MWD	molecular weight distribution
m	meta
NMR	nuclear magnetic resonance
ODCB	ortho-dichlorobenzene
o	ortho
p	para
PE	polyethylene

PP	polypropylene
% conv.	percent conversion
PDI	polydispersity index
Ph	phenyl
ppm	parts per million
q	quartet
R	alkyl group
t	triplet
rac	racemic
r.t	room temperature
s	strong (ESMS)
T_g	glass transition temperature
TCE	1,1,2,2-tetrachloroethane
TEA	triethylaluminum
TMA	trimethylaluminum
Trityl	triphenylmethyl
THF	tetrahydrofuran
w	weak (ESMS)
wt %	weight percent

CHAPTER 1

INTRODUCTION AND LITERATURE REVIEW

1.0 Introduction

From automobile tires to compact disks, polymers have become an invaluable component of modern daily life. Polymers therefore remain the subject of tremendous research efforts, particularly in the novel polymer design, as well as in the development of polymerization technologies with enhanced economic and environmental efficiencies. The significance of this research is evidenced by the large number of papers published on topics like polymer modification, new polymer synthesis, theoretical polymer studies and new catalyst development.[1]

Polyolefins have become a significant focal point of such research. Polyolefins form the basis of a multi-billion dollar industry annually, and materials such as polyethylene (PE) and polypropylene (PP) are extensively employed due to their excellent combination of mechanical and chemical properties as well as their processibility.[2] Traditionally, polyethylene is synthesized by free radical polymerization methods, but extreme reaction conditions (high temperatures and pressures) are generally required.[3] In addition, high molecular weight polypropylene cannot be made via free radical polymerization because of hydrogen transfer to monomer and formation of the highly favoured and resonance-stabilized allylic radicals.[4] This results in polypropylene oligomers. The free radical polymerization of olefins is therefore not without its disadvantages.

Such shortcomings naturally drove research efforts from traditional free radical methods towards novel and more efficient means of obtaining polyolefins. The discovery

in the late 1950's of Ziegler/Natta coordination polymerization has revolutionized ethylene and high molecular weight propylene polymerization and allowed access to new stereoregular polymeric materials, such as isotactic polypropylene. Coordination polymerization has therefore become an important foundation for the continued development of polyolefin technology, likely due to its advantageous stereochemical control, higher activities and high molecular weight polymers.[5] Specifically, single site metallocenes and late metal transition metal olefin polymerization represent a current hot topic.[6] The design of early and late metal catalysts, for example, by tuning ligand structures surrounding the metal environment, can provide access to a variety of polymers with unique properties (e.g. stereoregular polymers). Furthermore, such catalysts may also provide a method for the polymerization of monomers or combination of monomers that could not be traditionally homo- or copolymerized (e.g. ethylene-propylene copolymers). Hence, coordination polymerization can provide access to potentially useful and innovative polymeric materials.

Despite their current continued use, polyolefins do have some deficiencies that have limited their applicability. Their lack of polar functionality groups within the polymer framework leads to problems associated with adhesion, dyeability, paintability, printability and even compatibility with other functionalized polymers.[7] To date, there have been many studies examining the incorporation of functional polar groups (e.g. ester, halo, hydroxyl, etc.) within polyolefins and relevant studies will be discussed herein. Currently, the main challenge associated with the homo- and copolymerization of polar monomers with early metals (e.g. Ti, Zr) systems is catalyst poisoning. Here, the polar functionality binds to the oxophilic early metal center, thereby hindering monomer

insertion. On the other hand, late metal (e.g. Ni, Pd) catalysts are less oxophilic and therefore are able to tolerate polar groups and allow for subsequent olefin coordination.

With this objective in mind, Part One of this thesis is focused on utilizing Brookhart's palladium catalyst (**i**) and examining the homopolymerization of acrylonitrile and its copolymerization with ethylene. The second component of this thesis deals with using early metal (e.g. Ti, Zr) metallocene catalysts and for the homo- and copolymerization of protected, long chain polar monomers. The specific polar monomer chosen was 9-decenol (**ii**). The OH group was masked with carbon and silicon aryl and alkyl ethers (**iii**), and the protecting group abilities of these compounds were evaluated in attempted copolymerizations.

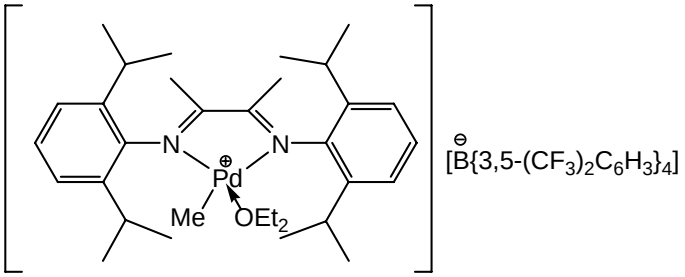

i

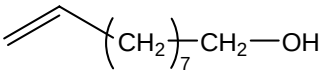

ii

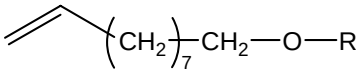

iii R = CR'_3, SiR'_3
R' = H or alkyl or aryl

Part 1

Late Metal Insertion Reaction Studies of Acrylonitrile and Copolymerization Behaviour of Acrylonitrile with Ethylene.

1.1 Literature Review

1.1.1 Introduction

Currently, polyolefin production is most successfully achieved via coordination Ziegler-Natta catalysis using early transition metals. In particular, the use of activated group 4 metallocene catalysts of the type $[Cp'_2MR]^+$ (Cp' = substituted cyclopentadienyl, M = Ti, Zr, Hf, R = alkyl) is well known for studies of the coordination polymerization of non-polar olefins (Figure 1).[8]

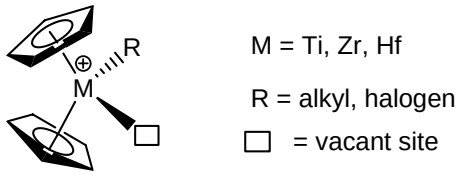

Figure 1. Typical activated cationic metallocene catalyst.

However, this class of compounds has not been useful in the homopolymerization of polar functional monomers such as acrylates, vinyl halides, vinyl amides or for the copolymerization of these monomers with ethylene or propylene. The difficulty with these group 4 metal catalysts is the preferred binding of the highly Lewis basic groups of the polar monomer with the very oxophilic and Lewis acidic metal center. This

'poisoning' of the catalyst prevents the olefin binding in an η^2 fashion to the metal center, thereby hindering migratory insertion and preventing coordination polymerization (Scheme 1).

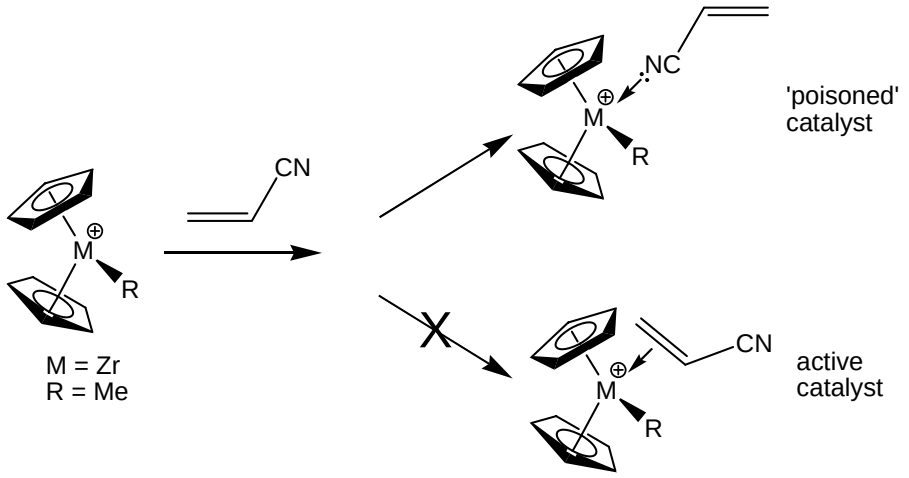

Scheme 1. Pathway for polar monomer addition to group 4 metallocene catalysts.

While polar monomers are readily polymerized by radical and ionic processes[9], intimate control of the overall polymer stereochemistry to generate highly iso- or syndiotactic polymeric materials has not yet been attained. In conjunction with this, feasible and mild routes to copolymers of linear olefins (such as ethylene and propylene) with polar monomers have not been found. The great potential for these types of copolymers to combine the unique properties of non-polar and polar groups into a single polymer chain explains the intense research undergoing today.[10]

To overcome the problem of catalyst poisoning, the first part of this thesis takes the approach of examining the use of the extensively studied late metal catalysts, in

particular, palladium complexes.[6] Late metal catalysts are relatively weakly electrophilic and are expected to tolerate polar monomers more effectively than early metal catalysts. Brookhart and Gibson have shown well known examples of these type of late metal catalysts, using aryl-substituted α-diimine Pd(II) and Ni(II) complexes (Figure 2).[6]

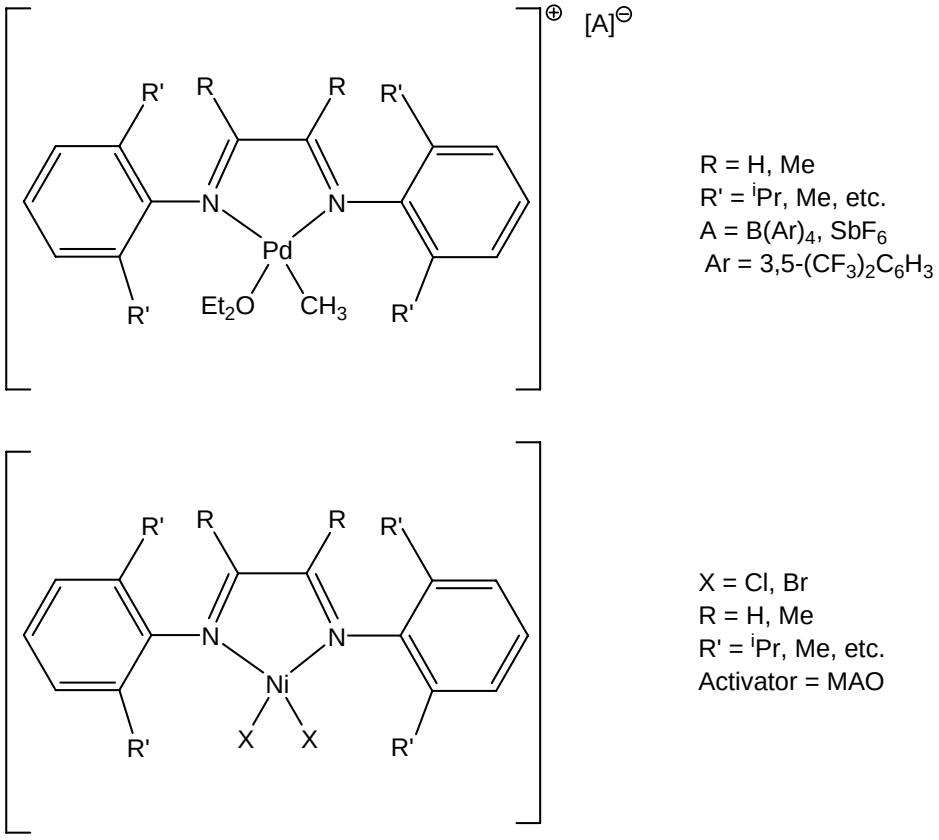

Figure 2. Pd(II) and Ni(II) late metal catalysts.

To probe the use of such late metal catalysts and gain a general understanding of the fundamental processes involved in non-polar and polar olefin homo- and copolymerization, the next section discusses the pertinent details of radical and coordination polymerization.

1.1.2 Polymerization Mechanisms in this Thesis

The syntheses of polyacrylonitrile (PAN), polyethylene (PE) and polypropylene (PP) are traditionally carried out by chain growth polymerization methods, such as free radical for PAN and coordination 'Ziegler-Natta' type polymerizations for PE and PP. The detailed mechanisms of each will be discussed below.

1.1.3 Chain Growth Polymerization

The utilization of chain growth (sometimes called chain reaction) polymerization is vast and very effective in the polymer industry. Initiation occurs by generating a reactive chain end (either a radical, an ion or a transition metal complex) on an alkene or substituted alkene. Propagation entails linking many monomer units to this reactive chain end and forming a polymer chain. This type of polymerization is further driven by the exothermicity (up to 20 kcal/mol), due to the conversion of the monomer π bond to a σ bond in the polymer main chain. A general pathway is shown in Scheme 2.

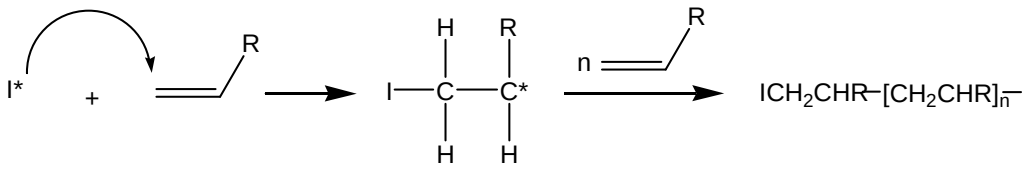

Scheme 2. General chain growth polymerization.

Termination reactions usually occur in chain reaction polymerizations. This can occur when monomer has depleted, thereby giving the chance for the active chain ends to react with another molecule or substrate and render the chain end unreactive (e.g.

coupling of radical). The type of reactive chain end describes the type of polymerization invoked. For example, if the reactive chain end is a radical, a radical polymerization is involved. This thesis addresses radical and coordination polymerizations.

1.1.4 Free Radical Polymerization Mechanism

Free radical polymerization is a widely employed mode of polymerization commercially, due to its great versatility and insensitivity to impurities as compared to other conventional methods. A wide range of vinyl monomers can be polymerized via free radical polymerization, including both polar and non-polar monomers such as acrylonitrile and styrene. However, free radical polymerization lacks control over the stereoregularity of the resulting polymers. In addition, a well-defined route to block copolymer synthesis is not possible by radical means. Also, broad molecular weight distributions are generally obtained. Despite these negatives, much research continues in the field of radical polymerization to improve upon its faults, particularly in the area of minimizing termination reactions, which can adversely affect the molecular weight of the final polymer.

1.1.4.1 Initiation

The initiation step involves generating primary radicals, usually from one of four major sources: (i) peroxides and hydroperoxides, (ii) azo compounds, (iii) redox initiators and (iv) photoinitiators. The first compounds (i) and (ii) are frequently used and are thermally unstable when heated, decomposing into their corresponding radical molecules. A good example is benzyl peroxide, which upon heating, forms two molecules of

benzoyloxy radicals, which can undergo further side reactions due to the cage effect created by the solvent molecules (Scheme 3a-c).[11b] Once the primary radicals are formed, they can attack the double bond of a monomer and generate an unpaired electron active center on the other end of the chain. (Scheme 3d).

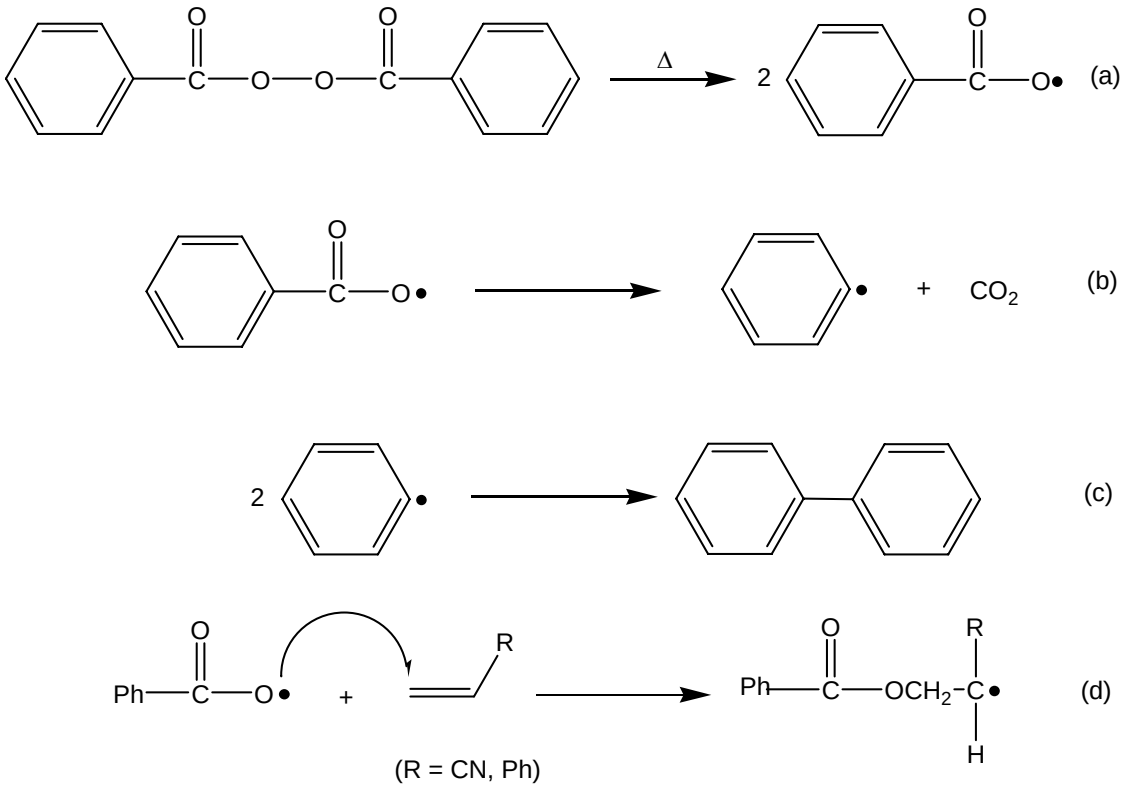

Scheme 3. Peroxide initiation reactions.

1.1.4.2 Propagation

The propagation step of free radical polymerization involves subsequent addition of the initiator radical to the double bonds of more monomer units to form a propagating polymer chain of n+1 units (Scheme 4). The mode of addition tends to be head to tail, as shown in Scheme 4. This is mainly due to both steric and electronic effects. Steric repulsion favours attack by the radical on the less hindered carbon of the double bond and resonance stabilization favours the more stable radical.[11] While head to tail addition is almost exclusively the favoured product, head to head addition can also occur and these are found in fluorine containing polymers (e.g. poly (vinyl fluoride)).[11]

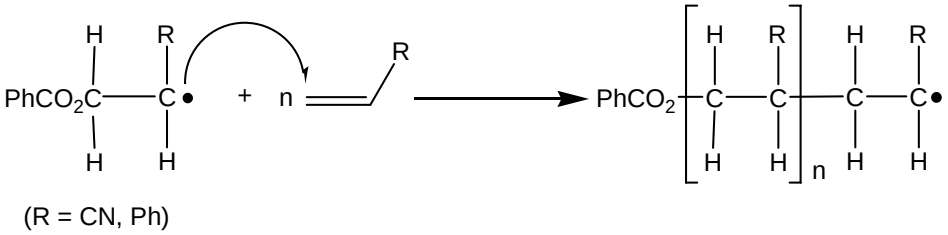

(R = CN, Ph)

Scheme 4. Radical propagation.

1.1.4.3 Chain transfer

Chain transfer is the process of transferring a radical propagating polymer chain end to that of another species. This transfer occurs frequently and tends to terminate one chain and initiate a new radical source. The effect of this transfer is a lowering of the molecular weight of the resulting polymer. An example of a chain transfer reaction can be seen upon the addition of a modifier, such a thiol (Scheme 5).[11] Thiols are added to help achieve desired molecular weight distribution for a particular application.

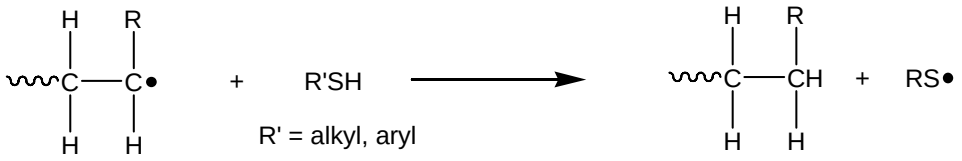

Scheme 5. Thiol assisted chain transfer reaction.

1.1.4.4 Termination

There are two main ways for a propagating radical to terminate during propagation: (1) combination (or radical coupling) and (2) disproportionation. Combination involves coupling of two propagating radical ends, resulting in two initiator fragments at the ends of the polymer chain and head to head linkage. In contrast, disproportionation involves atom transfer from one chain to another (typically hydrogen), resulting in a polymer chain with only one initiator fragment per polymer chain (Scheme 6).[11]

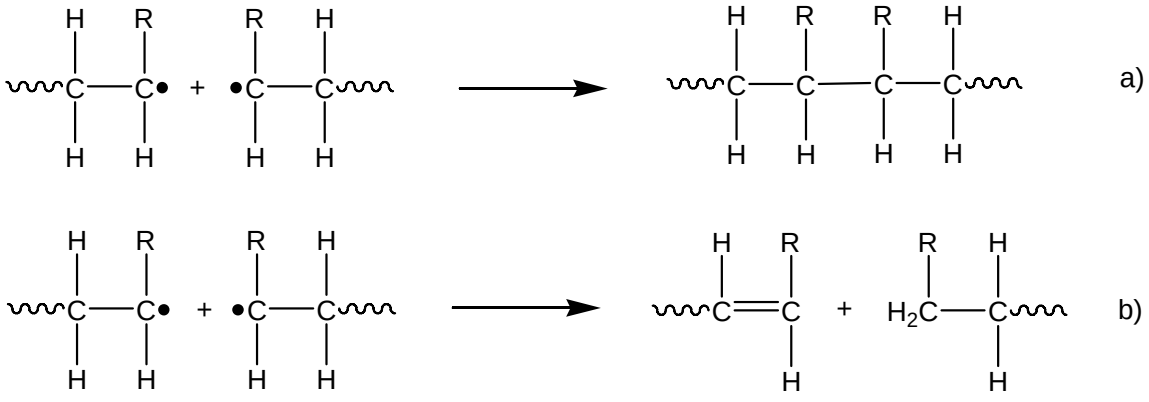

Scheme 6. a) Combination and b) disproportionation pathways in radical polymerization.

1.1.5 Coordination Polymerization

Coordination (or Ziegler-Natta) polymerization has progressed significantly since its inception and is currently an area of intense research. Coordination polymerization, discovered in the 1950's by Ziegler and Natta, provides access to unique polymeric materials, in particular stereoregular polyolefins, which are difficult to obtain via other conventional polymerization techniques (i.e. free radical). Karl Ziegler discovered that a combination of certain transition metals (e.g. $TiCl_3$) and organometallic compounds (e.g. $AlEt_3$) polymerizes ethylene to linear high density polyethylene (HDPE) at ambient temperatures and pressures.[12] This finding was important as it produced much tougher and higher melting polyethylene than the high pressure free radical initiator route, which typically produces low-density polyethylene (LDPE).[3] Soon after Ziegler's discovery, Giulio Natta found that Ziegler's type catalysts were able to polymerize α-olefins (e.g. propylene) into stereoregular polymers. This discovery led to the development of new materials and a new era of catalyst systems utilizing mainly non-polar monomers such as dienes and 1-alkenes .[13] These discoveries by Ziegler and Natta eventually lead to the Nobel Prize in chemistry in 1963.

Today, the most studied systems in coordination polymerization involves using the 16 electron precursor group 4 early metallocenes of the type Cp'_2MR_2 (Cp' = substituted cyclopentadienyl; M = Ti, Zr, Hf; R = alkyl or halogen). This catalyst geometry is shown in Figure 3.

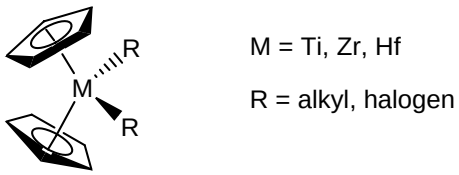

Figure 3. An example of a group 4 metallocene catalyst.

The activation of such precursors has been investigated extensively and will be discussed in the next section.

1.1.5.1 Activation of Coordination Polymerization Catalysts

Group 4 metallocene compounds are traditionally generated by the methylation of the metal center in a group 4 metallocene dihalogen complex with an alkyl aluminum cocatalyst (Scheme 7a); or for a group 4 metallocene dialkyl compound, an alkyl abstracting agent is used to abstract the methyl from the metal center to generate an ion pair with a weakly coordinating anion (Scheme 7b).

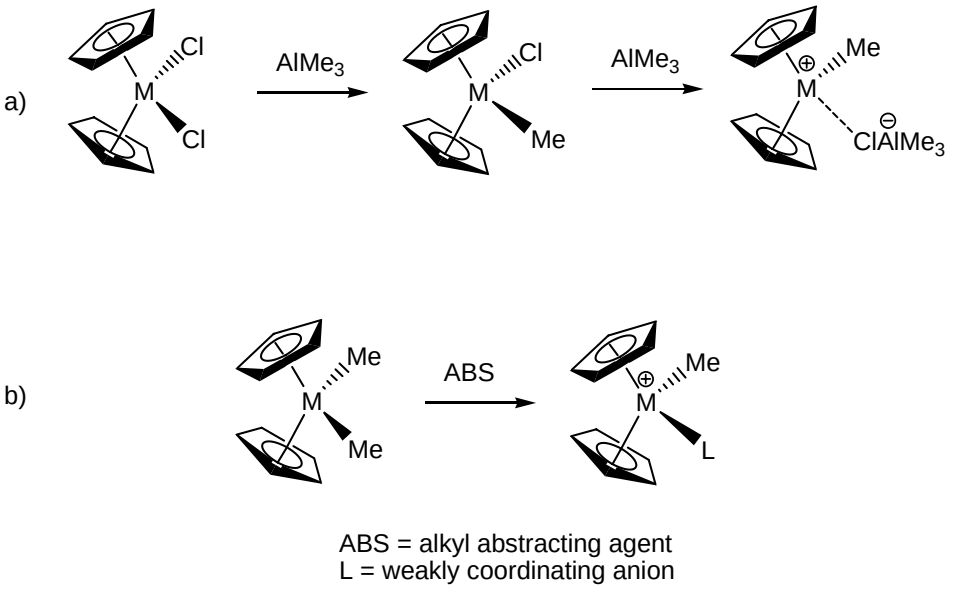

Scheme 7. Activation pathways for group 4 metallocene precursors.

The use of trialkylaluminum as a cocatalyst is very effective for heterogeneous catalyst systems (such as $TiCl_3$) in producing linear high molecular weight polyethylene.[12] However when group 4 metallocene dihalides (i.e. Cp_2TiCl_2) are activated with

trialkylaluminums, the resulting species are poor catalysts for ethylene polymerization and are inactive for propylene and higher α-olefin polymerization.[14] This finding diminished the commercial viability of these catalysts. However, when Sinn and Kaminsky[15] studied the effects of adding water to the inactive polymerization system $Cp_2ZrMe_2/AlMe_3$, they found a high activity for ethylene polymerization. This revolutionary discovery of this highly effective activator, known as MAO (methylaluminoxane), initiated a resurgence in the area of metallocene catalysis.

Methylaluminoxane $[-Al(Me)-O-]_n$ (n = 5 – 20) is synthesized by the controlled hydrolysis of trimethylaluminum. It is a highly effective activator for group 4 metallocenes to generate catalyst systems that are highly active for polymerizing ethylene, propylene and higher α-olefins.[16] There has been intense research with MAO since its initial discovery by Sinn and Kaminsky, but the exact structure of MAO is still ambiguous. There are many proposed structures for MAO, including: i) one dimensional linear chains, ii) cyclic rings and iii) three dimensional clusters . The three dimensional cage structure was based on the isolable and X-ray crystallographically characterized *tert*-butylaluminoxanes (iv) (Figure 4).[17]

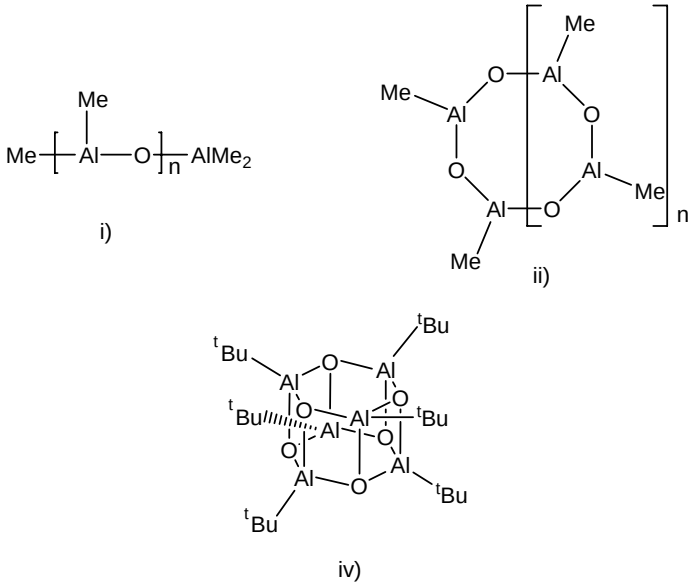

Figure 4. Sample possible structures of MAO.

The activation of group 4 metallocene precatalysts with MAO is proposed to occur via halogen abstraction and methylation of the metallocene, followed by a second halogen abstraction by MAO to generate the active cationic metallocene catalyst (Scheme 8).

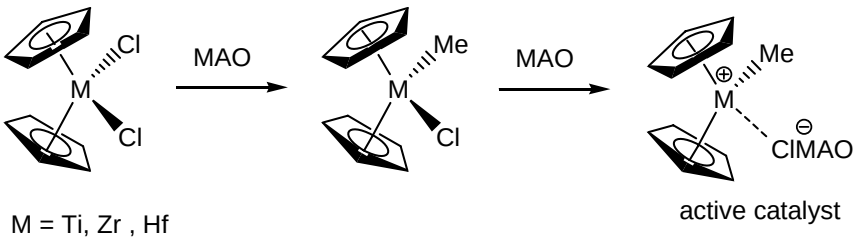

Scheme 8. Proposed mechanism of MAO activation.

In typical olefin polymerizations, MAO to catalyst ratios can range from hundreds to several thousands. MAO is also used as a scavenger for impurities which decrease catalyst activity (e.g. water, oxygen, etc.).

Beginning in the 1990's, Marks[18] and Ewen[19] independently reported the use of the strong Lewis acid, tris(perfluorophenyl)borane, $B(C_6F_5)_3$, in a stoichiometric amount, as an activator for dialkyl group 4 metallocene precatalysts (Scheme 9). The activated zwitterionic catalyst produced was a highly efficient catalyst for olefin polymerization. As a result of this discovery, research interests into coordination olefin polymerization have flourished. This zwitterionic catalyst was isolated and characterized crystallographically by Marks and extensive research has followed in this area to gain a better understanding of the reactivity of this catalyst under differing reaction conditions.[18] Despite being one of the most widely used cocatalysts in metallocene chemistry, this zwitterionic catalyst has a tendency for the anion $RB(C_6F_5)_3^-$ to block the catalyst active site, inhibiting monomer coordination to the active metal center, thereby decreasing the catalytic activity.[18]

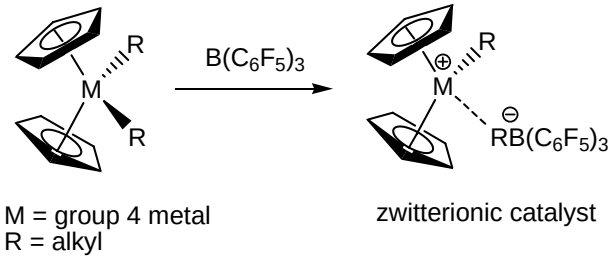

Scheme 9. Formation of zwitterionic catalyst.

To overcome this unfavourable interaction from a polymerization standpoint, Marks[20] and Piers[21] have developed many new more sterically demanding perfluorophenylboranes. For example, the Marks group have made compounds such as tris(2,2',2''-perfluorobiphenyl)borane (PBB)[20a], bis(pentafluorophenyl)(2-perfluorobiphenyl)borane (BPB)[20b] and tris(β-perfluoronaphthyl)borane (PNB)[20c] (Figure 5).

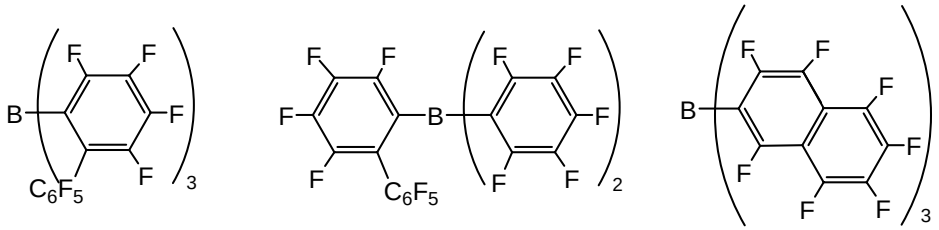

Figure 5. Bulkier perfluorophenylborane complexes.

Another successful approach of alkyl abstraction from metal alkyl complexes includes using triphenylcarbenium tetrakis(pentafluorophenyl)borate, $[Ph_3C][B(C_6F_5)_4]$.[19a,21] This strong alkide and hydride abstractor can readily cleave metal-alkyl bonds in group 4 metallocene and related metal alkyl systems. It has been shown to be a highly effective cocatalyst for olefin polymerization due to its anion, $B(C_6F_5)_4^-$, being less weakly coordinating than the anions formed from using $B(C_6F_5)_3$ (i.e. $RB(C_6F_5)_3^-$). Some problems associated with catalyst systems containing $B(C_6F_5)_4^-$ are poor solubility in hydrocarbon solvents, poor thermal stability and difficulty in crystallizing the cationic intermediates.[22] To help with these issues, new functionalized fluoroarylborate salts such as in Figure 6, make the study of these catalyst complexes

more facile.[22,23] However, despite these modifications, the activity of these fluoroarylborate salts are only comparable to $[Ph_3C][B(C_6F_5)_4]$.

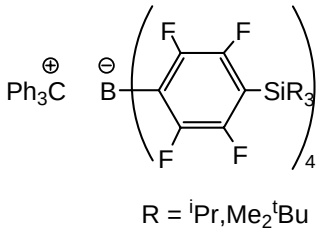

Figure 6. Functionalized fluoroarylborate.

One final group of pertinent compounds for activating metal-alkyl precatalysts involves ammonium salts of the form $[HNMe_2Ph][B(C_6F_5)_4]$. The use of these salts results in the protonation of one of the metal-alkyl bonds to generate the free alkane and the cationic active catalyst (Scheme 10). However, problems with these systems involve the liberation of the Lewis base, NMe_2Ph, which can coordinate to the active metal center and inhibit monomer coordination and subsequent insertion.[24]

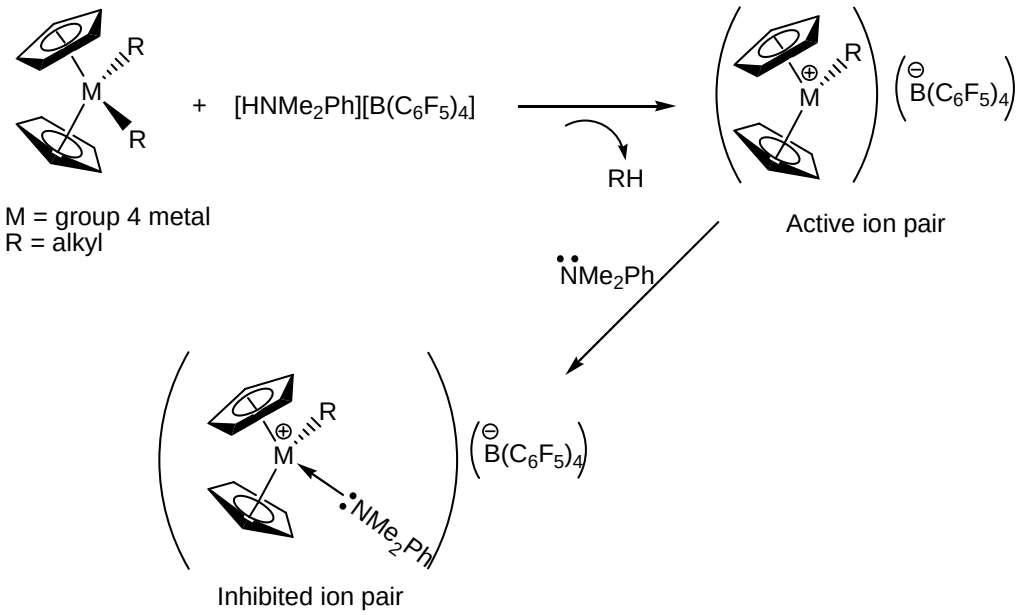

Scheme 10. Protonolysis of metal-alkyl bond and possible inhibition by Lewis base.

1.1.6 Coordination Polymerization Mechanism

The four steps involved in coordination polymerization are: i) initiation, ii) propagation, iii) termination and iv) chain transfer. These will be discussed below.

i) Initiation

The accepted initiation process in group 4 metallocene-type polymerizations proceeds via activation of the metallocene precatalyst to the 14 electron cationic intermediate. Next, displacement of the weakly coordinating anion by monomer is achieved to generate an η^2-alkene complex. Lastly, migration of the alkyl R group to the alkene, through a four centered transition state, occurs and a vacant site is regenerated for additional monomer insertion (Scheme 11).

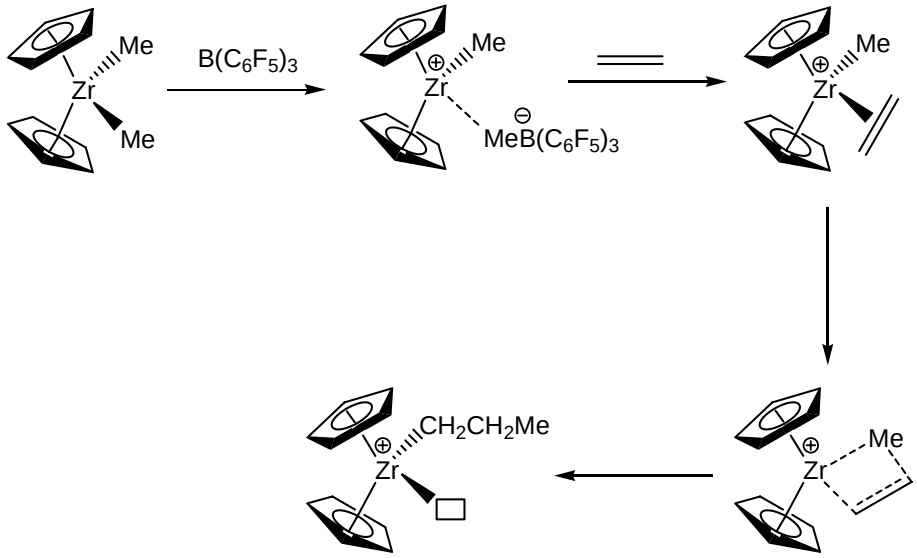

Scheme 11. Initiation mechanism.

ii) Propagation

Propagation involves monomer coordination to the newly formed vacant site after initiation followed by migratory insertion. Repeated monomer coordination and insertion leads to polymer chain growth (Scheme 12).

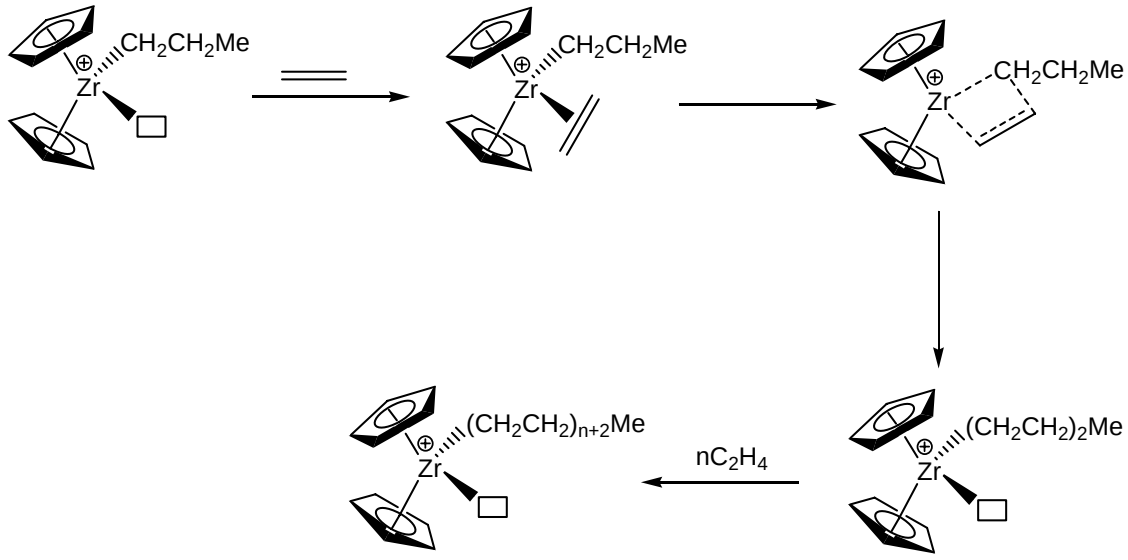

Scheme 12. Propagation mechanism.

iii) Termination

The process of termination in coordination polymerization is achieved by adding a polar additive such as water or methanol, resulting in proton transfer to the growing chain and termination of chain growth. The resulting complex, either a metal hydroxide or alkoxide, is incapable of further propagation (Scheme 13).

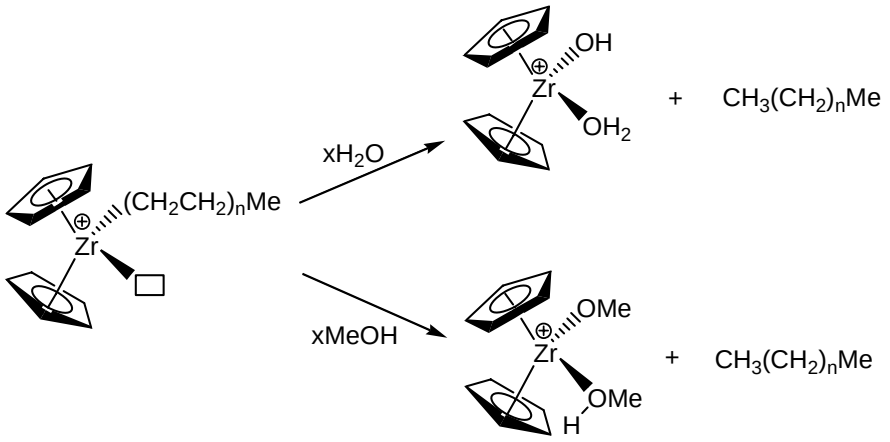

Scheme 13. Termination pathways using water or methanol.

iv) Chain Transfer

During propagation, the growing polymer chains can transfer a β-hydrogen to the metal or monomer through a process known as β-hydrogen elimination. With respect to transfer to the metal, the growing polymer chain transfers its β-hydrogen through a β-agostic interaction, instead of a new monomer coordinating to the metal center. This interaction leads to hydride transfer to the metal and an unsaturated polymer chain (Scheme 14). Monomer may then displace the unsaturated polymer chain. The metal hydride can reinitiate a new polymer chain or reinsertion may occur, followed by either branching or continued polymerization of the initial chain.

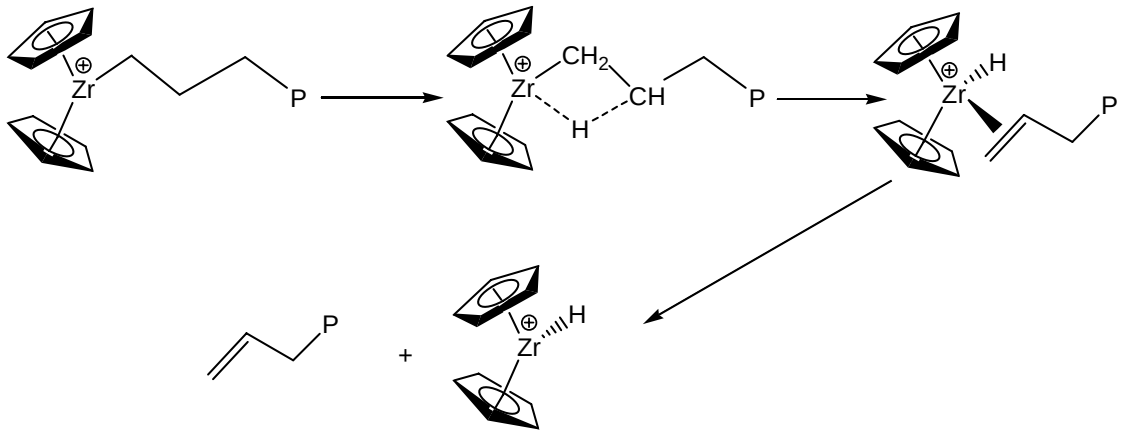

Scheme 14. β-hydrogen elimination to metal center.

The β-hydrogen transfer to monomer mentioned above occurs similarly to that in Scheme 14, except that monomer is coordinated to the metal center along with the growing polymer chain. Direct transfer of the β-hydrogen from the growing chain to the monomer occurs, thereby creating a new growing chain on the metal and release of a terminal olefin.[25]

Another important mode of chain transfer in coordination polymerization is transfer to aluminum, when using MAO or alkylaluminum as a cocatalyst. This is known as a transalkylation reaction. Here, the growing polymer chain is transferred to aluminum and aluminum transfers its alkyl group to the metal, creating a new metal-alkyl catalyst (Scheme 15). This aluminum end-capped polymer can transfer back to the metal catalyst, or if quenched in acidified media, can result in dead polymer with a methyl end-group. The new metal-alkyl catalyst can coordinate new monomer and start a new chain growth.[25]

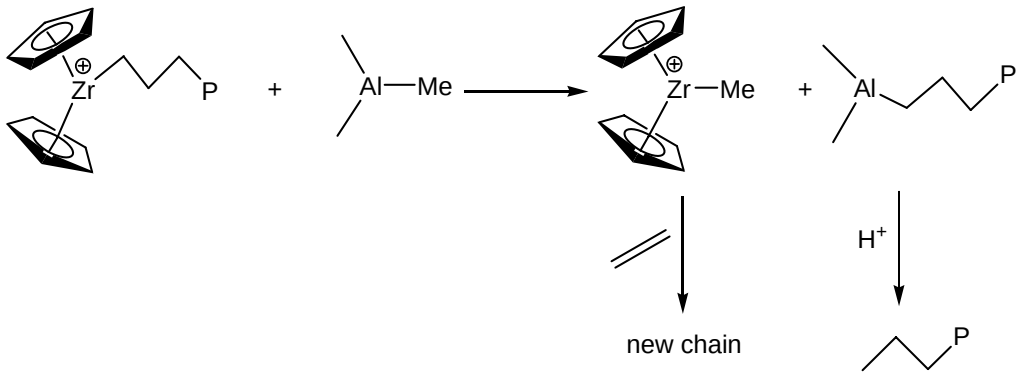

Scheme 15. Chain transfer to aluminum.

In conjunction with the modes of chain transfer above, some other important chain transfer reactions to mention are hydrogenolysis and β-alkyl elimination.

Hydrogenolysis involves the addition of hydrogen gas to the coordination polymerization mixture and results in the elimination of a saturated dead polymer chain and formation of a metal-hydride catalyst, which is capable of starting new chain growth (Scheme 16).[26] This method can be used to control the molecular weight of the final polymer.

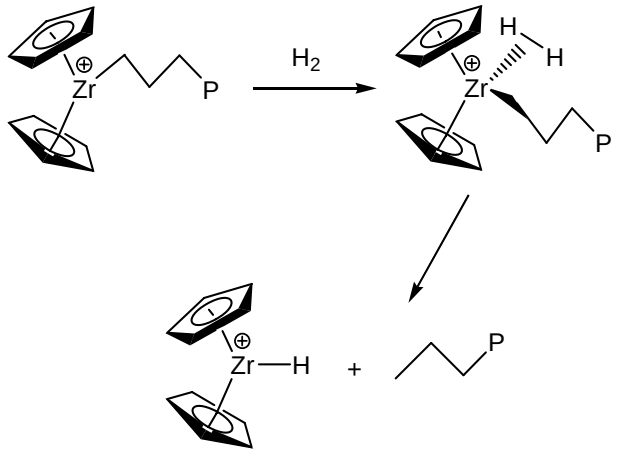

Scheme 16. Chain transfer via hydrogenolysis.

β-alkyl elimination (in particular β-Me elimination) is a process that has been observed in substituted cyclopentadienyl systems (such as pentamethylcyclopentadienyl complexes) with metals such as Zr, Hf, Sc.[27] The resulting products are an unsaturated polymer chain end and a new metal-alkyl catalyst, capable of further polymerization (Scheme 17).

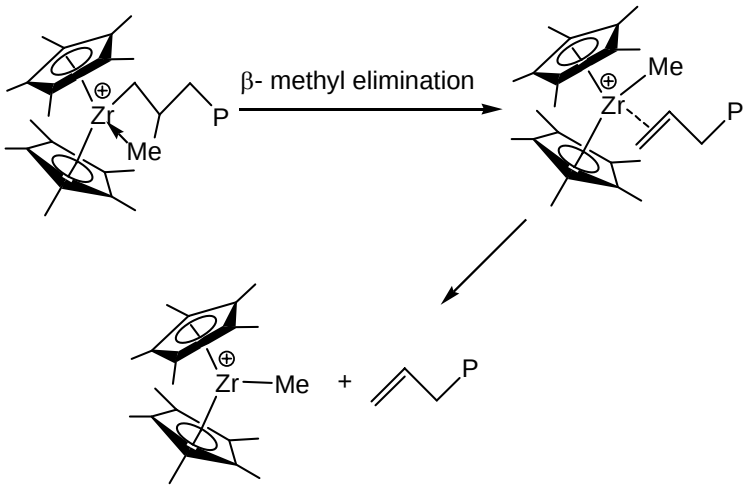

Scheme 17. Chain transfer via β-methyl elimination.

1.1.7 Polymers Discussed in this Thesis

The following section discusses the polymers used, synthesized or attempted to synthesize in this thesis.

Polyethylene (PE)

Polyethylene is a commodity polymer of great importance, as is seen with continually rising sales and demands each year.[28] Practical applications of polyethylene include packaging films, cable insulation, housewares and coatings. Three main types of polyethylene exist: high density polyethylene (HDPE), low density polyethylene (LDPE)

and linear-low density polyethylene (LLDPE). Each form of polyethylene (Figure 7) has its own unique properties and they are synthesized via different methods. HDPE is a highly crystalline polymer, with a high melting temperature (T_m = 120 ^oC), and it is generally made by Ziegler-Natta processes. HDPE has very few or no branches. LLDPE is also made via Ziegler-Natta processes, but here the ethylene is copolymerized with α-olefins (such as 1-butene or 1-hexene) to produce random branched copolymers. The incorporated long chain branches along the polymer main chain disrupt crystal packing and lower the melting temperature of the polymer. LDPE is synthesized via free radical processes at high temperatures and pressures. This polymer usually contains many branches (i.e. Me, Et and longer) along the polymer main chain.

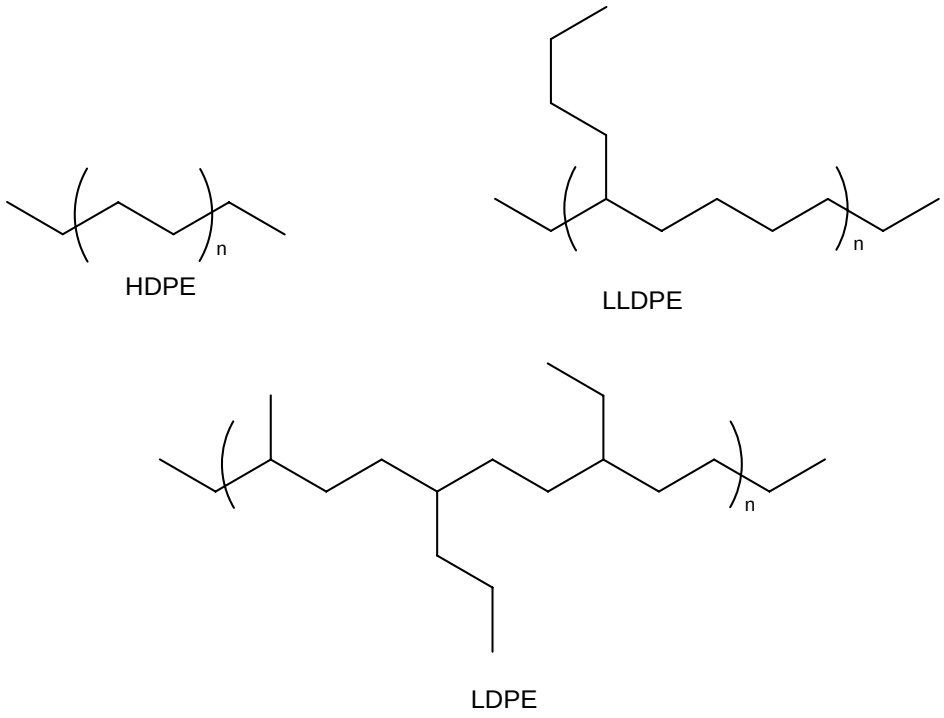

Figure 7. Three types of PE.

Polypropylene (PP)

Polypropylene is a widely used polymer with good mechanical properties. Uses for polypropylene range from plastic patio furniture to long lasting integral hinges to food storage containers. Properties of great chemical resistance and high melting temperature (T_m = 165-180 ^oC) make polypropylene superior to polyethylene in applications that require heat resistance. There are three main types of polypropylene polymers: isotactic, syndiotactic and atactic (Figure 8). Each stereochemically different polypropylene polymer has unique properties such as glass transition temperature (T_g) and crystalline melting temperature (T_m). In this thesis, atactic and isotactic polypropylene homo- and copolymers are synthesized.

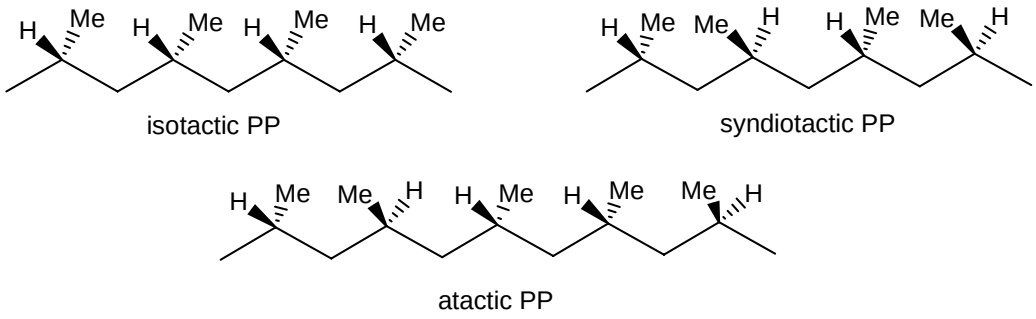

Figure 8. Tacticity forms of polypropylenes.

Polyacrylonitrile (PAN)

Polyacrylonitrile is an important polymer due to its unique and attractive properties. These include chemical resistance, rigidity, toughness, heat resistance and low gas permeability. PAN is typically prepared by free radical polymerization and results in linear polymer (Figure 9). PAN can be also made by anionic polymerization. However,

lower molecular weight and highly branched PAN is produced due to side reactions that incur such as 'back biting' or attack of the propagating anion on the cyano group.[28]

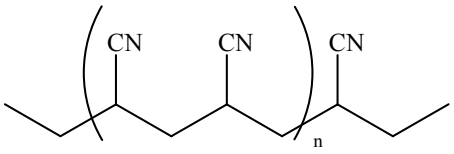

Figure 9. General structure of polyacrylonitrile.

Hydrogenated Butadiene-Nitrile Rubber (HBNR)

HBNR is currently synthesized by first copolymerizing acrylonitrile and butadiene by a radical process and then partially hydrogenating the resulting copolymer as shown in Scheme 18.[29] This copolymer is very strong and versatile with properties such as operating temperatures up to 165 ^{o}C and no degradation with exposure to heat, oil or chemicals. These findings have resulted in applications of HBNR in the automotive industry, particularly demanding applications requiring great chemical resistance such as seals, gaskets and hoses.

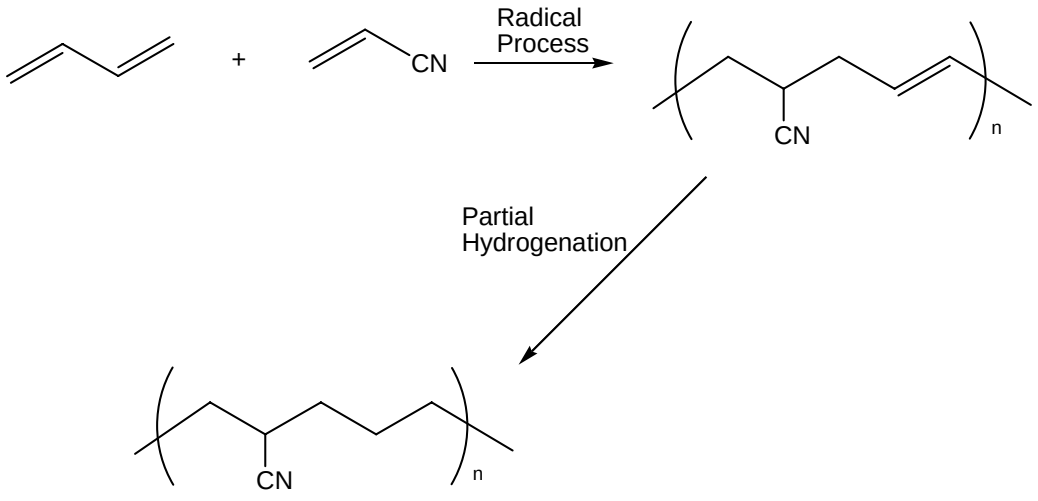

Scheme 18. Commercial synthesis of HBNR.

A major disadvantage of the commercial production of HBNR is the expensive batch process to hydrogenate the unsaturated copolymer. A potential solution to this issue would be to *directly* copolymerize ethylene and acrylonitrile using a transition-metal mediated process.

1.2 Palladium Metal Catalysts for Polymerization Studies

As discussed in Section 1.0, there is a significant problem of polymerizing polar monomers with highly Lewis acidic early metal catalysts. Typically, the functional group "poisons" the active catalyst by coordination to the metal center instead of η^2- olefin coordination, which is required for insertion. One approach to polar monomer insertion which may prove to be effective is the use of late metal catalysts such as those discussed in Section 1.0. These Brookhart and Gibson type late metal catalysts, based on nickel and palladium, are less electrophilic than their early metal counterparts and may be able to tolerate polar monomers more effectively.

Cationic α-diimine complexes of the type $[PdMe(L)(\alpha\text{-diimine})]^+$ (**1**: L = solvent or neutral ligand, Figure 10) have been shown to be effective catalysts for ethylene

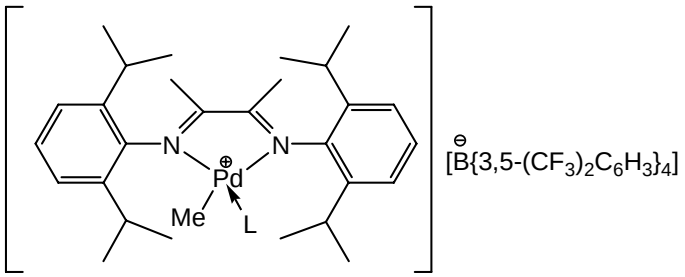

1

Figure 10. Cationic α-diimine catalyst.

polymerization, and copolymerization of ethylene with acrylates and methacrylates.[6] The copolymerization mechanism for this system is shown in Scheme 19. It has been shown

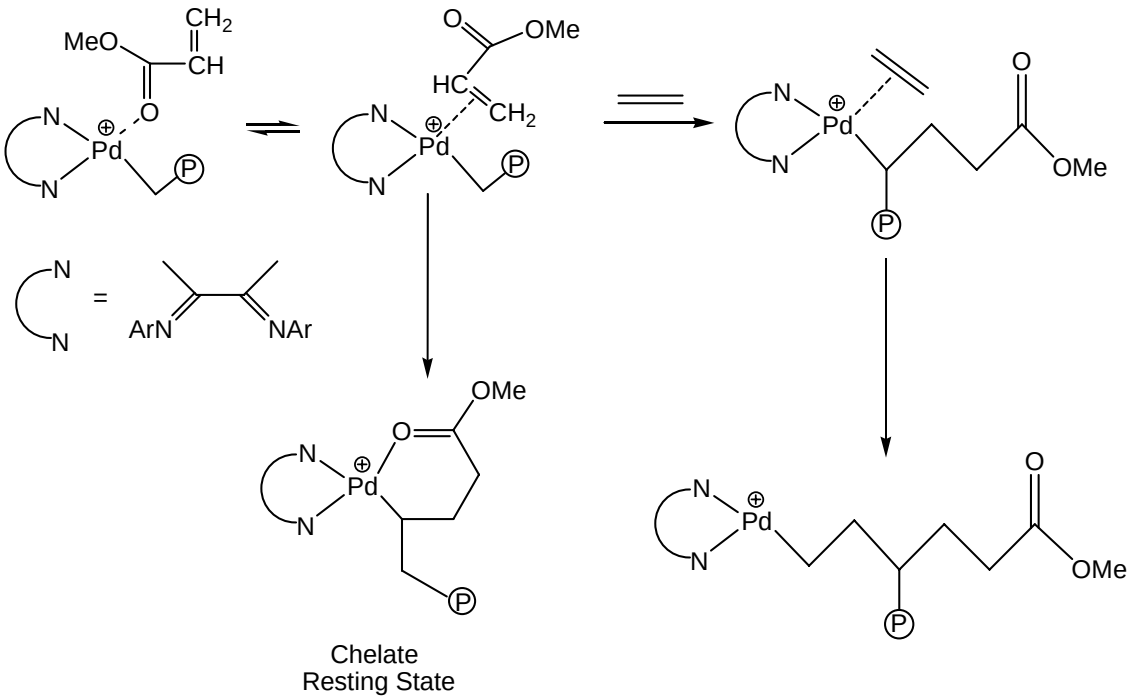

Scheme 19. Copolymerization mechanism of methyl acrylate with catalyst **1**.

through theoretical[30] and experimental[6,31] means that the polar group of the acrylate does bind to the metal center. However, the polar group can dissociate to allow monomer to bind to the metal center and insertion can ensue. As polymerization proceeds, the activity of this system is decreased due to the formation of a strong chelate resting state as shown in Scheme 19. This six-membered chelate with strong binding of the oxygen to the Pd metal has been found to be a highly favoured resting state, retarding monomer insertion, even at high ethylene pressures.[6] This realization explains why much of the polar monomer incorporated into the polymer chain is at the chain ends.

Jordan and coworkers[32] have investigated vinyl chloride polymerization with a similar system, (α-diimine)$PdMe_2$/ $B(C_6F_5)_3$. They found that 1,2 vinyl chloride insertion occurs in the Pd-Me bond to generate the expected first inserted product, of the type Pd-$CH_2CHClMe$. However, this species undergoes facile β-chloride elimination to the metal to form propylene and polymerization inactive palladium chloride compounds (Scheme 20).

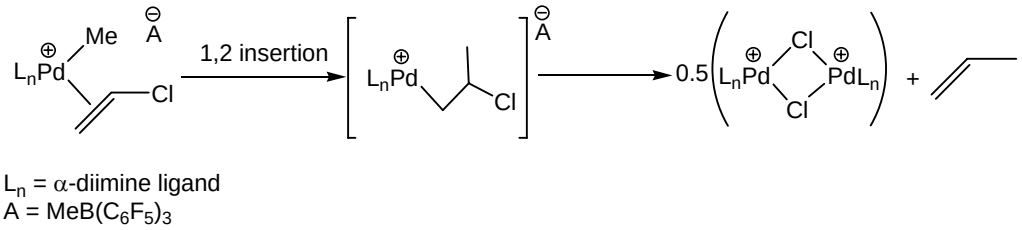

L_n = α-diimine ligand
A = $MeB(C_6F_5)_3$

Scheme 20. β-chloride elimination in an (α-diimine)$PdMe_2$/ $B(C_6F_5)_3$ system.

Computational studies have been done on palladium species of type **1** and similar complexes in order to determine the mode of binding when acrylonitrile is added to catalyst **1**.[30] It was found that σ-coordination to the metal via the nitrogen is 13 kcal/mol more favoured then π-bonding via the C=C bond (i.e. η^2-coordination). Interestingly, the barrier to insertion via η^2-coordinated acrylonitrile has been calculated to be similar to that of ethylene.[30] However, this insertion barrier calculation is very sensitive to the ligands surrounding the metal center and also the reaction conditions.[30c] In addition, catalysts of type **1** where the labile ligand is acrylonitrile or aryl nitriles instead of diethyl ether, were found to be active catalysts for the copolymerization of ethylene and 1-alkenes with methyl methacrylates.[6d] This signifies that substitution of the N- bond

ligands on the metal by olefins is possible and facile. In fact, historically it has been known that weakly coordinating olefins such as isobutene or styrene can readily displace the benzonitrile ligands from $PdCl_2(PhCN)_2$ to generate complexes of the form $[PdCl_2(alkene)_2]_2$.[31] In contrast to β-chloride elimination in vinyl chloride polymerization as discussed above, β-cyano elimination is less likely due to the larger difference in the bond strength of the C-CN bond (~132 kcal/mol) as compared to C-Cl (~94 kcal/mol).[33]

1.3 Research Aims for Part 1 of this Thesis

In Part 1 of this thesis, Brookhart's diimine catalyst **1** (L = OEt_2) (Figure 10) is *exclusively* studied for its homopolymerization behaviour of acrylonitrile and copolymerization with ethylene. As this work was being completed, two other groups, Wu *et al.*[34a] and Groux *et al.*[34b] published research similar to this work, but, our focus was quite different. Wu *et al.*[34a] studied six cationic palladium species with various bidentate N-donor ligands (Figure 11a, including diimine ligand catalyst **1**), and its room temperature acrylonitrile coordination and insertion chemistry. Groux *et al.*[34b] discussed a complementary study where neutral and anionic complexes of palladium species involving bulky ligands such as phenoxydiazene or phenoxyaldimine (Figure 11b) were utilized.

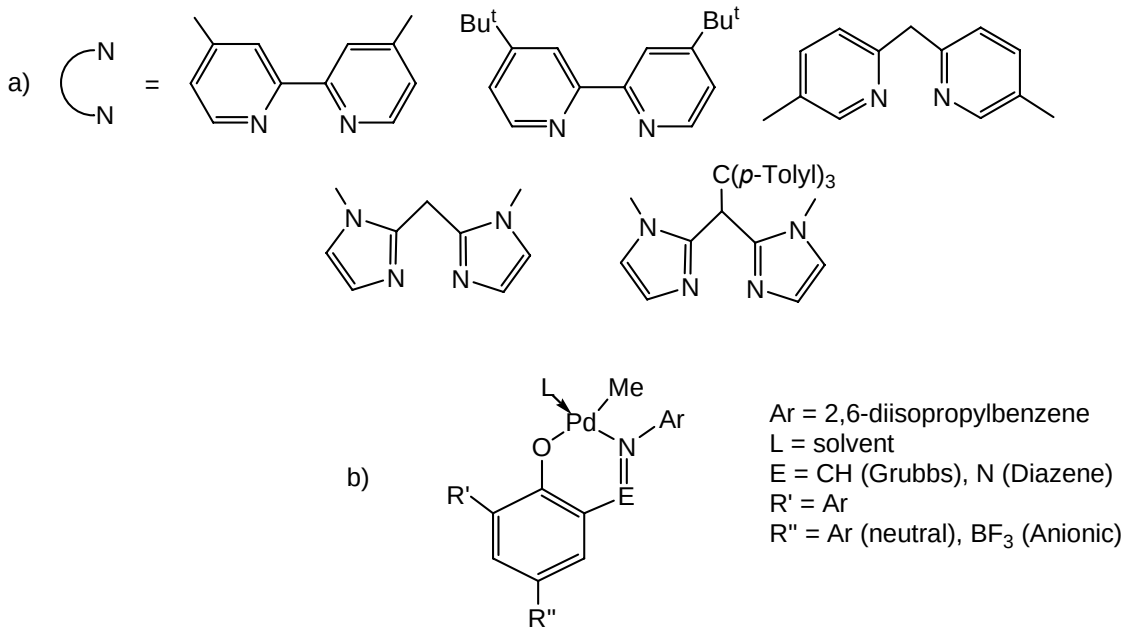

Figure 11. a) Bidentate N-donor ligands and b) phenoxydiazene or phenoxyaldimine ligands.

It was found by Wu *et al.* that palladium species, bearing the ligands shown in Figure 11a, react with acrylonitrile to form N-bond adducts $[L_2PdMe(NCCH{=}CH_2)]^+$. All these coordinated complexes undergo 2,1 insertion at 23 ^oC, *except* catalyst **1**, to form the insertion product $L_2Pd\{CH(CN)Et\}^+$, which instead forms mixed aggregates of the type $[L_2Pd(CH(CN)Et)]_n^{n+}$(Scheme 21). These mixed aggregates are proposed to be linked through the Pd metal via Pd-CHEtCN-----Pd interactions, and are a possible reason for the lack of insertion reactions due to effective competition with monomer binding.[34a] It is important to note that catalyst **1** was given very little attention in this study but is the *main focus* of this study.

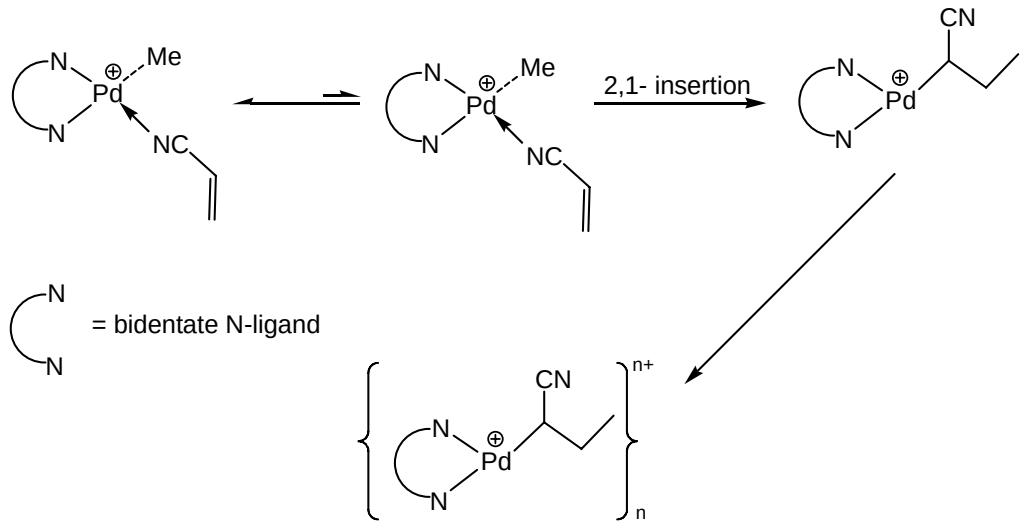

Scheme 21. AN insertion and generation of aggregates of the type $[L_2Pd(CH(CN)Et)]_n^{n+}$.

The study by Groux *et al.*[34b] involved neutral and anionic ligands, with the reasoning that these analogues of ligands favour acrylonitrile π-coordination over σ–N bond species, as evidenced by DFT calculations. This ligand tuning may favour the incidence of insertion reactions. Results of their study do show that acrylonitrile insertion occurs with these ligand types, but dimers and/or trimers were isolated which featured bridging α-cyano groups.[34b]

In Part 1 of this thesis, we report two novel and unprecedented observations. In addition to characterizing the N-bond coordinated acrylonitrile complex to catalyst **1** (complex **2**, Figure 12), we also show that complex **2** exists in solution as two interconverting rotamers. This is rationalized by the ring current effect of the aryl groups on the ligand interacting with the vinylic protons on AN, therefore producing unusual chemical shifts in the ^{1}H NMR. Secondly, we report that under forcing conditions, AN insertion into catalyst **1** occurs, a phenomenon not reported previously. In addition to this,

we investigated the copolymerization behaviour of these inserted reactions pathways with ethylene.

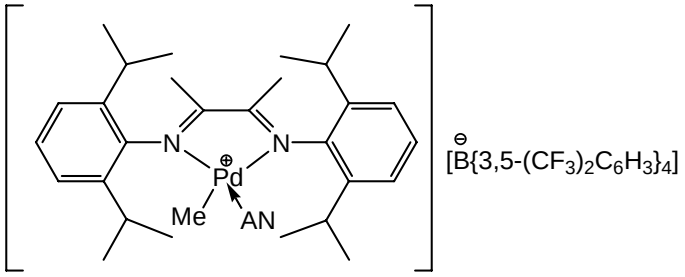

2

Part 2

Early Metal Copolymerization Studies of Polar Monomers $CH_2=CH(CH_2)_7CH_2OR$ (R = Me, $PhCH_2$, Ph_3C, Me_3Si, Ph_3Si) with Ethylene and Propylene.

1.4 Introduction

A polymer that contains two different repeat units is called a *copolymer*, and the process by which it is synthesized is called *copolymerization*. Copolymers offer the potential to combine the individual properties of the two different homopolymers (A and B) into one material. There are many different types of copolymers (Figure 12): a) alternating, where perfect alternation occurs between two different repeat units; b) block, where blocks of one type of homopolymer are attached to blocks of another type of homopolymer; c) random, where there is no specific order of the two different repeat units along the copolymer chain and d) graft, where one or more blocks of one type of homopolymer are grafted as arms or branches onto a different homopolymer main chain.[35]

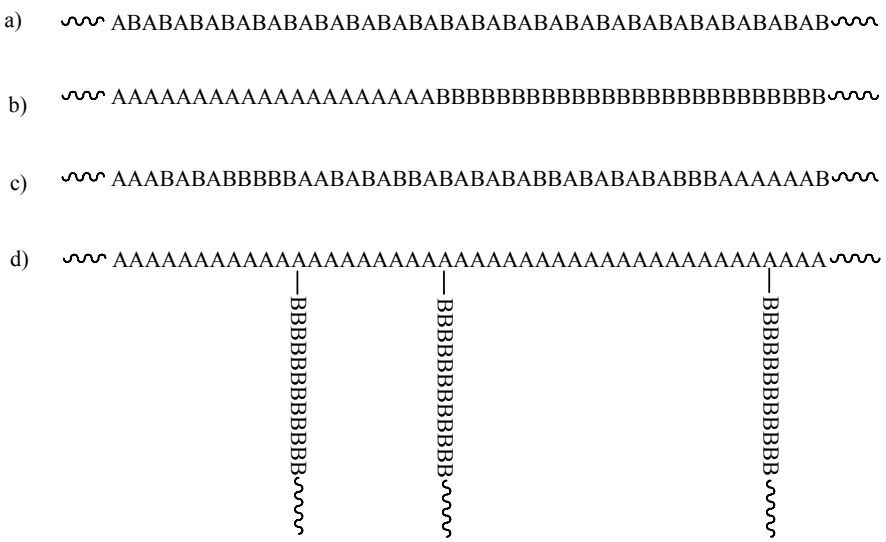

Figure 12. Structures of a) alternating, b) block, c) random and d) graft copolymers.

A good example of how the properties of a homopolymer can significantly change upon introduction of comonomers (such as non-polar 1-butene, 1-hexene, etc) is polyethylene (see section **1.1.7**). Introduction of polar monomers into homopolymers, such as polyethylene or polypropylene, can open the possibilities for new materials with improved properties.

1.5 Polar Monomer Copolymers

The random incorporation of polar groups such as ester, halo, cyano, hydroxyl, etc. into polyethylene and polypropylene can generate materials with enhanced properties such as adhesion, paintability and toughness.[7] As mentioned, the most effective catalysts for *homopolymerization* of ethylene and propylene are Ziegler catalysts (section **1.1.1**), but they do not perform well in the presence of polar functional groups due to coordination of the functional group to the oxophilic catalyst center and thereby "poisoning" the catalyst from insertion to occur (as shown in section **1.1.1**). Therefore, novel routes to random copolymers containing polar and nonpolar segments are desirable.

In contrast to part 1 of this thesis, where late metal catalysts were the focus, the second part of this thesis focuses on early metal (e.g. Ti, Zr) metallocene catalysts. Despite their highly oxophilic nature, metallocene catalysts offer several desirable advantages for copolymerization studies. For example, with the proper tailoring of the ligands on the metallocene catalyst, high stereochemical control (e.g. isotactic polypropylene) of the resulting polymer is possible. In addition, there are known examples of successful copolymerizations of ethylene with α-olefins[37] and copolymerizations of propylene with α-olefins[38]. In principle, proper masking of the

functional group on the polar monomer, prior to polymerization, should provide a route to the target copolymers. A good example of this is the masking of hydroxyl terminated monomers of the type $CH_2=CH(CH_2)_nCH_2OH$ (n = 0-12) with aluminum alkyls (eq. 1, 2).[39]

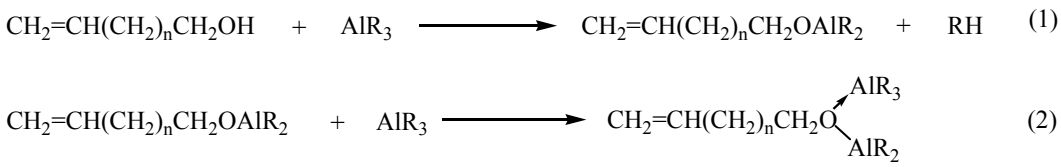

$$CH_2=CH(CH_2)_nCH_2OH + AlR_3 \longrightarrow CH_2=CH(CH_2)_nCH_2OAlR_2 + RH \quad (1)$$

$$CH_2=CH(CH_2)_nCH_2OAlR_2 + AlR_3 \longrightarrow CH_2=CH(CH_2)_nCH_2O\begin{matrix}AlR_3\\ \diagdown\\ \diagup\\ AlR_2\end{matrix} \quad (2)$$

The strategy involved was to sterically hinder the oxygen moieties with the bulky aluminum groups, thereby preventing coordination to the metal center and deactivation of the catalyst. Furthermore, upon hydrolysis, retrieval of the hydroxyl groups could be achieved in the final polymer.

1.6 Literature Review

For the scope of this thesis, the main focus will be on *in chain* or *direct* copolymerizations strategies and post polymerization treatment will not be reviewed.

The types of protecting groups used in the literature are comprised of different elemental alkyl groups. These are discussed below.

1.6.1 Aluminum Alkyl Masking Agents

To date, many attempts have been made to produce random copolymers of ethylene and propylene with 1-alkenes containing hydroxyl end groups by masking the

hydroxyl polar monomers with aluminum alkyls (as shown in **2.2**). The general polymerization procedure (Scheme 22) used for most of these copolymerizations involves combining one of a library of dichlorozirconocene catalysts (Figure 13), an aluminum alkyl masked polar monomer (either pre-formed or generated *in situ*) olefin, solvent (typically toluene) and MAO (100-10000 equivalents). In some cases, more aluminum alkyl is added to further aid in complexing the polar monomer.

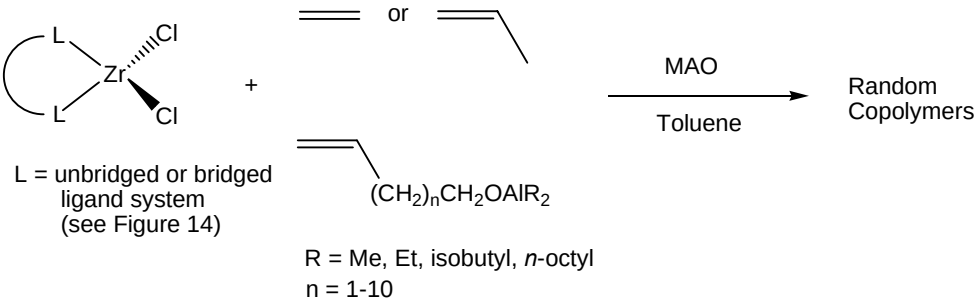

Scheme 22. General copolymerization procedure using aluminum alkyls.

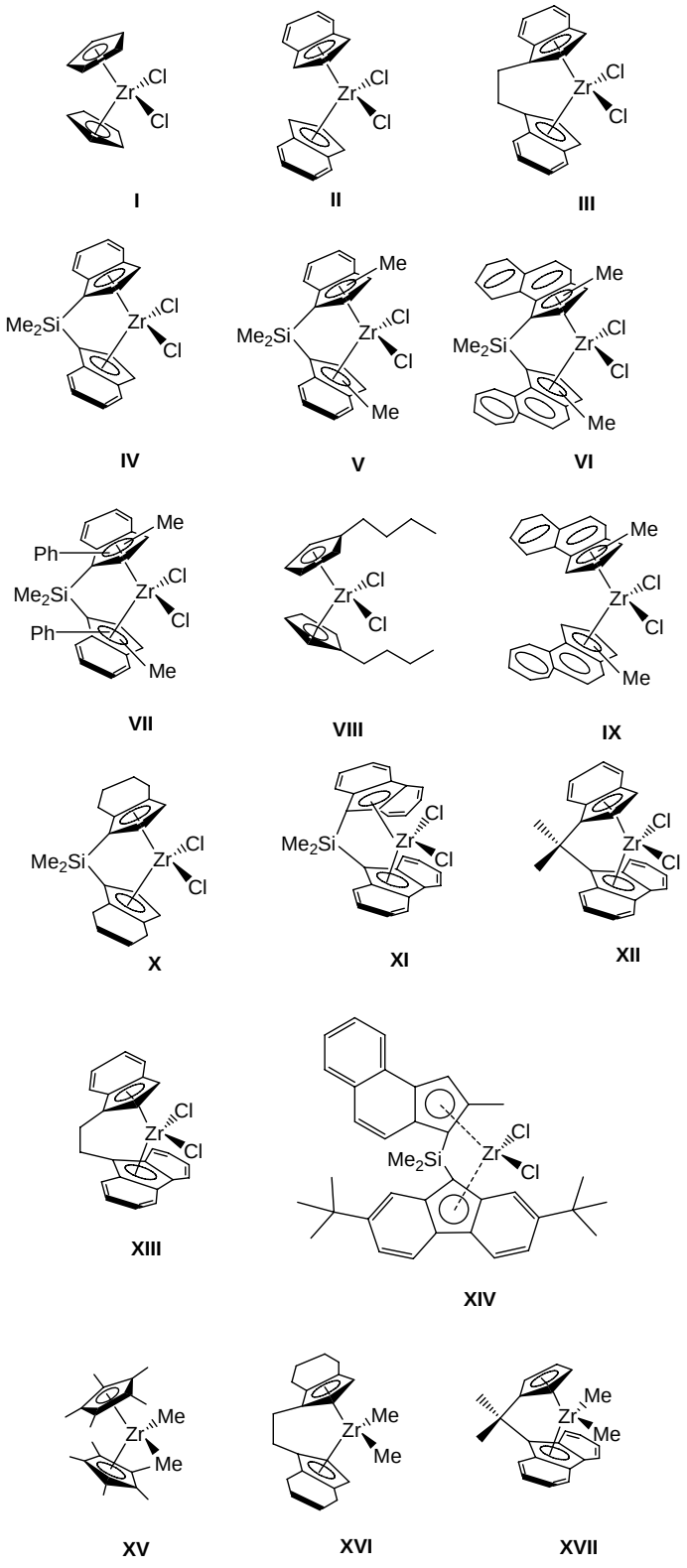

Figure 13. Library of zirconocene catalyst precursors.

Löfgren *et al*. have reported extensive studies of copolymers of ethylene and propylene with several long and short chain hydroxyl functionalized alkenes using dichlorozirconocenes (Figure 13, **I** – **VIII**) activated with MAO.[39a-i] They have shown that polar monomer incorporations occurred but were relatively low (1 wt % to 3.6 mol %); however, incorporations seem to be higher when long chain polar monomers were used. In addition, they found increasing the polar monomer concentration resulted in catalyst deactivation and lowered polymer molecular weights and yields. Interestingly, the amount of MAO added played an important role, as increasing the aluminum to zirconium or polar monomer ratio raised activities, and adding triisobutylaluminum (TIBAL) to these MAO systems also increased polymerization activities. This could be attributed to further complexation of the polar monomer by TIBAL in conjunction with MAO, therefore hindering the destruction of the active catalyst. Despite the low incorporations of polar monomer, a blend of the copolymers containing small amounts of hydroxyl groups actually improved the surface adhesion properties compared to that of the homopolymer.[39j]

Many other researchers have reported similar studies using zirconocene-based catalysts (**III**, **IV**, **X**, **XI**, **XII, XIII,** Figure 13) activated with MAO and masking/pretreating polar monomers with alkyl aluminums and/or pretreating with MAO.[40] These results showed high incorporations with long chain monomers, such as 10-undecenol and 5-hexenol, of up to 10 (catalyst **III**)[40e], 50 (catalyst **XIII**) [40f,k] and 37 (catalyst **XIV**) [40g,l] mol %, depending on the reaction conditions. However, short chain polar monomers, such as allyl alcohol, gave very low incorporations under similar

conditions.[40j,l,n] The highly incorporated 50 mol % copolymer material was found to be highly hydrophilic via contact angle measurements.[40k]

1.6.2 Silyl Masking Agents

Another approach to the masking of the hydroxyl ends involves using hydrolysable silyl ethers, mainly containing $OSiMe_3$ groups, initially introduced in the mid to late 1960's with $TiCl_3$-based catalysts.[41a,b] More recently, there have been numerous studies with metallocene-based catalysts (such as **IV**, **XV**, Figure 13), [41c-g] although improved incorporations, conversions and molecular weights have not been observed compared to aluminum masking. For example, Sivaram and Rajesh[42] found that the copolymerization of ethylene with various silicon monomers, such as with trimethylsilyloxydimethylvinylsilane (TMSD) and vinylethoxydimethylsilane (VEDS) (Scheme 23), with catalyst **IV**, showed *no* copolymerization activity with ethylene. This is most likely due to catalyst poisoning due to the ethoxy and silyloxy groups coordinating to the active center. Similar results were seen by Fink *et al.*[41d] using catalyst **IV,** where hydroxyl monomers were protected by trimethylsilyl groups and copolymerized with ethylene. However, when bulkier groups on the silicon were used, such as triisopropylsilyl (TIPS), good catalyst activities and comonomer contents were obtained (up to 2.2 mol %).

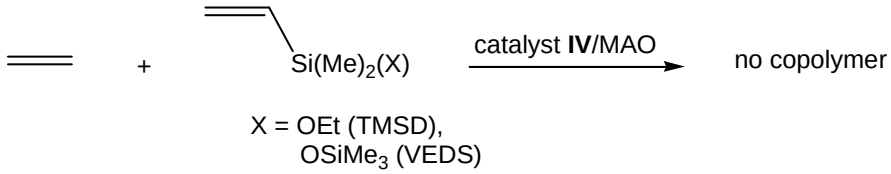

Scheme 23. Copolymerization of ethylene with vinyl silanes.

Another example of the silyloxy masking approach was that reported by Waymouth *et al.*[41c] where the silicon functionalized monomer 4-TMSO-1,6-heptadiene was reacted with $[Cp^*_2HfMe][B(C_6F_5)_4]$ in neat monomer at - 25 ^oC to yield poly(methylene-3,5-(1-trimethylsiloxy)cyclohexanediyl) with $M_w = 1.42 \times 10^4$, PDI = 3.1 and a conversion of 38 % (Scheme 24). Upon treatment of this polymer with aqueous HCl, the polyalcohol was obtained.

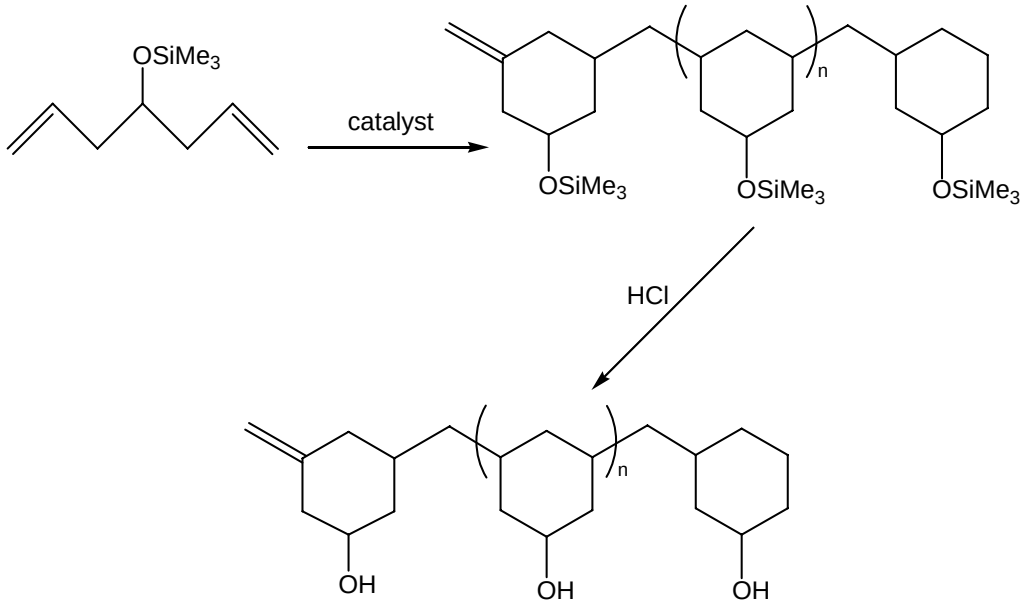

Scheme 24. Polymerization of silyl protected alcohol.

To provide further success with silicon protected monomers, the use of long spacers between the vinyl group and the protected hydroxyl group, in conjunction with a bulkier substituent on the silicon (such as a phenyl group), could provide access to more incorporated comonomer and accompanied by no diminished polymerization activity.

1.6.3 Boron Alkyl Masking Agents

The masking of oxygen containing monomers with boron alkyl groups followed by homo- and copolymerization with olefins has been extensively studied by Chung *et al.*[43] This approach was initiated by homopolymerizing a boron protected,{ 9-borabicyclo[3.3.1]nonane (9-BBN)}, vinyl monomer with a heterogeneous Ziegler/Natta catalyst ($TiCl_3/Al(Et_2)Cl$) to generate a polyorganoborane. This polymer could be easily transformed to the polyalcohol on treatment with $NaOH/H_2O_2$ (Scheme 25). This method is effective since the borane is a Lewis acid itself and is stable with respect to the Ziegler/Natta catalyst (e.g. titanium and aluminum), thereby avoiding side reactions.[43a]

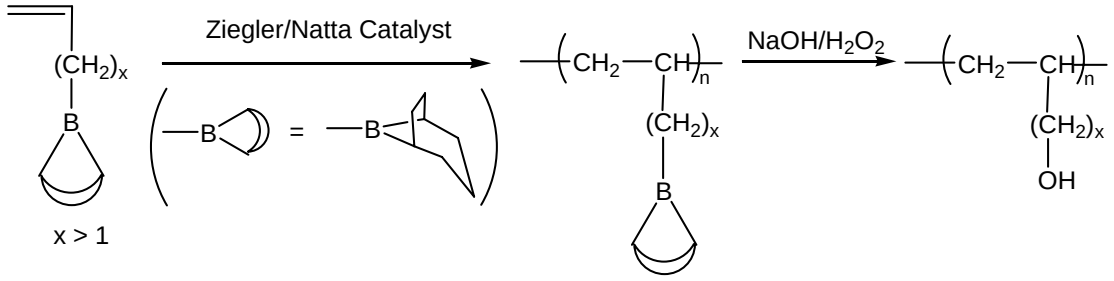

Scheme 25. Boron protected homopolymerization studies.

The weight-average molecular weight of the polyborane produced was determined by first converting the polyborane to the polyester for ease of GPC measurement, and it was found to be above a million grams per mole. Further structural analysis by ^{11}B NMR, IR and TGA confirmed the synthesis of both polyborane and polyalcohol.

Next, Chung *et al.*[43b] examined the borane protected monomer 5-hexenyl-(9-BBN), and its ability to copolymerize with 1-octene using a Ziegler/Natta catalyst ($TiCl_3/Al(Et_2)Cl$) (Scheme 26). They found that the borane monomer was only slightly

less reactive than 1-octene, therefore providing access to the synthesis of copolymers with a wide range of compositions.[43b] After obtaining the copolymer, further oxidation of the poly(octene-*co*-borane) copolymer generated the copolymer poly(octene-*co*-hexenol). The comparison of GPC profiles and glass transition temperatures (only one transition seen for each copolymer) showed that the copolymer established homogeneity. Also, the T_g of the copolymer decreased as the content of hydroxyl groups increased. In a subsequent paper, Chung *et al.*[43c] examined in more depth the reactivity and incorporation of this monomer, 5-hexenyl-(9-BBN), with several α-olefins such as propylene, 1-butene and 1-octene. It was found that propylene copolymerization had the least incorporation of borane (up to 5 mol %), octene the highest (62 mol %) and 1-butene is intermediate (15-37 mol %). This trend is what is expected for heterogeneous Ziegler/Natta polymerization, where the smaller the alkene, the higher the reactivity.[43c] However, as the α-olefin is lengthened, this trend becomes less evident. The copolymers poly(propylene-*co*-5-hexenyl-9-BBN) and poly(1-butene-*co*-5-hexenyl-9-BBN), which have incorporations less than 10 mol % of borane monomer, were insoluble in common organic solvents at room temperature. However, they were soluble at high temperatures. Interestingly, the poly(1-octene-*co*-5-hexenyl-(9-BBN)) was soluble in hydrocarbon solvents (e.g. heptanes) at room temperature regardless of percent composition.

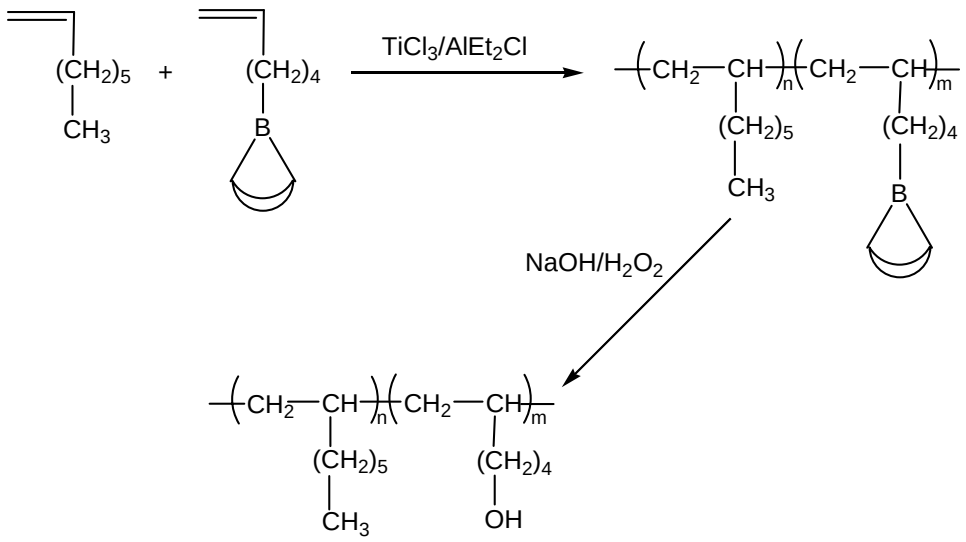

Scheme 26. Copolymerization with boron protecting groups.

A final example involves the copolymerization of borane protected monomers with α-olefins using homogeneous metallocene catalysts **I** and **II (**Figure 13). The advantages of using metallocene catalysts over the traditional heterogeneous Ziegler/Natta catalysts include excellent incorporation of higher α-olefins while maintaining relatively narrow molecular weights and composition distribution. In addition, better stereochemical control of the polymer microstructure is possible with metallocenes.[43d] The metallocene catalysts **I** (Cp_2ZrCl_2) and **II** ($Et(Ind)_2ZrCl_2$) were activated with MAO and the borane protected monomer 5-hexenyl-(9-BBN) was copolymerized with ethylene. Chung found that using the catalyst system $Et(Ind)_2ZrCl_2$/MAO gave the best incorporation of borane monomer, which was quantitative, under the conditions employed (45 psi ethylene, > 5000 equivalents of MAO, 30 ^oC) of up to 2.30 mol %.[43d] Interestingly, the catalyst activity actually increased when the amount of borane monomer was increased, which is not typically observed. The system Cp_2ZrCl_2/MAO gave lower incorporations (1.22 mol %) under similar conditions, but when the heterogeneous Ziegler/Natta catalysts

$TiCl_3/AlEt_2Cl$ were tested, no borane incorporation was detected in the copolymer. All copolymers were successfully converted to the hydroxyl copolymers via $NaOH/H_2O_2$ treatment at 40 ^oC for 3 hours.

1.6.4 Nitrogen Masking Agents

In the preceding sections, the masking agents of aluminum, silicon and boron alkyls were used to either protect the oxygen functionality (i.e. AlR_3, $-SiR_3$) or incorporate the functional group (i.e. BR_3) and which is converted upon work up to the hydroxyl functional group. In this section, examples of nitrogen alkyls (or silyl alkyl analogues) are given and shown to either homopolymerize or copolymerize with α-olefins in the presence of metallocene type catalysts.

Mülhaupt *et al*.[44] have successfully copolymerized ethylene with *N*,*N*-bis(trimethylsilyl)-1-amino-10-undecene, in the presence of the homogeneous catalyst system *rac*-$Me_2Si(2\text{-}MeBenz[e]Ind)_2ZrCl_2$ (**XVIII**) and MAO, to short chain branched linear low density polyethylene with pendent aminoalkyl groups after hydrolysis of the silylated amines (Scheme 27).

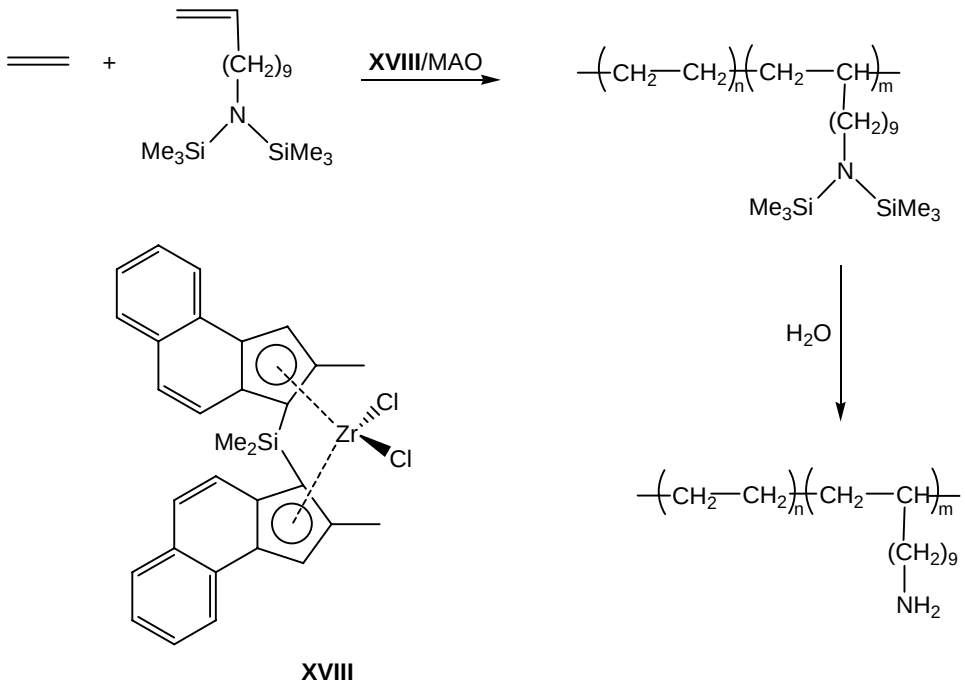

XVIII

Scheme 27. Nitrogen masked alkenes for copolymerization studies.

Characterization was done by ^{1}H NMR, IR, elemental analyses and DSC, and analysis showed that incorporations of up to 19 wt % (3.7 mol %) of the amine were obtained into the copolymer. It should be noted that Al:Zr concentrations were on the order of 16 000.

Waymouth *et al*.[45a] utilized a series of different symmetric zirconocene dimethyl precursors, L_nZrMe_2, (**XV**, **XVI**, **XVII**, Figure 13); and these precatalysts were activated with anilinium borate $[HNMe_2Ph][B(C_6F_5)_4]$ to polymerize a series of 5-amino-1-pentenes and a 4-amino-1-butene with different R groups on the nitrogen (R = methyl, ethyl, isopropyl and phenyl). It was found that the 5-(*N*,*N*-diisopropylamino)-1-pentene monomer showed the highest activity with the $[Cp^*_2ZrMe][B(C_6F_5)_4]$ catalyst system. Clearly, steric effects play an important role in preventing the nitrogen from binding to the metal center, as seen with a 70 fold decrease in activity when dimethyl groups are on the nitrogen atom.[45a] This $[Cp^*_2ZrMe][B(C_6F_5)_4]$ catalyst system was also found to be

four times more reactive than $Cp^*_2ZrCl_2$/MAO system and 180 times more than the heterogeneous $TiCl_3/Al(i\text{-}Bu)_3$ catalyst system. This result shows potential for ion pair utilization for functional monomer homo- and copolymerization studies. Also, it was reported that similar activities were obtained for 1-hexene polymerization with C_{2v}-symmetric $[Cp^*_2ZrMe][B(C_6F_5)_4]$ with respect to 5-(*N*,*N*-diisopropylamino)-1-pentene. However, when the C_2-symmetric *rac*-(ethylenebis(tetrahydroindenyl)$ZrMe_2$ was used, 1-hexene polymerization was 30 times more reactive than the aminopentene.[45a] Finally, a series of different polymer tacticities could be achieved with these amino monomers depending on the catalyst system used (e.g. syndiotactic poly(aminopentene) with a C_s-symmetric catalyst, or isotactic poly(aminopentene) with a C_2-symmetric catalyst).

Soon after the previous results, Waymouth *et al*.[45b] reported the copolymerization of 5-(*N*,*N*-diisopropylamino)-1-pentene with 1-hexene or 4-methyl-1-pentene using metallocene/borate system (Scheme 28).

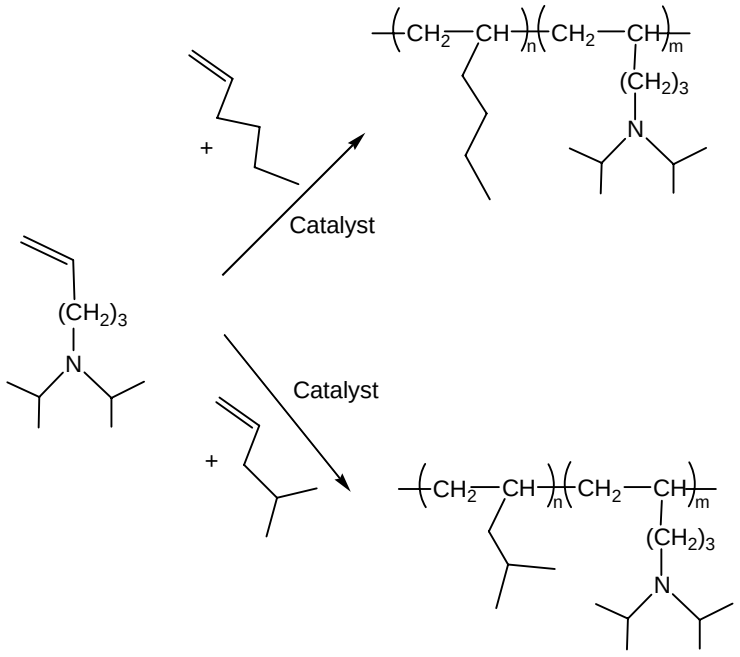

Scheme 28. Copolymerization of amino protected olefins with α-olefins.

The selected catalysts were [Cp^*_2ZrMe][$B(C_6F_5)_4$] and [*rac*-(ethylenebis(tetrahydroindenyl)ZrMe][$B(C_6F_5)_4$], due to their previous good performance with aminopentene monomers,[45a] and for the synthesis of functionalized atactic and isotactic polymeric materials. They found that direct copolymerization of these aminopentenes with monoalkenes using the homogeneous catalysts mentioned above is possible, giving up to 50 % conversion of amine into the copolymer with 1-hexene, and up to 17 % conversion with 4-methyl-1-pentene using [*rac*-(ethylenebis(tetrahydroindenyl)ZrMe][$B(C_6F_5)_4$] as catalyst. As for the catalyst [Cp^*_2ZrMe][$B(C_6F_5)_4$], only 4-methyl-1-pentene incorporation (up to 17 % conversion of amine) was reported.

A final example of the introduction of a nitrogen functionalized monomer into a polyolefin comes from Imuta *et al.*[46] They utilized a novel stereorigid, bulky zirconium catalyst (**XIV**, Figure 13) and a pretreated allyl amine (**XVIV**, Figure 14) with a trialkylaluminum (either TEA or TIBA), and copolymerized it with ethylene in the presence of MAO. It was confirmed by ^1H and ^{13}C NMR that allyl amine (**XX**, Figure 14) incorporations were low (0.22 to 0.57 mol %) under the reaction conditions, and most incorporations were located at the polyolefin chain ends.[46]

XVIV **XX**

Figure 14. Zirconium catalyst and monomers used for allyl amine-capped polyolefins.

1.7 Research Aims of Part 2 of this Thesis

The research aims of Part 2 of this thesis were to develop new polymeric materials via direct copolymerization (Scheme 29) of polar monomers with olefins (e.g. ethylene, propylene) utilizing protecting group strategy on the functional polar monomers (mainly oxygen containing monomers). The main catalyst systems employed were early metal (e.g. Zr, Ti) metallocene catalysts with different symmetries (e.g. C_2, C_{2v}), in order to obtain different polymer microstructures (i.e. isotactic, atactic polymer) to probe the possibility of improved properties such as adhesion, toughness, etc.

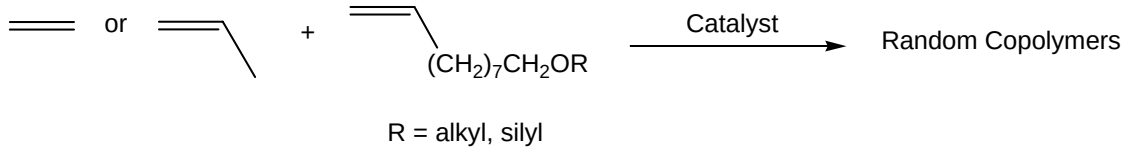

Scheme 29. General route employed to copolymer synthesis.

The general strategy introduced was developed after taking into consideration the problem of catalyst poisoning, with respect to early metals. Some important factors employed for this study include: a) separating the vinyl group from the functional heteratom (i.e. oxygen) with long methylene spacers increases the chance that the heteroatom will less likely interfere will insertion reactions, b) increasing the steric bulk around the heteratom to inhibit coordination to the active center, c) protecting the heteratom with electron-withdrawing groups or back-donating ability groups, thus decreasing the basicity of the heteratom and d) addition of a Lewis acid (e.g. AlR_3) to further complex the polar monomer and make it even less likely to coordinate to the

active center. Therefore, a series of ether monomers (CH_2=$CH(CH_2)_8OR$) were developed from the commercially available 9-decen-1-ol, each with varied degrees of steric bulk on the oxygen (R = Me, CH_2Ph, $CHPh_2$, CPh_3). In addition, silyl ethers of the long chain 9-decen-1-ol monomer (R = $SiMe_3$, $SiPh_3$) were prepared and were expected to be effective comonomers due to the ability of silicon to efficiently delocalize the π electrons on oxygen through π-bonding.[47] All of these synthesized vinyl and silyl ethers were copolymerized with ethylene or propylene under ambient conditions (1 atm, 25 ^oC, toluene) using dichlorozirconocene catalysts activated with MAO. The copolymers were characterized by ^1H and ^{13}C NMR, differential scanning calorimetry (DSC) and infrared spectroscopy. As a control, propylene-1-hexene copolymerizations were examined using the same catalyst system as above and compared to the polar monomer copolymerization results.

Furthermore, ^1H NMR monitoring reactions of the homopolymerization of these vinyl and silyl ethers were investigated with the zwitterionic compound $Cp_2ZrMe_2/B(C_6F_5)_3$ to probe the effectiveness of the protecting group on the ethers and their homopolymerizing behaviour.

Finally, inconsistent copolymerization results apparently arising from the effects of 'aging' MAO resulted in an investigation of how aging MAO affects polar monomer copolymerization studies with propylene.

REFERENCES FOR CHAPTER 1

1. See for example, (a) Hu, Y.; Dong, J-Y. *Coord. Chem. Rev.* **2006**, *250*, 47. (b) Miller, S. A.; Schwerdtfeger, E. D. *Polymer Preprints*, **2007**, *48(1)*, 187. (c) Michalak, A.; Ziegler, T. *J. Am. Chem. Soc.* **2001**, *123*, 12266. (d) Naga, N *J. Polym. Sci., Part A: Polym. Chem.* **2006**, *44*, 6083.
2. Odian, G. G. *Principles of Polymerization*, 4th ed.; Wiley-Interscience: Hoboken, N.J., 2004; pp 300-302.
3. Doak, K. W. *Encyclopedia of Polymer Science and Engineering*; Wiley-Interscience: New York, New York, 1986; vol. 6, pp 386-429.
4. Stevens, M. P. *Polymer Chemistry: An Introduction,* 3rd ed.; Oxford University Press Inc: New York, New York, 1999, p 181.
5. Odian, G. G. *Principles of Polymerization*, 4th ed.; Wiley-Interscience: Hoboken, N.J., 2004; p 641.
6. (a) Ittel, S. D.; Johnson, L. K.; Brookhart, M. *Chem. Rev*. **2000**, *100*, 1169. (b) Johnson, L. K.; Killian, C. M.; Brookhart, M. *J. Am. Chem. Soc.* **1995**, *117*, 6414. (c) Johnson, L. K.; Mecking, S.; Brookhart, M. *J. Am. Chem. Soc.* **1996**, *118*, 267. (d) Mecking, S.; Johnson, L. K.; Wang, L.; Brookhart, M. *J. Am. Chem. Soc.* **1998**, *120*, 888.
7. Yanjarappa, M. J.; Sivaram, S. *Prog. Poly. Sci.* **2002**, *27*, 1347.
8. (a) Bochmann, M. *J. Chem. Soc., Dalton Trans*. **1996**, 255. (b) Kaminsky, W.; Arndt, M. *Adv. Polym. Sci*. **1997**, *127*, 143. (c) Chien J. C. W. In *Topics in Catalysis*; Marks, T. J; Stevens, J. C. Eds., J.C. Baltzer AG, Science Publishers,

1999; vol. 7, p 125. (d) Alt, H. G.; Köppl, A. *Chem. Rev*. **2000**, *100*, 1205. (e) Chen, E. Y-X.; Marks, T. J. *Chem. Rev*. **2000**, *100*, 1391.

9. (a) Odian, G. G. *Principles of Polymerization*, 4th ed.; Wiley-Interscience: Hoboken, N.J., 2004, Chapters 3 and 5. (b) Matyjaszewski, K. editor, *Advances in Controlled/living Radical Polymerization*, ACS Symposium Series 854, American Chemical Society, Washington, DC, 2003. (c) Matyjaszewski, K.; Davis, T. P. editors, *Handbook of Radical Polymerization*, Wiley-Interscience, Hoboken, N.J.: 2002. (d) Quirk, R. P., editor, *Applications of Anionic Polymerization Research*, ACS Symposium Series 696, American Chemical Society, Washington, DC, 1998.
10. (a) Boffa, L. S.; Novak, B. M. *Chem. Rev*. **2000**, *100*, 1479. (b) Gibson, V. C.; Spitzmesser, S. K. *Chem. Rev*. **2003**, *103*, 283. (c) Chung, T. C. M., *Functionalization of Polyolefins*; Academic Press: San Diego, 2002.
11. (a) Odian, G. G. *Principles of Polymerization*, 4th ed.; Wiley-Interscience: Hoboken, N.J., 2004, p 326. (b) Stevens, M. P. *Polymer Chemistry: An Introduction*, 3rd ed.; Oxford University Press Inc.: New York, New York, 1999, pp 169-186.
12. (a) Ziegler, K. *Angew. Chem.* **1964**, *76*, 545. (b) Ziegler, K., Hollzkamp, E., Breil, H., Martin, H. *Angew. Chem.* **1955**, *67*, 426, 541.
13. Natta, G.; Pasquon, I.; Zambelli, A. *J. Am. Chem. Soc.* **1962**, *84*, 1488.
14. (a) Breslow, D. S.; Newburg, N. R. *J. Am. Chem. Soc.* **1957**, *79*, 5072. (b) Natta, G.; Pino, P.; Mazzanti, U.; Giannini, E.; Mantica, E.; Peraldo, E. *J. Polym. Sci.*, **1957**, *26*, 120.

15. Sinn, H.; Kaminsky, W. *Adv. Organomet. Chem.* **1980**, *18*, 99.

16. For example, see (a) Ewen, J. A.; Jones, R. L.; Razavi, A. Ferrara, J. D. *J. Am. Chem. Soc.* **1988**, *110*, 6255.

17. Barron, A. R. *J. Am. Chem. Soc.* **1993**, *115*, 4971.

18. Yang, X.; Stern, C. L.; Marks, T. J. *J. Am. Chem. Soc.* **1994**, *116*, 10015.

19. (a) Ewen, J. A.; Elder, M. J. Eur. Patent Appl. 426,638, **1991**; (b) U. S. Pat. 5,561,092, **1996**.

20. (a) Chen, Y.-X.; Yang, S.; Stern, C. L.; Marks, T. J. *J. Am. Chem. Soc.* **1996**, *118*, 12451. (b) Li, L.; Stern, C. L.; Marks, T. J. *Organometallics* **2000**, *19*, 3332. (c) Li, L.; Marks, T. J. *Organometallics* **1998**, *17*, 3996.

21. Chien, J. C.; Tsai, W.-M.; Rausch, M. D. *J. Am. Chem. Soc.* **1991**, *113*, 8570.

22. Jia, L.; Yang, X.; Ishihara, A.; Marks, T. J. *Organometallics*, **1995**, *14*, 3135.

23. Jia, L.; Yang, X.; Stern, C. L.; *Organometallics*, **1997**, *16*, 842.

24. Bavarian, N.; Baird, M. C., *Organometallics*, **2005**, *24*, 2889.

25. Resconi, L.; Camurati, I.; Sudmeijer, O. *Top. Catal.*, **1999**, *7*, 145.

26. For example, (a) Pino, P.; Cioni, P.; Wei., J *J. Am. Chem. Soc.* **1987**, *109*, 6189. (b) Busico, V.; Cipullo, R.; Chadwick, J. C.; Modder, J. F.; Sudmeijer, O. *Macromolecules* **1994**, *27*, 7538. (c) Carvill, A.; Tritto, I.; Locatelli, P.; Sacchi, M. C. *Macromolecules* **1997**, *30*, 7056.

27. (a) Hajela, S.; Bercaw, J. E. *Organometallics*, **1994**, *13*, 1147. (b) Guo, Z.; Swenson, D.; Jordan, R. F. *Organometallics*, **1994**, *13*, 1424. (c) Eshius, J.; Tan, Y.; Teuan, J. H.; Renkema, J. *J. Mol. Catal.* **1990**, *62*, 277.

28. (a) Ono, H.; Hisatani, K.; Kamide, K. *Polymer J.,* **1993**, ***25***, 245. (b) Odian, G. G. *Principles of Polymerization*, 4th ed.; Wiley-Interscience: Hoboken, N.J., 2004; p 751.

29. Kemperman, Th.; Koch, S.; Sumner, J., editors, *Manual for the Rubber Industry*, 2nd ed.; Bayer AG, Leverkusen, 1993.

30. (a) Deubel, D. V.; Ziegler, T. *Organometallics* **2002**, *21*, 1603. (b) Deubel, D. V.; Ziegler, T. *Organometallics* **2002**, *21*, 4432. (c) Ziegler, T., private communication.

31. Kharasch, M. S.; Seyler, R. C.; Mayo, F. R. *J. Am. Chem. Soc.* **1938**, *60*, 882.

32. Foley, S. R.; Stockland, R. A.; Shen, H.; Jordan, R. F. *J. Am. Chem. Soc*. **2003**, *125*, 4350.

33. These bond strengths were calculated using thermodynamic data available at http:webbook.nist.gov/chemistry. We thank Prof. J. A. Stone for informing us of this source.

34. (a) Wu, F.; Foley, S. R.; Burns, C. T.; Jordan, R. F. *J. Am. Chem. Soc.* **2005**, *127*, 1841. (b) Groux, L. F.; Weiss, T.; Reddy, D. N.; Chase, P. A.; Piers, W. E.; Ziegler, T.; Parvez, M.; Benet-Bucholz, J. *J. Am. Chem. Soc.* **2005**, *127*, 1854.

35. Stevens, M. P. *Polymer Chemistry: An Introduction,* 3rd ed.; Oxford University Press Inc.: New York, New York, 1999; pp 7-8.

36. See for example, Matyjaszewski, K. *Cationic Polymerizations: mechanisms, synthesis and applications.* Marcel Dekker, Inc.: New York, 1996.

37. See, for instance, (a) Lehmus, P.; Harkki, O.; Leino, R.; Luttikhedde, H. J. G.; Nasman, J. H.; Seppala, J. V. *Macromol. Chem. Phys.* **1998**, *199*, 1965. (b) Auer, M.; Nicolas, R.; Vesterinen, A.; Luttikhedde, H.; Wilen, C.-E. *J. Polym. Sci., Part A: Polym. Chem.* **2004**, *42*, 1350. (c) Kokko, E.; Lehmus, P.; Leino, R.; Luttikhedde, H. J. G.; Ekholm, P.; Naesman, J. H.; Seppaelae, J. V. *Macromolecules*, **2000**, *33*, 9200. (d) Simanke, A. G.; Galland, G. B.; Freitas, L. L.; Da Jornada, J. A. H.; Quijada, R.; Mauler, R. S. *Macromol. Chem. Phys*. **2001**, *202*, 172.

38. See, for instance, (a) Arnold, M.; Henschke, O.; Knorr, J. *Macromol. Chem. Phys*. **1996**, *197*, 563. (b) Arnold, M.; Bornemann, S.; Köller, F.; Menke, T. J.; Kressler, J. *Macromol. Chem. Phys*. **1998**, *199*, 2647. (c) Arnold, M.; Bornemann, S.; Schade, B.; Henschke, O. *Kautschuk Gummi Kunststoffe* **2001**, *54*, 300. (d) Quijada, R.; Guevara, J. L.; Galland, G. B.; Rabagliati, F. M.; Lopez-Majada, J. M. *Polymer*, **2005**, *46*, 1567.

39. (a) Aaltonen, P.; Löfgren, B. *Macromolecules* **1995**, *28*, 5357. (b) Aaltonen, P.; Fink, G.; Löfgren, B.; Seppälä, J. *Macromolecules* **1996**, *29*, 5255. (c) Aaltonen, P.; Löfgren, B. *Eur. Polym. J*. **1997**, *33*, 1187. (d) Hakala, K.; Lofgren, B.; Helaja, T. *Eur. Polym. J.* **1998**, *34(8)*, 1093. (e) Ahjopalo, L.; Löfgren, B.; Hakala, K.; Pietilä, L.-O. *Eur. Polym. J.* **1999**, *35*, 1519. (f) Helaja, T.; Hakala, K.; Helaja, J.; Löfgren, B. *J. Organometal. Chem*. **1999**, *579*, 164. (g) Hakala, K.; Helaja, T.; Löfgren, B. *J. Polym. Sci., Part A: Polym. Chem*. **2000**, *38*, 1966. (h) Paavola, S.; Uotila, R.; Löfgren, B.; Seppala, J. V. *React. Funct. Polym.* **2004**, *61*, 53. (i) Paavola, S.; Löfgren, B.; Seppaela, J. V. *Eur. Poly. J.* **2005**, *41*, 2861. (j) Anttila,

U.; Hakala, K.; Helaja, T.; Lofgren, B.; Seppala, J. *J. Polym. Sci., Part A: Polym. Chem*. **1999**, *37*, 3099.

40. (a) Wilén, C.-E.; Näsman, J. H. *Macromolecules* **1994**, *27*, 4051. (b) Wilén, C.-E.; Luttikhedde, H.; Hjertberg, T.; Näsman, J. H. *Macromolecules* **1996**, *29*, 8569. (c) Jiang, G. J.; Chiu, H.-W. *Polymer Preprints* **1998**, *39*, 318. (d) Hwu, J. M.; Jiang, G. J. *Polymer Preprints* **1999**, *40*, 177. (e) Marques, M. M.; Correia, S. G.; Ascenso, J. R.; Ribeiro, A. F. G.; Gomes, P. T.; Dias, A. R.; Foster, P.; Rausch, M. D.; Chien, J. C. W. *J. Polym. Sci. Part A: Polym. Chem*. **1999**, *37*, 2457. (f) Hagihara, H.; Murata, M.; Uozumi, T. *Macromol. Rapid Comm*. **2001**, *22*, 353. (g) Imuta, J.-I.; Toda, Y.; Kashiwa, N. *Chem. Lett*. **2001**, 710. (h) Kaya, A.; Jakisch, L.; Komber, H.; Voigt, D.; Pionteck, J.; Voit, B.; Schulze, U. *Macromol. Rapid Comm*. **2001**, *22*, 972. (i) Wendt, R. A.; Fink, G. *Macromol. Chem. Phys*. **2002**, *203*, 1071. (j) Imuta, J.; Kashiwa, N.; Toda, Y. *J. Am. Chem. Soc*. **2002**, *124*, 1176. (k) Hagihara, H.; Tsuchihara, K.; Takeuchi, K.; Murata, M.; Ozaki, H.; Shiono, T.. *J. Polym. Sci., Part A: Polym. Chem.* **2004**, *42*, 52. (l) Kashiwa, N.; Matsugi, T.; Kojoh, S.; Kaneko, H.; Kawahara, N.; Matsuo, S.; Nobori, T.; Imuta, J. *J. Polym. Sci., Part A: Polym. Chem.* **2003**, *41*, 3657. (m) Hagihara, H.; Tsuchihara, K.; Sugiyama, J.; Takeuchi, K.; Shiono, T. *J. Polym. Sci., Part A: Polym. Chem.* **2004**, *42*, 5600. (n) Hagihara, H.; Tsuchihara, K.; Sugiyama, J.; Takeuchi, K.; Shiono, T. *Macromolecules* **2004**, *37*, 5145. (o) Hippi, U.; Korhonen, M.; Paavola, S.; Seppaelae, J. *Macromol. Mat. Eng.* **2004**, *289*, 714. (p) Zhang, X.; Chen, S.; Li, H.; Zhang, Z.; Lu, Y.; Wu, C.; Hu, Y. *J. Polym. Sci.: Part A: Polym. Chem.*, **2005**, *43*, 5944. (q) Kawahara, N.; Kojoh, S.; Matsuo, S.;

Kaneko, H.; Matsugi, T.; Kashiwa, N. *J. Mol. Catal. A: Chem.* **2005**, *241*, 156. (r) Jiang, G. J.; Hwu, J. M. Book of Abstracts, 218th ACS National Meeting, New Orleans, Aug. 22-26 1999, POLY-448. (s) Jiang, G. J.; Chiu, H.-W. Book of Abstracts, 215th ACS National Meeting, Dallas, March 29-April 2 (1998), POLY-073. (t) Ferreira, M. L.; Belelli, P. G.; Damiani, D. E. *Macromol. Chem. Phys*. **2001**, *202*, 830. (u) Wendt, R. A.; Angermund, K.; Jensen, V.; Thiel, W.; Fink, G. *Macromol. Chem. Phys*. **2004**, *205*, 308.

41. (a) Giannini, U.; Brückner, G.; Pellino, E.; Cassata, A. *J. Polym. Sci. Polym. Let. Ed*. **1967**, *5*, 527. (b) , U.; Brückner, G.; Pellino, E.; Cassata, A.. *J. Polym. Sci., Polym. Symp*. **1968**, 157. (c) Kesti, M. R.; Coates, G. W.; Waymouth, R. M. *J. Am. Chem. Soc*. **1992**, *114*, 9679. (d) Goretzki, R.; Fink, G. *Macromol. Rapid Comm*. **1998**, *19*, 511. (e) Goretzki, R.; Fink, G. *Macromol. Chem. Phys*. **1999**, *200*, 881. (f) Sivak, A. J.; Cullo, L. A. Ziegler-Natta polymerization of siloxy group-containing alkenes in preparation of polymers containing functional groups. PCT Int. Appl. **1988**, 59 pp. CODEN: PIXXD2 WO 8808856 A1 19881117. (g) Sivak, A. J.; Cullo, L.A. Alkene-alkenylsilane copolymers with high stereoregularity. (Aristech Chemical Corp., USA). Eur. Pat. Appl. (1990), 38 pp. CODEN: EPXXDW EP 363990 A2 19900418.
42. Rajesh Kumar K, Sivaram S. Unpublished results (see reference 7).
43. (a) Chung, T. C. *Macromolecules*, **1988**, *21*, 865. (b) Ramakrishnan, S.; Berluche, E.; Chung, T. C. *Macromolecules*, **1990**, *23*, 378. (c) Rhubright, D.; Chung, T. C. *Macromolecules*, **1993**, *26*, 3019. (d) Lu, H.L.; Chung, T. C. *Journal of Molecular Catalysis A: Chemical*, **1997**, *115*, 115.

44. Schineider, M. J.; Schafer, R.; Mulhaupt, R. *Polymer*, **1997**, *38*, 2455.

45. (a) Stehling, U. M.; Stein, K. M; Kesti, M. R.; Waymouth, R. M. *Macromolecules*, **1998**, *31*, 2019. (b) Stehling, U. M.; Stein, K. M; Fisher, D.; Waymouth, R. M. *Macromolecules*, **1998**, *32*, 14.

46. Imuta, J.; Toda, Y.; Matsugi, T.; Kaneko, H.; Matsuo, S.; Kojoh, S.; Kashiwa, N. *Chem. Let.*, **2003**, *32*, 656.

47. (a) Bassindale, A. R.; Taylor, P. G. *The Chemistry of Organic Silicon Compounds*, *Editors:* Patai, S.; Rappoport, Z. Wiley; Chichester, UK, 1989, *Chap. 12*, 809. (b) Brook, M. A. *Silicon in Organic, Organometallic, and Polymer Chemistry,* Wiley and Sons: New York, 2000, pp 31-34, 201-203.

CHAPTER 2

EXPERIMENTAL

2.1.1 Chemical Supplies

All research chemicals were purchased from Aldrich unless stated otherwise. All deuterated NMR solvents were purchased from Cambridge Isotope Laboratories Inc.

2.1.1.1 Part 1: Diimine-Palladium(II)-Acrylonitrile Insertion Studies

$PdCl_2$ was obtained on loan from Johnson Matthey. Sodium tetrakis-(3,5-bistrifluoromethylphenyl)borate $[Na][BAr^f_4]$ (where Ar^f = 3,5-$(CF_3)_2C_6H_3$) was purchased from Boulder Scientific Chemicals. Acrylonitrile (AN) was purified of moisture and inhibitor by stirring over CaH_2 for a day; it was then vacuum distilled into a Schlenk tube and stored in a refrigerator (3 ^oC). Diimine ligand[1] ArN=C(Me)C(Me)=NAr (Ar = 2,6-$C_6H_3(C_3H_7)_2$) designated as (N-N), $CODPdCl_2$ (COD = 1,5-cyclooctadiene)[2] and $(N\text{-}N)PdMe_2$,[3] were synthesized via standard literature procedures.

2.1.1.2 Part 2: Polar Monomer Homo- and Copolymerization Studies

The catalysts Cp_2ZrCl_2, Ind_2ZrCl_2 and *rac*-$Et(Ind)_2ZrCl_2$, (Cp = C_5H_5, Ind = C_9H_7, Et = C_2H_4) were used as received from Aldrich. Cp_2ZrMe_2[4] and *rac*-$Et(Ind)_2ZrMe_2$[5] were synthesized as in the literature. 9-Decen-1-ol (98 % Alfa Aesar), $SiHPh_3$, $NH(Me_3Si)_2$ and benzyl chloride were degassed and dried over 4 Å molecular sieves prior to use. NaH, CH_3I, $CHPh_2Br$, $LiClO_4$ and CPh_3Cl were used as received.

Aluminum oxide, basic, 150 mesh, 58 Å was dried under vacuum overnight and stored in the glovebox. Tris(pentafluoro)borane ($B(C_6F_5)_3$) was synthesized according to the literature.[6] Ethylene (Grade 3.0) and propylene (Grade 2.5, 99.5%) were supplied by Praxair and were further dried by passing through a column of activated 4 Å molecular sieves. 1-Hexene was stirred over calcium hydride overnight, vacuum distilled and stored over 4 Å molecular sieves in the glovebox. The methylaluminoxane (MAO) used was either Aldrich (10 wt % in toluene) or Akzo Nobel (6.9 wt % in toluene) and each was used as received or modified as stated. *Caution: MAO is pyrophoric and must be carefully handled under an inert atmosphere.*

2.1.2 Physical and Analytical Methods

All reactions were carried out under purified argon using standard Schlenk line techniques. The purchased deoxygenated solvents toluene, ethyl ether, hexanes, dichloromethane and tetrahydrofuran were dried by passing through a dried alumina column. For THF, ethyl ether and CH_2Cl_2 further drying was done by storing over activated 4Å molecular sieves. Toluene-d_8 and benzene-d_6 were dried over sodium/benzophenone, CD_2Cl_2 over calcium hydride, and $CDCl_3$ and DMSO-d_6 over 4Å molecular sieves. 1,1,2,2-tetrachloroethane-d_2, chlorobenzene-d_6 and *o*-dichlorobenzene were used as received.

^1H, $^{13}C\{^1H\}$ and COSY NMR spectra were run on Bruker AV300, -400, -500 or -600 spectrometers, chemical shifts being referenced to the residual proton signals of the deuterated solvents. All samples were prepared in 5 mm diameter tubes with approximately 0.4 mL of the selected deuterated solvent. The samples run at ambient

temperatures were those in $CDCl_3$, CD_2Cl_2, benzene-d_6 or toluene-d_8. High temperature NMR spectra were run in either 1,1,2,2-tetrachloroethane-d_2 (TCE-d_2) at 120 ^oC, chlorobenzene-d_5 at 120 ^oC or a mixture of *o*-dichlorobenzene/C_6D_6 (95/5 v/v) at 80 ^oC. High temperature ^{13}C NMR for the copolymers synthesized were run using 7000-10000 scans, a flipping angle of 74^o and an acquisition time of 1.5 seconds.

Electrospray mass spectrometry (ESMS) experiments were run in positive and negative ion modes on Quattro VG and Applied Biosystems/MDS Sciex QSTAR XL instruments at a cone voltage typically of 20 V; nitrogen was used as the nebulizing gas, CH_2Cl_2 as the carrier solvent. The ions were in all cases complex multiplets, and the m/e values quoted below are for the strongest line in each multiplet. Elemental analyses were carried out by Canadian Microanalytical Services of Delta, B.C., and molecular mechanics calculations were carried out by Dr. Michael Baird using PCModel version 8.0.

Temperature readings for selected polymerizations were monitored using a SPER Scientific 800005/Advanced Thermometer W/RS232 thermocouple. The resolution is 0.1 ^oC.

Differential scanning calorimetry (DSC) was run on a Perkin Elmer DSC 7 (TAC 7/DX). DSC aluminum pans were charged with 2-7 mg of polymer and were ramped at a rate of 5.00 or 10.00 ^oC/min; starting at a temperature range of 30 ^oC and ramping up to 250 ^oC. Three ramping cycles were done for each sample. Typically, the second cycle was chosen for analysis.

IR analysis was done on a Perkin Elmer Spectrum One FT-IR spectrometer at a spectral resolution of 4 cm^{-1}. Samples were prepared by dissolving the copolymer in the

appropriate solvent and depositing the copolymer on one KBr plate. Slow evaporation of the solvent left a thin film that was analyzed.

2.2 Part 1: Syntheses for Diimine-Palladium(II)-Acrylonitrile Insertion Studies

2.2.1 Synthesis of Oxonium Acid $[H(Et_2O)_2][BAr^f_4]$ (Ar^f = 3,5-$(CF_3)_2C_6H_3$)

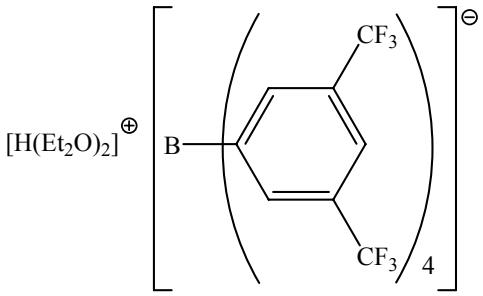

This compound was synthesized as in the literature with slight modifications.[7] 1.0 g of sodium tetrakis(3,5-bistrifluoromethylphenyl)borate (1.1 mmol) was added to 25 mL of ethyl ether in a 100 ml Schlenk flask that was pre-charged with activated 4 Å molecular sieves. This solution was allowed to stir for several hours. Next, this solution was transferred to a new Schlenk flask, via syringe, and cooled to 0 ^oC. Excess HCl (1.1 mL of a 2.0 M in ethyl ether) was added to another Schlenk flask, and diluted further with 15 mL of ethyl ether and cooled to 0 ^oC. The salt solution was then added to the HCl solution dropwise and the solution was left to stir for 30 min at 0 ^oC. The stirring was halted and the solution was left to stand to allow the NaCl to settle. The clear solution was decanted and concentrated *in vacuo* to approximately 10 mL. The solution was then cooled to -78 ^oC, hexanes (10 mL) were added to induce further precipitation and then the

supernatant was removed. The remaining white solid was dried and stored in the glovebox freezer at -30 ^{o}C. Yield: 0.750 g (80 %). ^{1}H NMR (300 MHz, CD_2Cl_2) δ 11.0 (v br. 1H, Et_2OH), 7.72 (br, 8H, *o*-H), 7.57 (br, 4H, *p*-H), 3.94 (br, 8H, CH_2), 1.37 (t, 12H, CH_3). Lit[7]: (CD_2Cl_2) δ 11.1 (v br. 1H, Et_2OH), 7.70 (br, 8H, *o*-H), 7.55 (br, 4H, *p*-H), 3.85 (br, 8H, CH_2), 1.32 (t, 12H, CH_3).

2.2.2 Synthesis of [(N-N)PdMe(OEt$_2$)][BAr$^f_4$] (Ar^f = 3,5-(CF$_3$)$_2$C$_6$H$_3$) (1)

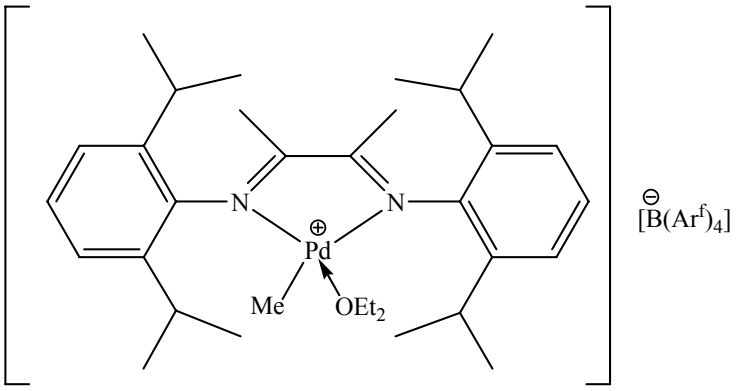

The compound [Pd(N–N)Me(OEt$_2$)][BAr$^f_4$] was prepared as in the literature.[3] Solid (N-N)PdMe$_2$ (100 mg, 0.185 mmol) and [H(Et$_2$O)$_2$][BAr$_4$] (187 mg, 0.185 mmol) were charged into a 100 mL Schlenk flask in the glovebox. Next, the flask was taken out of the glovebox and cooled to -78 ^{o}C, under argon. Pre-cooled ethyl ether (15 mL) was added to the flask and the mixture was stirred for 15 min at -78 ^{o}C. The mixture was allowed to warm to r.t. briefly (15 min) and then the solvent was removed *in vacuo* to yield an orange powder **1** (165 mg, 62 %) which was stored in the glovebox freezer at -30 ^{o}C. ^{1}H NMR (500 MHz, CD_2Cl_2, -60 ^{o}C) δ 7.70 (s, 8H, *o*-H), 7.58 (s, 4H, *p*-H), 7.47 – 7.10 (m, 6H, aryl H), 3.20 (q, 4H, O(CH_2CH_3)$_2$), 2.88 (septet, 2H, *CH*Me$_2$), 2.82 (septet, 2H, *C'H*Me$_2$), 2.19 and 2.16 (N=C(*Me*)-C'(*Me*)=N), 1.35, 1.30, 1.16 and 1.15 (d, 6H

each, J = 6.4 – 6.8 CH*Me*Me, C'HMe*Me*), 1.08 (t, 3H, J = 6.9 Hz, O(CH_2CH_3)$_2$), 0.34 (s, 3H, Pd*Me*). Lit[3]: (400 MHz, CD_2Cl_2, -60 ^oC) δ 7.71 (s, 8H, *o*-H), 7.58 (s, 4H, *p*-H), 7.4 – 7.0 (m, 6H, aryl H), 3.18 (q, 4H, J = 7.1 Hz, O(CH_2CH_3)$_2$), 2.86 (septet, 2H, J = 6.65 Hz, *CH*Me$_2$), 2.80 (septet, 2H, J = 6.55 Hz, *C'H*Me$_2$), 2.18 and 2.15 (N=C(*Me*)-C'(*Me*)=N), 1.34, 1.29, 1.14 and 1.13 (d, 6H each, J = 6.4 – 6.7 Hz, CH*Me*Me, C'HMe*Me*), 1.06 (t, 3H, J = 6.9 Hz, O(CH_2CH_3)$_2$), 0.33 (s, 3 H, Pd*Me*).

2.2.3 Synthesis of Cationic Nitrile Complex [(N-N)PdMeAN][BAr$^f_4$] (2)

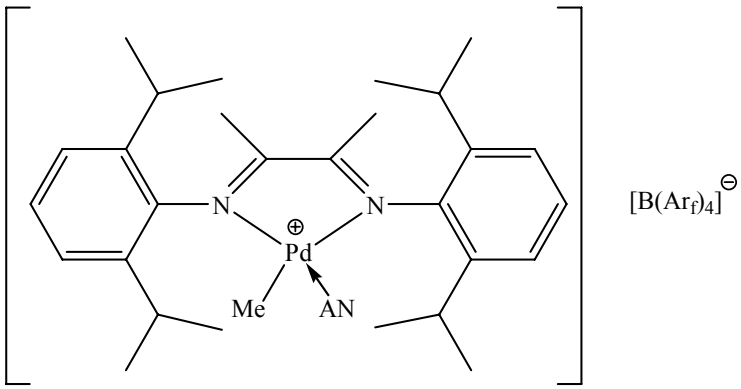

An orange solution of 200 mg of [Pd(N–N)Me(OEt$_2$)][BAr$^f_4$] (0.137 mmol) in 2 mL AN was stirred under argon for 2 hours. The AN was then removed under reduced pressure, and the resulting oil was washed with hexanes and dried overnight under vacuum to give a yellow solid. Yield: 177 mg, 90 %. ^{1}H NMR (CD_2Cl_2, 298K) δ 7.74 (s, 8H, BAr$^f_4$ H$_o$), 7.58 (s, 4H, BAr$^f_4$ H$_p$), 7.43 (m, 2H, H$_{aryl}$), 7.37 (m, 4H, H$_{aryl}$), 6.21 (d, 1H, ^3J(HH) = 12 Hz, CH*H*CHCN), 5.85 (d, 1H, ^3J(HH) = 18 Hz, C*H*HCHCN), 5.45 (dd, 1H, ^3J(HH) = 12, 18 Hz, CH$_2$C*H*CN), 2.92 (m, 4H, C*H*Me$_2$), 2.26 (s, 3H, N=CCH_3), 2.24

(s, 3H, N=CCH_3), 1.38 and 1.26 (m, 12H each, CHCH_3C'H_3), 0.58 (s, 3H, PdCH_3). Anal. Calcd for $C_{64}H_{58}BF_{24}N_3Pd$: C, 53.29; H, 4.05; N, 2.91. Found C, 53.21; H, 4.07; N, 2.80.

2.2.4 Reactions of [(N-N)PdMeAN][BAr^f_4] (2) with Acrylonitrile

In a typical reaction, 35-45 mg of **2** were dissolved in 1 mL of AN and the solution was stirred under argon (a) at room temperature for 12 h, (b) at 50 ºC for 2 h, or (c) at reflux (77 ºC) for 12 h. As polyacrylonitrile was formed in (c), a blank run, in the absence of **2**, was also run. In all cases, the AN was then removed under reduced pressure and the resulting oily materials were washed with hexanes, dried overnight under vacuum and characterized by ^{1}H NMR spectroscopy and ESMS.

2.3 Part 2: Copolymerization Studies of Olefins with Polar Monomers

2.3.1 Synthesis of 10-Methoxy-dec-1-ene (A)

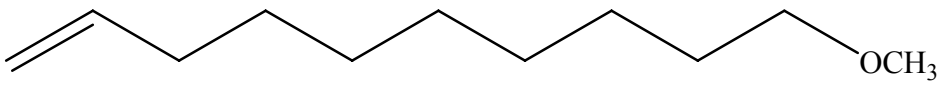

This monomer was synthesized according to the literature with modifications.[8] To a mixture of NaH (3.38 g, 0.14 mol, 1.1 equiv) in 250 mL dry THF was added 9-decenol (20.00 g, 0.128 mol, 1.0 equiv) dropwise at 0 ^{o}C. After stirring 2 hours at room temperature, methyl iodide (18.17 g, 0.128 mol, 1.0 equiv) was added at 0 ^{o}C. This solution was allowed to stir overnight. The solvent was then removed *in vacuo* and 100 mL of dry hexanes were added. This mixture was then filtered through a medium Schlenk

frit to remove NaI. The resulting hexane solution with product was purified by passing through a 5-6 cm column of activated alumina and pumped down *in vacuo* to obtain a colourless liquid (13.7 g, 63%). ^{1}H NMR (400 MHz, $CDCl_3$) δ: 5.82 (dddd, $J_1 = J_2 = 6.7$, $J_3 = 10.0$, $J_4 = 17.0$ Hz, 1H), 4.99 ($J_1 = J_2 = 1.5$, $J_3 = 10.3$, $J_4 = 17.0$ Hz , 1H), 4.93 ($J_1 = J_2 = 1.3$, $J_3 = 2.2$, $J_4 = 10.0$ Hz, 1H), 3.37 (t, $J = 6.8$ Hz, 2H), 3.34 (s, 3H), 2.04 (m, 2H), 1.56 (m, 2H), 1.32 (m, 10H). ^{13}C NMR (100 MHz, $CDCl_3$) δ: 139.0, 114.2, 73.0, 58.5, 33.9, 29.8, 29.5, 29.2, 29.2 (overlapping), 29.0, 26.2. Lit[8]: ^{1}H NMR (500 MHz, $CDCl_3$) δ: 5.81 (dddd, $J_1 = J_2 = 6.7$, $J_3 = 10.4$, $J_4 = 17.1$ Hz, 1H), 4.99 ($J_1 = J_2 = 1.6$, $J_3 = 2.2$, $J_4 = 17.1$ Hz, 1H), 4.93 ($J_1 = J_2 = 1.3$, $J_3 = 2.2$, $J_4 = 10.2$ Hz , 1H), 3.36 (t, $J = 6.4$ Hz, 2H), 3.33 (s, 3H), 2.03 (m, 2H), 1.57 (m, 2H), 1.30 (m, 10H). ^{13}C NMR (125 MHz, $CDCl_3$) δ: 140.3, 114.6, 73.4, 61.0, 34.4, 30.1, 29.9, 29.8, 29.5, 29.3, 26.6.

2.3.2 Synthesis of 10-Benzyloxy-dec-1-ene (B)

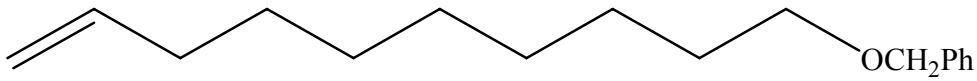

This monomer was synthesized according to the literature with modifications.[9a] To a mixture of NaH (0.767 g, 0.032 mol, 1.0 equiv) in 150 mL dry THF was added 9-decenol (5.00 g, 0.032 mol, 1.0 equiv) dropwise at room temperature. After stirring 2 hours at room temperature, benzyl chloride (4.05 g, 0.032 mol, 1.0 equiv) was added at room temperature and the resulting mixture was reflux for 16 h. After cooling down to room temperature, the solvent was removed *in vacuo* and 100 mL of dry hexanes were

added. This mixture was then filtered through a medium Schlenk frit to remove NaCl. The resulting hexane solution with product was purified by passing through a 5-6 cm column of activated alumina and reduced *in vacuo* to obtain a colourless liquid (1.5 g, 20%). ^{1}H NMR (400 MHz, $CDCl_3$) δ: 7.40-7.22 (m, 5H), 5.83 (dddd, $J_1 = J_2 = 7$, $J_3 = 11$, $J_4 = 17$ Hz, 1H), 5.01 ($J = 17$ Hz, 1H), 4.94 ($J = 10$ Hz, 1H), 4.52 (s, 2H), 3.48 (t, $J = 7$ Hz, 2H), 2.05 (m, 2H), 1.63 (m, 2H), 1.35 (m, 10H). ^{13}C NMR (100 MHz, $CDCl_3$) δ: 139.4, 139.0, 128.6, 127.8, 127.7, 114.3, 73.1, 70.7, 34.0, 30.0, 29.6, 29.3, 29.1, 26.4. Lit: ^{1}H NMR (300 MHz, $CDCl_3$)[9b] δ: 7.40-7.18 (s, 5H, Ar), 5.80 (1H, m, vinyl), 4.92 (2H, m, vinyl), 4.48 (2H, s, benzyl), 3.45 (2H, t, OCH_2), 2.03 (2H, m), 1.61 (2H, m), 1.35(2H, m). ^{13}C NMR (75 MHz, $CDCl_3$)[9a] δ: 139.1, 138.8, 128.3, 127.6, 127.5, 114.2, 72.9, 70.5, 33.9, 29.8, 29.4, 29.1, 28.9, 26.2.

2.3.3 Synthesis of 10-Trityloxy-dec-1-ene (C)

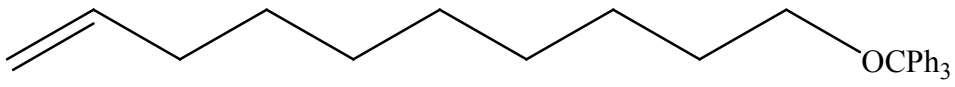

Referring to the preparation of **B**, we found that CPh_3Cl (5.58 g, 0.020 mol, 1.0 equiv) affords **C** as a colourless oil (3.19 g, 40%). ^{1}H NMR (500 MHz, $CDCl_3$) δ: 7.48 (m, 2H), 7.32 (m, 2H), 7.25 (m, 1H), 5.84 (dddd, $J_1 = J_2 = 8$, $J_3 = 11$, $J_4 = 18$ Hz, 1H), 5.02 ($J = 20$ Hz, 1H), 4.96 ($J = 14$ Hz, 1H), 3.08 (t, $J = 7$ Hz, 2H), 2.06 (m, 2H), 1.65 (m, 2H), 1.34 (m, 10H). ^{13}C NMR (125 MHz, $CDCl_3$) 145.0, 139.6, 129.1, 128.2, 127.2, 114.5, 86.7, 64.1, 34.2, 30.4, 29.9, 29.8, 29.5, 29.3, 26.7. Anal. Calcd for $C_{29}H_{34}O$: C, 87.39; H, 8.60. Found: C, 87.18; 8.65.

2.3.4 Synthesis of 10-Trimethylsiloxy-dec-1-ene (D)

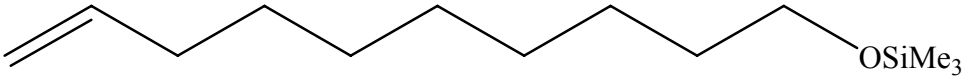

This compound was synthesized according to the solvent free process by Azizi and Saidi.[10] To a mixture of $(Me_3Si)_2NH$ (7.22 g, 0.044mol, 0.7 equiv) and $LiClO_4$ (3.4 g, 0.032 mol, 0.5 equiv) was added 9-decen-1-ol (10.00 g, 0.064 mol, 1 equiv) at room temperature and the mixture was allowed to stir overnight. Work up entailed adding CH_2Cl_2 to the crude reaction mixture and filtering through a medium Schlenk frit. The resulting solution was then passed over 5-6 cm of activated alumina and the solvent was reduced *in vacuo* to yield a colourless liquid (13 g, 89 %). ^{1}H NMR (400 MHz, $CDCl_3$) δ: 5.78 (dddd, $J_1 = J_2 = 7$, $J_3 = 10$, $J_4 = 17$ Hz, 1H), 4.96 ($J = 17$ Hz, 1H), 4.90 ($J = 11$ Hz, 1H), 3.55 (t, $J = 7$ Hz, 2H), 2.02 (m, 2H), 1.50 (m, 2H), 1.32 (m, 10H), 0.9 (s, 9H). ^{13}C NMR (100 MHz, $CDCl_3$) 139.3, 114.4, 62.9, 34.1, 33.0, 29.8, 29.7, 29.4, 29.2, 26.1. TOF-EI-MS ($[M + H]^+$, calc. 229.1909, found 229.1904).

2.3.5 Synthesis of 10-Triphenylsiloxy-dec-1-ene (E)

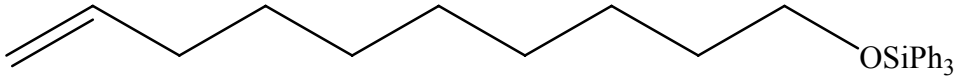

This compound was synthesized according to the process described by Piers *et al*.[11] To a mixture of 9-decen-1-ol (6.00 g, 0.038 mol, 1 equiv) and $HSiPh_3$ (10.00 g, 0.038 mol, 1 equiv) in 150 mL of dry toluene was added a 10 mL solution of $B(C_6F_5)_3$ (0.786 g, 1.5 mmol, 0.04 equiv) dropwise. Aliquots of the reaction were taken and analyzed by ^1H NMR. It was determined that the reaction was completed after stirring 68 hours at room temperature. The reaction mixture was filtered through a medium Schlenk frit and the solvent was removed *in vacuo*. 100 mL of hexanes were added to the reaction mixture and the solution was passed over 5-6 cm of activated alumina and the solvent was removed to yield a thick colourless oil (12.6 g, 80%). ^1H NMR (400 MHz, $CDCl_3$) δ: 7.79-7.43 (m, 15H), 5.92 (dddd, $J_1 = J_2 = 7$, $J_3 = 10$, $J_4 = 17$ Hz, 1H), 5.10 ($J = 18$ Hz, 1H), 5.04 ($J = 10$ Hz, 1H), 3.91 (t, $J = 7$ Hz, 2H), 2.14 (m, 2H), 1.70 (m, 2H), 1.40 (m, 10H). ^{13}C NMR (100 MHz, $CDCl_3$) 139.6, 135.8, 134.9, 130.3, 128.2, 114.6, 64.4, 34.2, 32.9, 29.8, 29.7, 29.5, 29.3, 26.2. TOF-EI-MS ($[M + H]^+$, calc. 415.2444, found 415.2457) Anal. Calcd for $C_{28}H_{34}OSi$: C, 81.10; H, 8.27. Found: C, 80.98; 7.93.

2.3.6 Synthesis of n-Decyl Methyl Ether (F)

This compound was synthesized according to the procedure described for compound **A**, but using *n*-decyl alcohol (15.00 g, 94.7 mmol). Yield: 11.0 g (67%). ^{1}H NMR (500 MHz, $CDCl_3$): δ 3.38 (t, *J* = 6.6 Hz, 2H), 3.34 (s, 3H), 1.58 (m, 2H), 1.28 (m, 14H), 0.89 (t, *J* = 6.9 Hz, 3H). Lit[12]: (360 MHz, $CDCl_3$): δ 3.34 (t, *J* = 6.5 Hz, 2H), 3.30 (s, 3H), 1.54 (m, 2H), 1.25 (m, 14H), 0.85 (t, 3H).

2.3.7 General Purity Test for Polar Monomers (A-E) Prior to Copolymerizations

For each monomer (**A-E**), water content was checked by preparing a Cp_2ZrMe_2 solution in C_6D_6 in an NMR tube, and then adding the desired polar monomer (5 - 10 molar equivalents). The spectra were analyzed for the absences of new resonances in the Cp region (δ 5.74 for the hydrolysis product $(Cp_2ZrMe)_2O$), any methane production (0.24 ppm) and for persistence of the Zr-Me resonance of Cp_2ZrMe_2 (-0.14 ppm).

2.3.8 General Procedure for Copolymerizations

The following procedure describes a typical copolymerization experiment and modifications to this procedure are noted where appropriate.

To a flame-dried 50 mL Schlenk tube were added 5 mg of *rac*-Et$(Ind)_2ZrCl_2$ and 15 mL of dry toluene. Propylene (1 atm) or ethylene (1 atm) was bubbled into this solution for 2 min to saturate the toluene/precatalyst solution. MAO (1000 equiv) in toluene was added to the Schlenk and the solution was stirred for 5 minutes prior to comonomer addition. The desired comonomer, either neat or in toluene solution, was added next, drop-wise over one minute, to the solution and the mixture was stirred for 20

or 30 minutes at room temperature while bubbling of ethylene or propylene was continued. The copolymerization was quenched with 70 mL of a HCl/ethanol (5 % HCl in ethanol) mixture and the reaction mixture was stirred overnight. The precipitated copolymers were then filtered, washed with ethanol, and dried under vacuum at 60 ^{o}C overnight. The copolymers were analyzed by ^{1}H and ^{13}C (where possible) NMR and IR spectroscopy and differential scanning calorimetry.

2.3.9 General Procedure for NMR Scale Monitoring Reactions for the Homopolymerization of Polar Monomers (A-E)

In the glovebox, a 5 mm NMR tube (either screw-cap or Teflon J-Young valve) was charged with $B(C_6F_5)_3$ (14 mg, 27.8 μmol) and 0.50 mL of the desired deuterated NMR solvent. In a separate vial, Cp_2ZrMe_2 (7 mg, 27.8 μmol) was dissolved in 0.25 mL of NMR solvent and then this Cp_2ZrMe_2 solution was added dropwise to the $B(C_6F_5)_3$ solution to form a yellow solution. This yellow solution should contain the ion pair $[Cp_2ZrMe][MeB(C_6F_5)_3]$ (see Scheme 10). To confirm successful ion pair formation, the ^{1}H NMR of this solution was taken. Next, this yellow solution was brought into the glovebox and the desired polar monomer (5 or 10 molar equivalents) was added to the ion pair. The tube was shaken and quickly taken to an NMR spectrometer whereby the reaction was monitored over 24 hours (The delay time from glovebox to NMR was found to be 8 minutes).

2.3.10 General Procedure for Attempted Upscale Homopolymerization of Polar Monomers (A-E)

In a 25 mL Schlenk flask, Cp_2ZrMe_2 (10 mg, 39.8 μmol) was added to 3 mL of a solution of $B(C_6F_5)_3$ (20 mg, 40 μmol) in the desired solvent. The bright yellow ion pair solution was stirred for 2 minutes. Next, the desired polar monomer (**A - E**) (20 to 100 equivalents) was added dropwise and the solution was stirred for 24 hours. The solvent was removed *in vacuo* and the remaining residue was either dissolved in a deuterated solvent for NMR analysis or taken for mass spectrometry analysis.

2.3.11 General Procedure for Preparing Modified MAO for Copolymerization Studies

The MAO (10 % wt in toluene) purchased from Aldrich was modified in four different ways to determine if the procedure would affect copolymerization results. The following four methods were used to modify MAO:

1) Heating the MAO solution for 18 hr under argon at 80 ^oC.

   In a typical experiment, after the heat modified MAO solution was cooled to room temperature, the modified MAO (1000 equiv.) was added to the precatalyst *rac*-$Et(Ind)_2ZrCl_2$ (5 mg) which was already in a saturated propylene/toluene solution. After 5 min, the desired polar monomer (100 equiv.) was added dropwise, and the reaction was stirred for 25 min followed by quenching with EtOH/HCl. The resulting reaction mixture was stirred overnight, filtered and dried in a vacuum oven at 60 ^oC overnight.

2) Pumping the 10 wt % solution of MAO overnight to dryness to remove residual TMA.

   In a typical experiment, after this vacuum modified MAO solution was redissolved in toluene, the modified MAO (1000 equiv.) was added to the precatalyst *rac*-Et(Ind)$_2$ZrCl$_2$ (5 mg) which was already in a saturated propylene/toluene solution. After 5 min. the desired polar monomer (100 equiv.) was added dropwise, and the reaction was stirred for 25 min followed by quenching with EtOH/HCl. The resulting reaction mixture was stirred overnight, filtered and dried in a vacuum oven at 60 ^{o}C overnight.

3) Adding 50 equivalents of air (21 % oxygen abundance in air, 15.0 mL), with respect to aluminum, in MAO, and stirring it overnight.

   In a typical experiment, the modified MAO (1000 equiv.) was added to the precatalyst *rac*-Et(Ind)$_2$ZrCl$_2$ (5 mg) which was already in a saturated propylene/toluene solution. After 5 min. the desired polar monomer (100 equiv.) was added dropwise and the reaction was stirred for 25 min, followed by quenching with EtOH/HCl. The resulting reaction mixture was stirred overnight, filtered and dried in a vacuum oven at 60 ^{o}C overnight.

4) Adding 50 equivalents of water (10.75 mL), with respect to aluminum, in MAO, and stirring it overnight.

   In a typical experiment, the modified MAO (1000 equiv.) was added to the precatalyst *rac*-Et(Ind)$_2$ZrCl$_2$ (5 mg) which was already in a saturated

propylene/toluene solution. After 5 min. the desired polar monomer (100 equiv.) was added dropwise and the reaction was stirred for 25 min, followed by quenching with EtOH/HCl. The resulting reaction mixture was stirred overnight, filtered and dried in a vacuum oven at 60 ^{o}C overnight.

Each of the four modified MAO samples prepared above were used as stated in the general copolymerization method (section **2.3.7**).

2.3.12 General Procedure for Copolymerization Studies of 1-Hexene with Propylene in the i) Absence and ii) Presence of Saturated n-Decyl Methyl Ether (F)

i) Following the procedure in Section **2.3.8**, 5 mg of catalyst *rac*-Et(Ind)$_2$ZrCl$_2$ and 15 mL of dry toluene were added to a flame-dried 50 mL Schlenk. Propylene (1 atm) was bubbled into this solution for 2 min to saturate the toluene/precatalyst solution. 1-Hexene (100 or 500 equivalents) was either premixed with the catalyst above or added 5 mins after MAO (1000 equivalents) addition. The mixture was stirred for 20 or 30 minutes at room temperature while bubbling of propylene was continued. The copolymerization was quenched with 70 mL of a HCl/ethanol (5 % HCl in ethanol) mixture and the resulting solution was stirred overnight. The precipitated copolymers were then filtered, washed with ethanol, and dried under vacuum at 60 ^{o}C overnight. The copolymers were analyzed by ^{1}H and ^{13}C (where possible) NMR and IR spectroscopy and differential scanning calorimetry.

ii) The same procedure was used as above in i), but 100 equivalents of the *n*-decyl methyl ether (**F**) were added *prior* to MAO addition to determine the effects of the ether on copolymerization results.

REFERENCES FOR CHAPTER 2

1. Dieck, T.; Svoboda, M.; Greiser, T. *Z. Naturforsch*, **1981**, *36b*, 823.
2. Drew, D.; Doyle, J. R. *Inorg. Synth.* **1972**, *13*, 47.
3. Johnson, L. K.; Killian, C. M.; Brookhart, M. *J. Am. Chem. Soc.* **1995**, *117*, 6414.
4. Samuel, E.; Rausch, M. D. *J. Am. Chem. Soc.* **1973**, *95*. 6263.
5. Chien, J. C. W.; Tsai, W-M.; Rausch, M. D. *J. Am. Chem. Soc.* **1991**, *113*, 8570.
6. Massey, A. G.; Park, A. J. *J. Organomet. Chem.*, **1964**, *2*, 245.
7. Brookhart, M.; Grant, B.; Volpe, A. F. Jr. *Organometallics*, **1992**, *11*, 3920.
8. Guan, Z.; Ma, X.S.; Chen, G. *J. Am. Chem. Soc.* **2003**, *125*, 6697.
9. a) Carballeira, N.M; Miranda, C. *Chem. Phys. Lipids,* **2003**, *124*, 63-67. b) Prugh, J. D.; Rooney, C. S.; Deana, A. A.; Ramijit, H. G. *J. Org. Chem.* **1986**, *51*, 648.
10. Azizi, N, Saidi, M. R. *Organometallics*, **2004**, *23*, 1457.
11. Blackwell, J. M.; Foster, K. L.; Beck, V. H.; Piers, W. E. *J. Org. Chem.,* **1999**, *64*, 4887.
12. Tulloch, A. P. *Chem. Phys. Lipids*, **1985**, *37*, 197.

CHAPTER 3

RESULTS AND DISCUSSION

3.1 Part 1: Late Metal Insertion Reaction Studies of Acrylonitrile and Copolymerization Behaviour of Acrylonitrile with Ethylene.

3.1.1 Synthesis and Structure of [(N-N)PdMeAN][BAr^f_4] (2)

As discussed in Section **1.3**, the focus of Part 1 of this thesis was to investigate the reactions of Brookhart's catalyst **1** with acrylonitrile (AN). Complex **1** was synthesized by reacting (N-N)$PdMe_2$ with the oxonium acid $[H(Et_2O)_2][BAr^f_4]$ (Ar^f = 3,5-$(CF_3)_2C_6H_3$) to generate the ether coordinated orange complex **1** in 62 % yield (Equation 3).

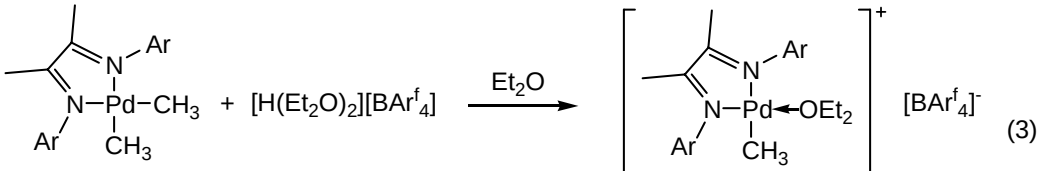

(Ar = 2,6-(*i*-Pr)$_2C_6H_3$)
(Ar^f = 3,5-$(CF_3)_2C_6H_3$)

1 (3)

Dissolution of the orange complex **1** in AN resulted in an immediate color change to yellow, suggesting the displacement of ether by AN to produce the cationic nitrile complex $[Pd(N–N)Me(AN)]^+$ (**2**) (Equation 4). Work up of complex **2** entailed stirring for one hour, pumping down the excess AN, repeated washings of the resulting solid with hexanes and drying overnight under reduced pressure.

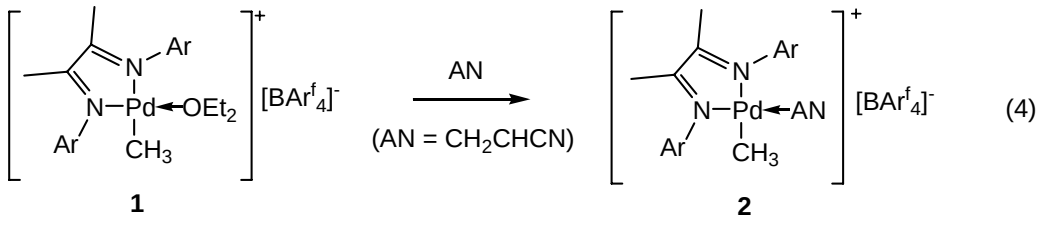

1 **2** (4)

(Ar^f = 3,5-$(CF_3)_2C_6H_3$)

The resulting yellow powder was shown by ^{1}H NMR spectroscopy, ESMS and elemental analyses to be [Pd(N–N)Me(AN)][BAr_4^f], which may exist in conformations such as **2a** and **2b** (to be discussed later).

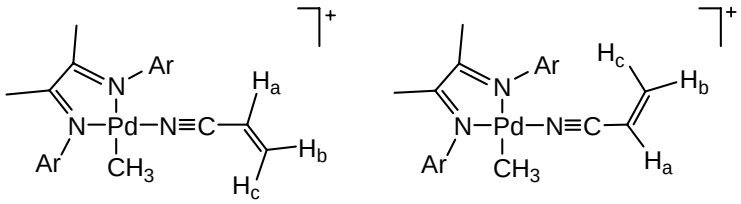

2a **2b**

Ar = 2,6-(*i*-Pr)$_2$C$_6$H$_3$

The molecular ion of **2** (578 Da) was readily observed in an ES mass spectrum and the isotope pattern of the molecular ion agreed closely with a calculated spectrum, clearly confirming the formulation of the complex as a coordination complex in which AN had replaced the ether ligand of **1** (Figure 15). Carrying out the reaction of **1** with AN in dichloromethane or ethyl ether resulted in the formation of the same product.

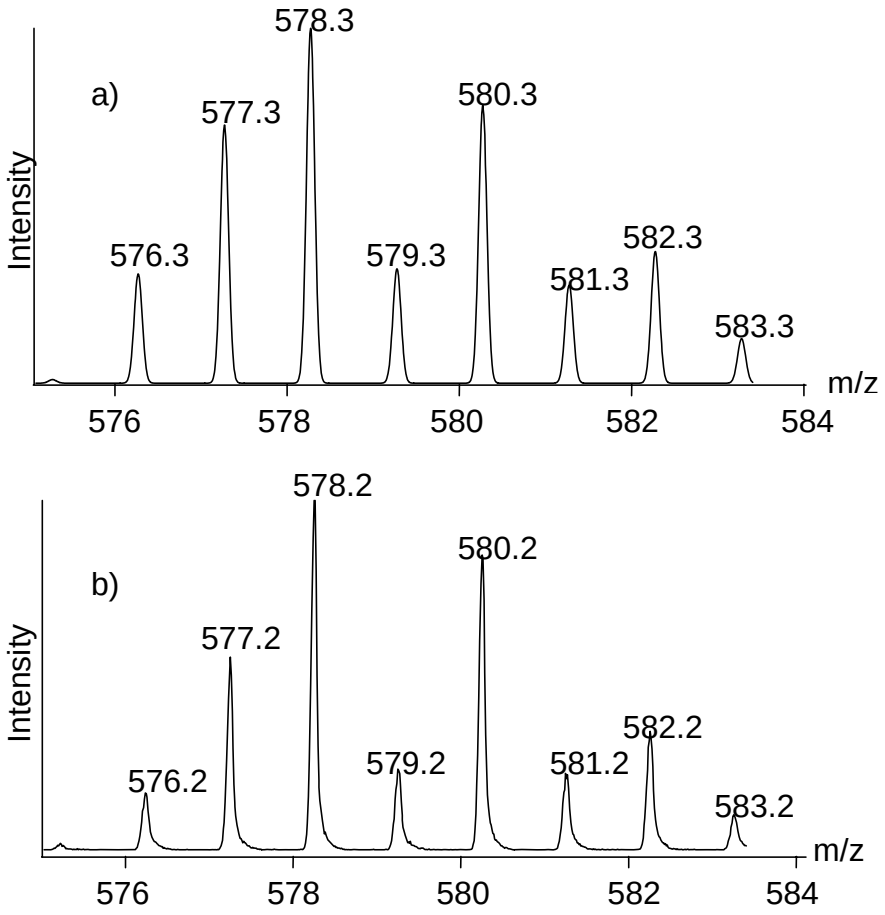

Figure 15. a) Calculated and b) observed isotope patterns for the molecular ion of **2**.

Wu *et al* have recently prepared (via the reaction of Pd(N–N)MeCl with $[Li(Et_2O)_{2.8}][B(C_6F_5)_4]$) but not isolated the analogous compound [Pd(N–N)Me(AN)][$B(C_6F_5)_4$], containing the same cation but a different anion.[1a] Aside from the additional $[BAr_4^f]^-$ resonances in the ^{1}H NMR spectrum of **2**, the room temperature NMR spectra of the two compounds compare well. Wu *et al.*[1a] and Groux *et al.*[1b] have also identified in solution a number of similar Pd-AN complexes, but in all cases, 2,1-insertion of the AN into the Pd-Me bond occurs relatively rapidly and no cationic AN complexes were actually isolated.

The olefinic resonances in a room temperature ^{1}H NMR spectrum of **2** (Figure 16) are informative with respect to structure. On coordination, the resonance of H_a shifts upfield from δ 5.71 in free AN to δ 5.45 (0.26 ppm), while that of H_b downfield from δ 6.09 to δ 6.21 (0.12 ppm). The H_c resonance shifts upfield from δ 6.22 to δ 5.85 (0.37 ppm). These coordination induced changes are very different from those of known η^2-AN complexes of metals in the +2 oxidation state,[2] as well as for those of the analogous η^2-propene complex (**A**, L = $MeCH{=}CH_2$); in these, all three vinyl hydrogen resonances shift upfield by 0.75 ppm or more.[3] In view of these observations, in addition to the previously mentioned computational results,[4] we conclude that the AN of **2** is coordinated through the nitrogen of AN. This conclusion is further supported by the shifting of the nitrile stretching frequency by 49 cm^{-1} to a higher frequency in the IR spectrum.[5a]

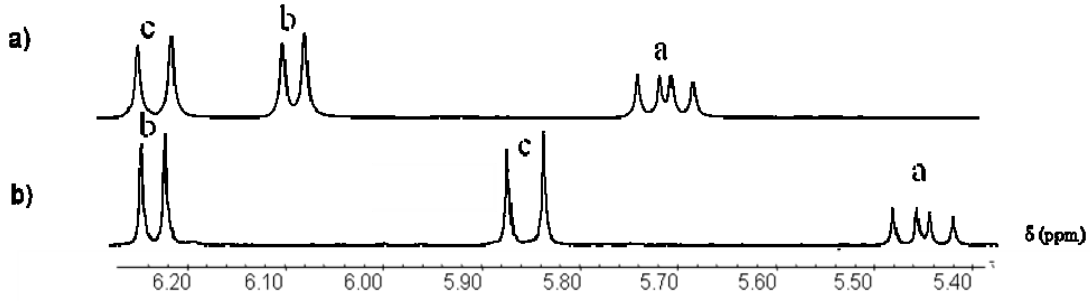

Figure 16. ^{1}H NMR (400 MHz, CD_2Cl_2) of a) acrylonitrile and b) complex **2** at room temperature.

Interestingly, variable temperature NMR studies of **2** suggest that this complex exists in solution as a mixture of at least two interconverting, isomeric forms. Reducing

the temperature from 298 K to 193 K results in reversible changes in the NMR spectrum, and the Pd-methyl resonance, as well as the resonances of H_b and H_c shift upfield by 0.2, 0.07 and 0.3 ppm, respectively. However, the resonances of H_a and the diimine ligand change relatively little (Figure 17).

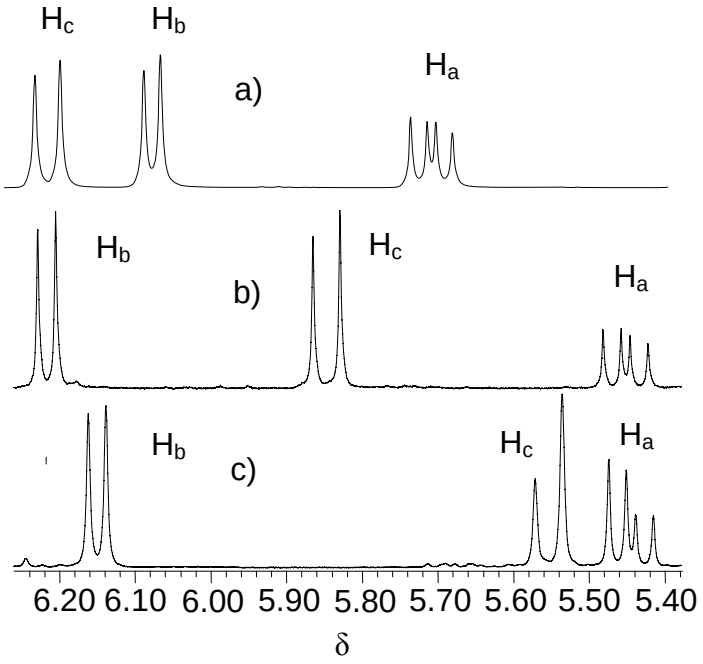

Figure 17. ^{1}H NMR (500 MHz, CD_2Cl_2) spectrum of the olefinic region of **2** at (b) 298 K and (c) 193 K. (a) is free acrylonitrile at 298 K.

We rationalize these observations in terms of rapid interconversion between two different conformations with different chemical shifts. Molecular mechanics calculations suggest that, because of the steric requirements of the bulky isopropyl groups, the plane of the coordinated AN ligand lies approximately in the molecular plane. Two such conformations are possible, one with H_c approximately eclipsing the Pd-methyl group (**2a**), the other with H_a approximately eclipsing the Pd-methyl group (**2b**; shown in Figure 18). In the latter, H_c could interact with the π face of the aryl ring and hence

experience significant shielding because of ring current effects,[5b] and indeed molecular mechanics calculations on conformation **2b** suggest close contacts between H_c and three

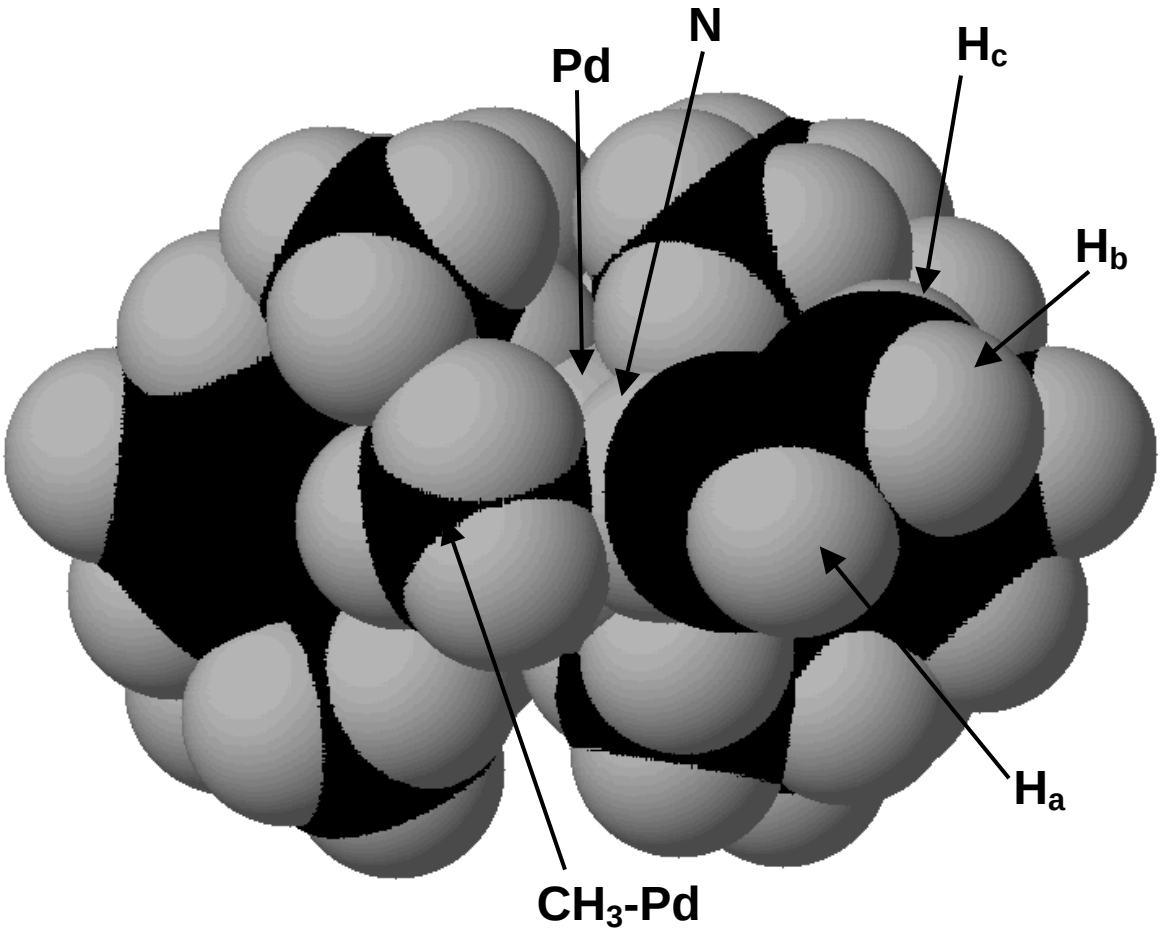

Figure 18. Space filling model of **2** showing how H_c lies close to an aryl ring in the preferred conformation **2b**.

of the ring carbon atoms. This is not the case for H_a and H_b in either conformation, and thus changing the relative populations of the two conformations results in the greatest ring current effects being on the chemical shift of the resonance of H_c, which is indeed observed. Increasing the population of **2b** results in an upfield shift of the resonance of H_c, and thus the observed temperature effects on the chemical shift of H_c suggest that **2b** is the more stable rotamer.

3.1.2 Reactions of [(N-N)PdMeAN][BAr$^f_4$] (2) with Acrylonitrile.

Although solutions of the $[B(C_6F_5)_4]^-$ salt of **2** are reported to be stable with respect to insertion at 23 ºC for several days,[1a] we find that compound **2** does engage in insertion reactions in the presence of free AN if given time and that secondary reactions occur under more forcing conditions. Thus **2** was stirred in neat AN at room temperature for 12 h, in neat AN at 50 ºC for 2 h, and refluxed in neat AN (77 ºC) for 12 h. All of the reactions were then worked up as in the case of complex **2**, and the products of the first two reactions were found to be yellowish powders, that of the 12 h reflux reaction a greenish-orange material.

The room temperature ^{1}H NMR spectra (olefinic region) of the three product mixtures are shown in Figure 19(b-d), where they are compared with the ^{1}H NMR spectrum of **2** in Figure 19(a). Magnified aliphatic regions of the three product mixtures, including that of complex **2**, are also shown in Figure 20(a-d). As can be seen, the spectra shown in Figures 19(b, c) are similar, exhibiting in addition to the resonances of **2** a new set of olefinic resonances at δ 6.32 (d, J = 12.1 Hz), apparently corresponding to H_b of a second AN complex **3** (discussed later), and a new H_a resonance at δ ~5.45 (m, confirmed

by a COSY experiment (Figure 21)). The new H_c resonance overlaps exactly with the analogous resonance of **2** at δ 5.85 (confirmed by relative integrations and by a COSY experiment). Also, the spectra in Figure 19d shows, in addition to free acrylonitrile, a new set of resonances corresponding to a complex **4**, which was found and assigned a structure after mass spectrometry analysis (discussed later). There are also new ligand resonances (Figure 20(b-d)) in the region δ 1.0-3.3, (and what possibly may be a new singlet Pd-Me resonance at δ 0.42, a 1:2:1 triplet at δ 0.23, a partially obscured multiplet at ~δ 0.41 and multiplets at ~δ 0.8-0.9). Thus the reactions clearly produce complex mixtures.

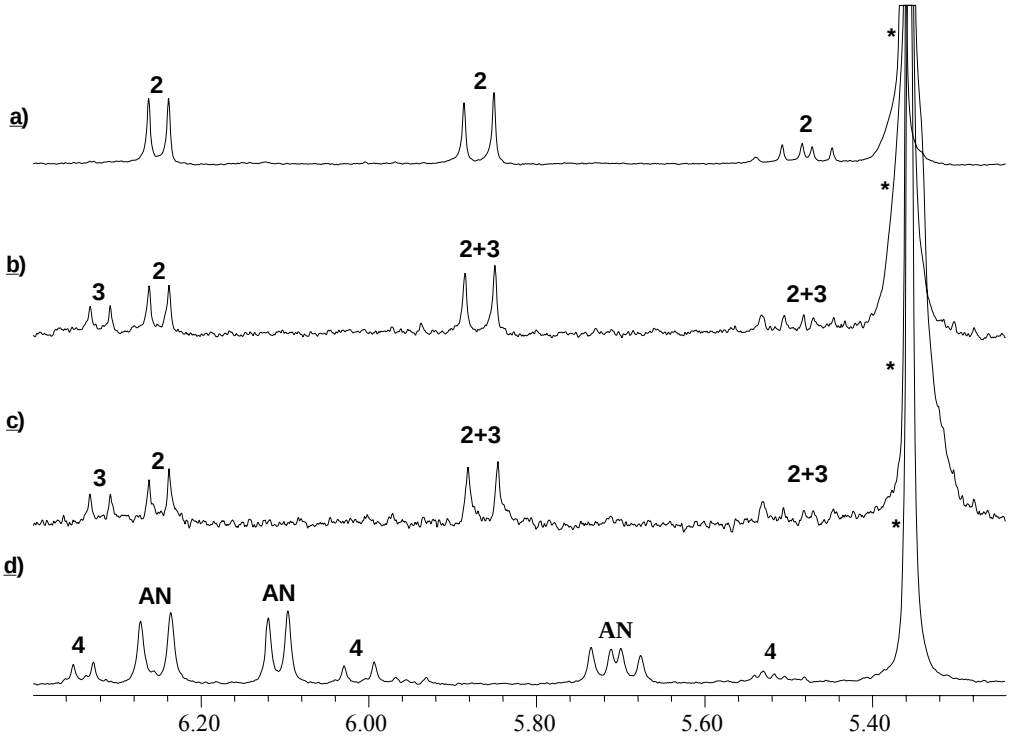

Figure 19. ^{1}H NMR (500 MHz, CD_2Cl_2) olefinic region of (a) compound **2**, (b) the product(s) formed at 50 ºC for 2 h, (c) the product(s) formed at room temperature for 12 h, (d) the product(s) formed under reflux for 12 h. (AN –free acrylonitrile).

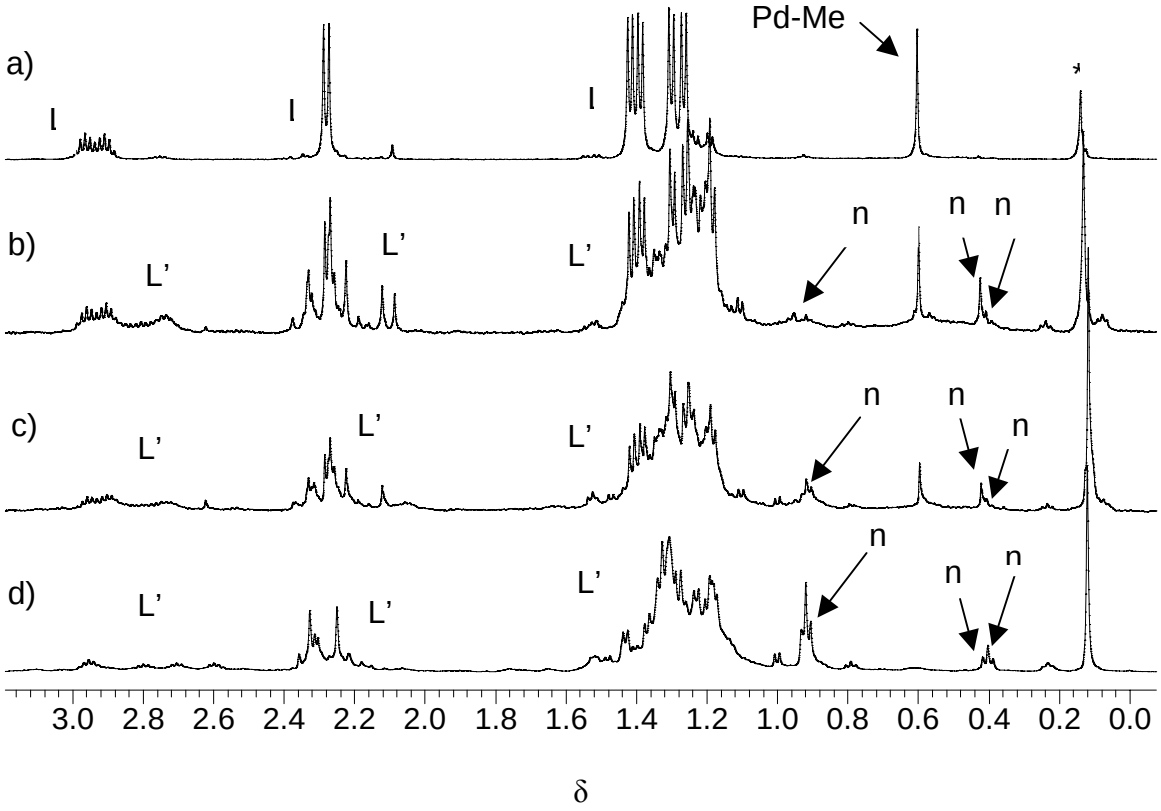

Figure 20. ^{1}H NMR (500 MHz, CD_2Cl_2) spectra of 0 - 3 ppm region of (a) compound **2**, (b) the product(s) formed at 50 ºC for 2 h, (c) the product(s) formed at room temperature for 12 h,(d) the product(s) formed under reflux for 12 h. (n - new product(s) peaks, L – ligand (complex **2**), L' – new ligand peaks (product mixtures),* - grease)

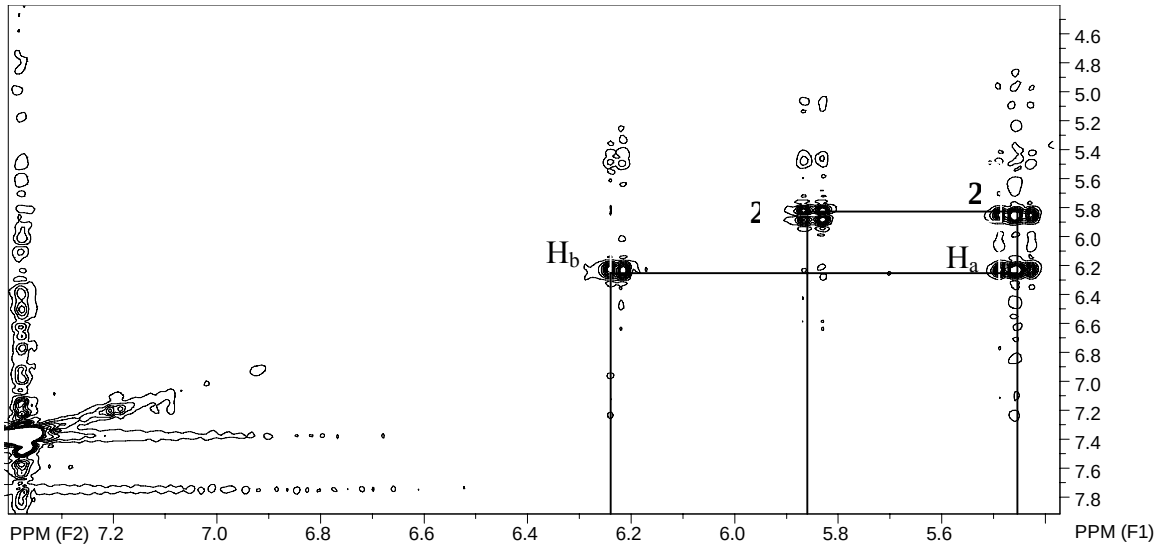

Figure 21. Olefinic region COSY spectrum (product(s) formed at 50 ºC for 2 h) correlating new H_a and H_b signals.

ES mass spectra were run in an attempt to identify the species in solution, and the mass spectra of the two product mixtures (Figure 19b,c) were also found to be similar. A sample mass spectrum of the product mixture obtained at 50 ^{o}C for 2 hours is shown in Figure 22. In addition to the molecular ion of **2** at 578 Da, both spectra exhibited singly charged ions at 592, 631 and 647 Da and several doubly charged ions (~553, ~564, ~572 and ~586 Da), characterized by their 0.5 Da spacings and very different isotope distribution patterns. Although the assignments of the doubly charged species are still unclear, the weak ion at 631 Da corresponds to the mass of a cation of stoichiometry $[Pd(N–N)(CH_2CHCN)_2Me)]^+$, containing two AN units in addition to the basic $[Pd(N–N)Me]^+$ moiety. The complex presumably results from the insertion of an AN unit followed by coordination of a second N-bonded AN to give a complex such as $[Pd(N–N)(CHCNCH_2Me)(CH_2CHCN)]^+$ (**3**) (Equation 5).

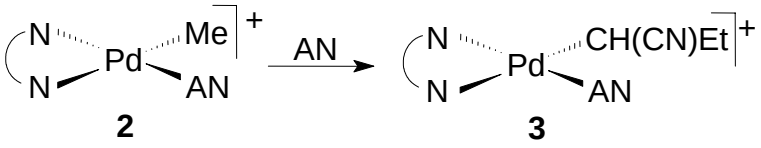

(5)

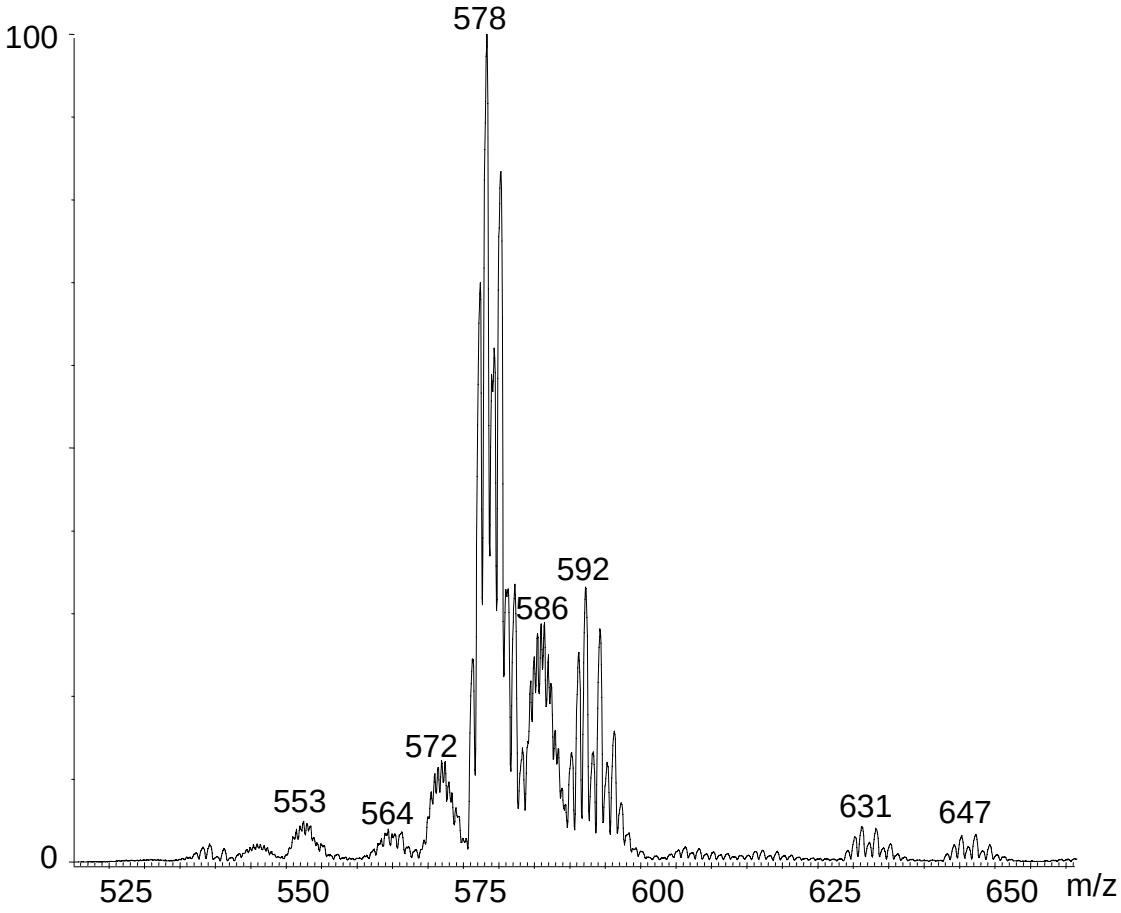

Figure 22. Low Resolution ES mass spectrum of the product mixture obtained at 50 ^{o}C for 2 hours.

A number of similar cationic species have been reported recently, and all involve 2,1-insertions to give 1-cyanopropyl complexes for which δ(CH) = 1.7-2.8 (m), δ(CH_2) = 1.0-1.7 (m) and δ(Me) = 0.65-1.00 (t).[1a] As can be seen in Figure 20(b, c), while much of both spectra are obscured in the range δ 0-4.0 by the very intense diimine resonances, the spectra do exhibit a 1:2:1 triplet at δ 0.23. We tentatively assign this triplet and the new

set of AN olefinic resonances in Figure 20(b, c) to **3**, and thus the NMR and ESMS data are consistent with **3** being the product of a 2,1-insertion of AN. A chemical shift of δ 0.23 is unusually high for the methyl group of a 1-cyanopropyl ligand,[1a] but may be rationalized on the basis of ring current effects as discussed above for compound **2**. Similar upfield shifts have been reported for propylene insertion complexes of the type $[Pd(N–N)(CH_2=CHMe)(CHMeCH_2)_nMe]$ and,[3] although not commented on at this time, may possibly be rationalized in the same way. In contrast, the series of analogous complexes by Wu *et al.*[1a] and Groux *et al.*[1b], in which there are no ligands which can induce ring current effects, exhibit normal chemical shifts for the 1-cyanopropyl ligands.

The medium intensity ion at 592 Da exhibits an isotope pattern appropriate for a complex of the stoichiometry $[Pd(N–N)(C_4H_5N)Me)]^+$ (**4**; C_4H_5N = crotononitrile, MeCH=CHCN). Crotononitrile is the product of β-hydrogen elimination from complex **3** (Equation 6), and the formation of **4** must involve release of the coordinated crotononitrile followed by substitution by it of the AN of a molecule of **2** (Equations 7, 8).

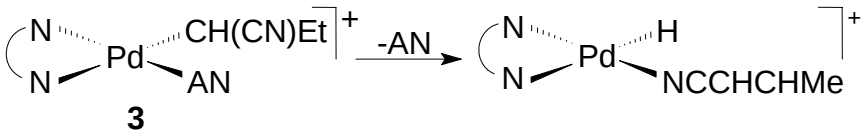

3 (6)

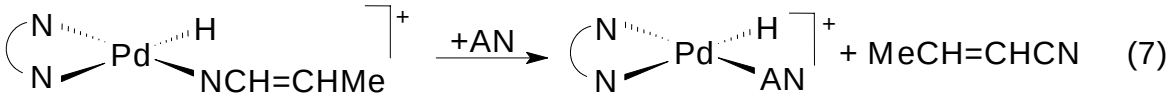

(7)

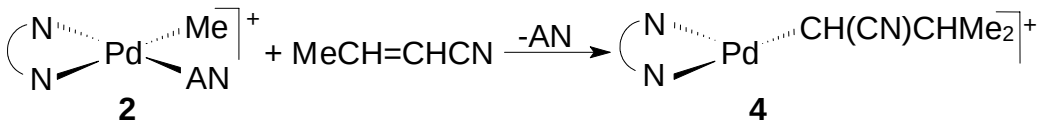

2 **4** (8)

It is difficult to convincingly rationalize the conversion of **2** to **4** in the presence of excess AN, but crotonitrile does have a much higher boiling point (120 °C) than does acrylonitrile (77 °C) and its relative concentration would increase as the volatiles are removed during workup. In any case, a high resolution ES mass spectrum was run to obtain an exact mass for the peak at 592 Da and the experimental value, 592.2903 Da, differed by only 3.3785 ppm from the calculated value for $C_{33}H_{48}N_3Pd$, 592.2882 Da. No other reasonable stoichiometry was within 17 ppm of the experimental value, and thus attribution of the multiplet at 592 Da to **4** seems firm. Since we observed no unexplained resonances in the olefinic region of the NMR spectrum, it seems likely that **4** contains an inserted C_4H_5N moiety, as in $[Pd(N–N)(CHCNCHMe_2)]^+$ (Equation 8). It is possible that the vacant site on the metal is occupied by an agostic interaction with one of the *i*-Pr groups.

The initially formed palladium-containing product of β-hydrogen elimination from **3** (Equation 6) would be the hydride complex $[Pd(N–N)(C_4H_5N)H)]^+$, isomeric with **2** and hence indistinguishable on the basis of mass spectrometry. A secondary product, $[Pd(N\text{-}N)(AN)H]^+$, would arise from substitution of the crotonitrile by AN (Equation 3), and a weak peak in the ES mass spectrum at 564 Da may be taken as evidence for the presence of this species although a close examination of the ^1H NMR spectra in the region δ 0 to –20 reveals no hydride resonance. Thus the species in solution may well be

the insertion product, $[Pd(N\text{-}N)(CHCNMe)]^+$ (**5**, Equation 9), with the vacant site on the metal occupied by an agostic interaction with one of the *i*-Pr groups .

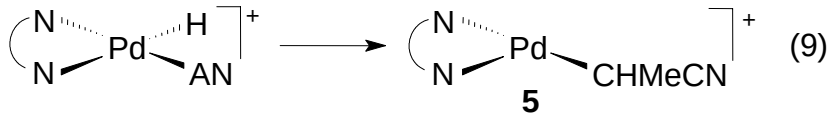

5 (9)

Figure 19 (d) shows the ^1H NMR spectrum of the products formed during 12 h of refluxing in AN. The spectrum exhibits many resonances in the region δ 1.0-3.3, suggesting the presence of a complex mixture. Interestingly, there are no resonances in the olefinic region and the above mentioned triplet at δ 0.23 and multiplet (now seen to be a triplet) at δ 0.41 and are much more apparent while the singlet at δ 0.42 has disappeared. The ES mass spectrum (Figure 23) exhibited multiplets at m/e = 509 (m), 564 (m), 578 (s), 598 (w), 605 (w), 631 (w), 649 (w) and 663 (w) Da, in addition to several others at higher masses. The multiplet at 509 Da exhibits an isotope pattern consistent with its formulation as **6**, i.e. a compound in which metallation of one of the isopropyl groups has occurred. This multiplet was not present in the mass spectra of the reaction mixtures obtained under less forcing conditions, and thus is probably a product of decomposition. As with **4** and **5**, it is possible that the vacant site on the metal is occupied by an agostic interaction with one of the *i*-Pr groups.

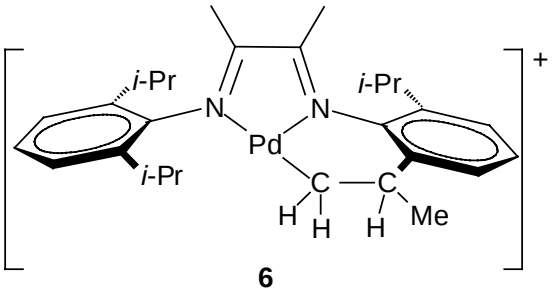

6

The peak at 564 Da, attributed to **5**, is much stronger than observed in the mass spectra discussed above. Again the ^{1}H NMR spectrum of the reaction mixture exhibits neither hydride nor olefinic resonances, and thus this species seems best formulated as the product of insertion. The multiplet at 631 Da has been discussed above, but those at 649 and 663 Da remain unidentified.

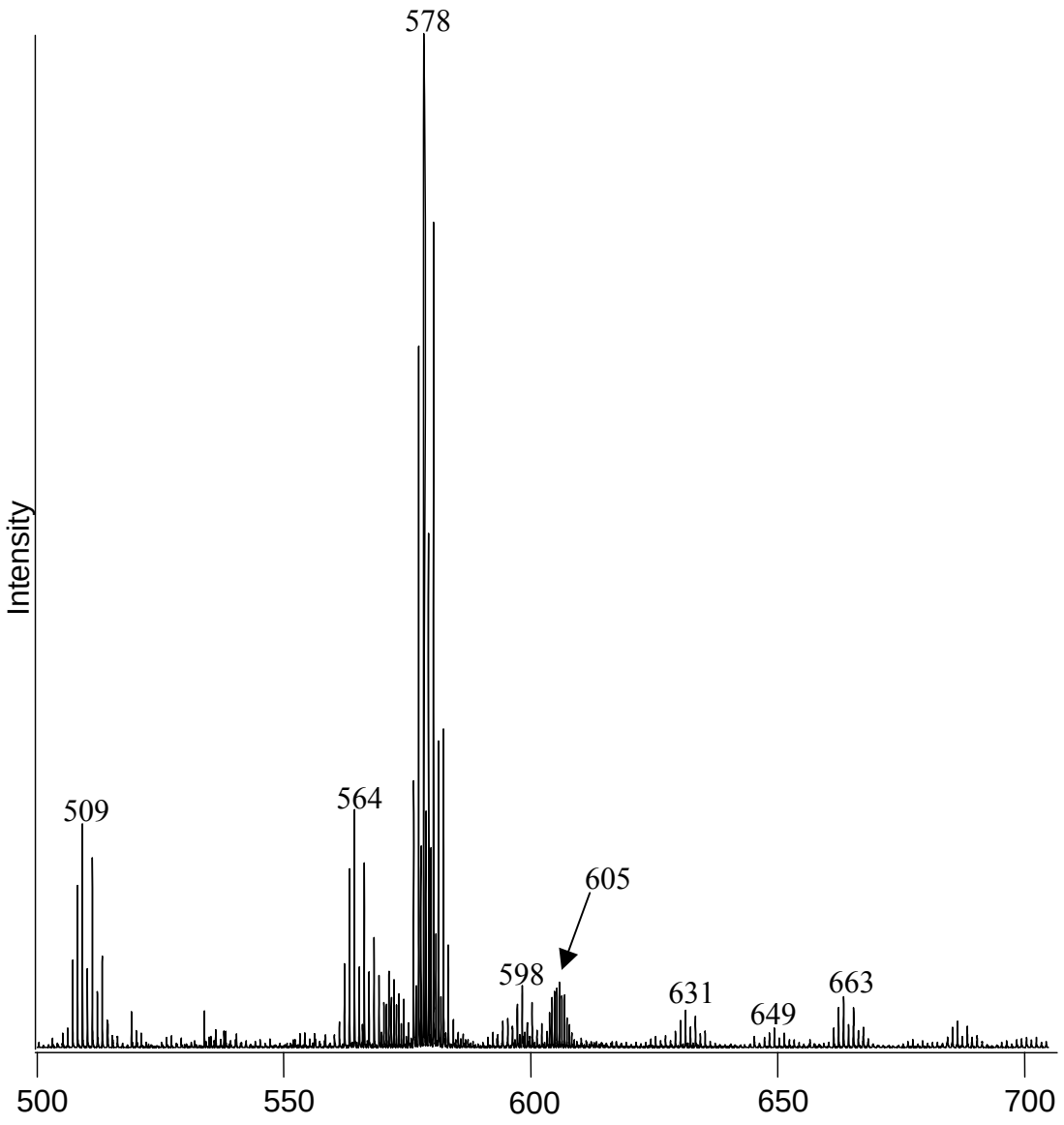

Figure 23. High resolution ES mass spectrum of the products formed during 12 h of refluxing in AN.

Interestingly, while the main set of peaks of the multiplets at 578, 598 and 631 Da exhibit the isotope patterns expected, all also contain sets of weaker peaks at masses differing from those of the main peaks by 0.5 Da and exhibiting the isotope patterns expected for the corresponding, dicationic dimers. Since the ^{1}H NMR spectrum of the

reaction mixture shows clearly that the molecules in solution do not contain coordinated AN, the new species must be dimeric, as in **7**.

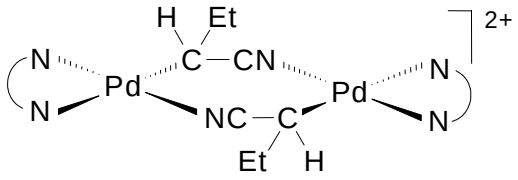

7

Thus dicationic, dinuclear species are readily formed in this system and probably involve bridging nitrile ligands as shown; similar results have been observed elsewhere and, in fact, dinuclear species have been shown to be a common secondary product following 2,1-insertion of AN into a Pd-Me bond.[1] We therefore tentatively assign the second methyl triplet resonance in the spectra of Figure 20(b, c, d) to the dimer **7**.

The question arises then as to whether the monomeric complexes exist in solution or whether they are formed via dimer dissociation within the mass spectrometer. This question cannot be answered, but ES mass spectra of similar platinum complexes have been shown to reflect the species in solution,[6a] and the monomeric species may well be stabilized by agostic interactions involving the diimine isopropyl groups. Somewhat similar platinum containing species have been noted elsewhere.[6b] Unfortunately, the identities of many of the species giving rise to the ions detected in the mass spectrum are as yet unknown.

3.1.3 Polymerization reactions involving [(N-N)PdMeAN][BAr^f_4] (2).

Interestingly, it was found that trace amounts of polyacrylonitrile were formed during the 12 h reflux reaction; a ^{1}H NMR spectrum of the resulting white precipitate in DMSO-d_6 exhibited broad resonances at δ 2.1 and 3.2, characteristic of polyacrylonitrile.[6c] However, in none of the mass spectra obtained to date have there been any series of peaks separated by 53 Da, as would be expected if multiple insertions of AN at palladium were occurring in this diimine system. Thus while a single insertion into a Pd-Me or Pd-H bond seems to occur slowly, subsequent insertions appear to be unachievable, a conclusion also reached elsewhere.[1] The small amounts of polyacrylonitrile obtained during the long reflux reactions are presumably a result of radical polymerization processes, possibly initiated by homolysis of Pd-CHCNEt bonds. Polyacrylonitrile does not form during control experiments, i.e. in the absence of **2**.

However, we have investigated the possibility of ethylene-AN co-polymerization by **2**. Bubbling ethylene through a solution of **2** in CD_2Cl_2 for 2 min results in a color change from yellow to orange, disappearance of the Pd-Me resonance and appearance of the peaks of the type of branched polyethylene reported previously.[3] The spectrum exhibits no resonance for free ethylene and the diimine resonances are changed very little, but there are vinyl resonances of coordinated acrylonitrile and they are shifted slightly upfield from those in the NMR spectrum of **2**. Thus the resting state in this catalytic system seems to be a complex of the type $[Pd(N–N)(AN)(polymeryl)]^+$(where polymeryl is a growing alkene chain).

On bubbling ethylene for 3 min through solutions of **2** in several solvents in the presence of a few equivalents of AN, we observe not copolymer formation but rather

serious inhibition of ethylene polymerization. The addition of a large excess of AN completely shuts down ethylene polymerization. Complementary experiments in which we attempted to homopolymerize AN in the presence of BPh_3 also failed; the Lewis acidic triarylborane apparently does not bind the nitrogen of the AN with sufficient strength to allow the olefinic moiety to coordinate preferentially.

RESULTS AND DISCUSSION

3.2 Part 2: Early Metal Copolymerization Studies of Polar Monomers $CH_2=CH(CH_2)_7CH_2OR$ (R = Me, $PhCH_2$, Ph_3C, Me_3Si, Ph_3Si) with Ethylene and Propylene.

3.2.1 Polar Monomer Synthesis

As discussed in Section **2.4**, the focus of Part 2 of this thesis was to develop new polymeric materials via direct copolymerization of polar monomers with olefins (e.g. ethylene, propylene) utilizing a protecting group strategy on the functional polar monomers. To achieve this goal, masking agents on the hydroxyl group of 9-decen-1-ol were chosen to encompass a variety of steric requirements (e.g. methyl (**A**), benzyl (**B**), trityl (**C**), trimethylsilyl (**D**) and triphenylsilyl (**E**)) and we wished to address the hypothesis that most bulky substituents would hinder ether oxygen coordination and thus result in a minimal inhibition of (co)polymerization. Of monomers **A**-**E**, all were prepared with modified literature procedures,[7-10] while monomer **C** has not been reported and it is characterized here, including elemental analysis. Monomers **D** and **E** have been cited in the literature[11], but no spectroscopic data for these compounds were given, and therefore the ^1H and ^{13}C NMR data are reported for the first time here. In addition, the synthesis of a saturated *n*-decyl methyl ether **F** is reported for a polymerization study to be discussed later (Section **3.2.3.4**). The outline syntheses of the monomers are given below as well as spectroscopic data for each.

3.2.1.1 Synthesis of 10-Methoxydecene (A) and 10-Benzyloxydecene (B)

The synthesis of monomers **A** and **B** were achieved by methods outlined by Guan *et al.*[7] and Carballeira *et al.*[8a], respectively. Deprotonation of the alcohol by sodium hydride was done in THF solution, followed by addition of the alkyl iodide/aryl chloride to afford the products **A** (63 % yield) or **B** (20 % yield) as clear liquids (Equation 10).

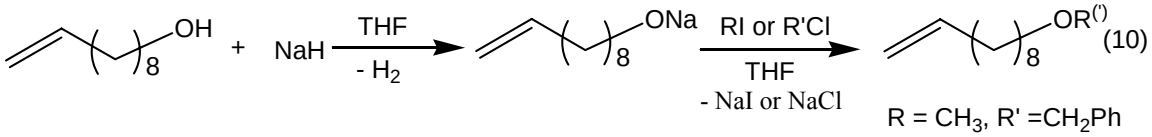

The monomers **A** and **B** were purified by passing each monomer over an activated alumina column (5 – 6 cm in height) with dry hexanes as the eluent, to remove any residual hydridic impurities. After removal of the hexanes, the monomers were isolated and stored under an inert atmosphere. This was a standard protocol for all synthesized monomers **A** – **E**. The ^{1}H NMR spectra of monomers **A** and **B** (shown in Figures 24 and 26a) are in good agreement with the literature values as are the ^{13}C NMR spectra (Figures 25 and 26b).[7,8] The complete peak assignments for each monomers **A** and **B** are given in Tables 1 - 4. These assignments were made on the basis of literature values.[7,8] As can be seen for monomer **A**, the -C*H*$_2$-OCH$_3$ group gives a characteristic triplet at δ 3.37, a singlet for the methoxy resonance -CH$_2$-OC*H*$_3$ at δ 3.34, and absence of –OH resonance (δ 2.29), signifying the successful masking of the alcohol. In addition, the vinyl region (δ 5.82, 4.99 and 4.93) and aliphatic region (δ 2.04-1.32) are also present with very little change in chemical shift compared to 9-decen-1-ol.[12] Monomer **B** has a similar spectrum to that of monomer **A**, in addition to new peaks in the phenyl region at δ 7.39 - 7.26 and a

new singlet at δ 4.52 corresponding to the -O-CH_2-Ph of the benzyl group. The product yield was poor (< 10 %), but enough was obtained and purified by alumina column treatment (as mentioned above) to be used in subsequent reactions.

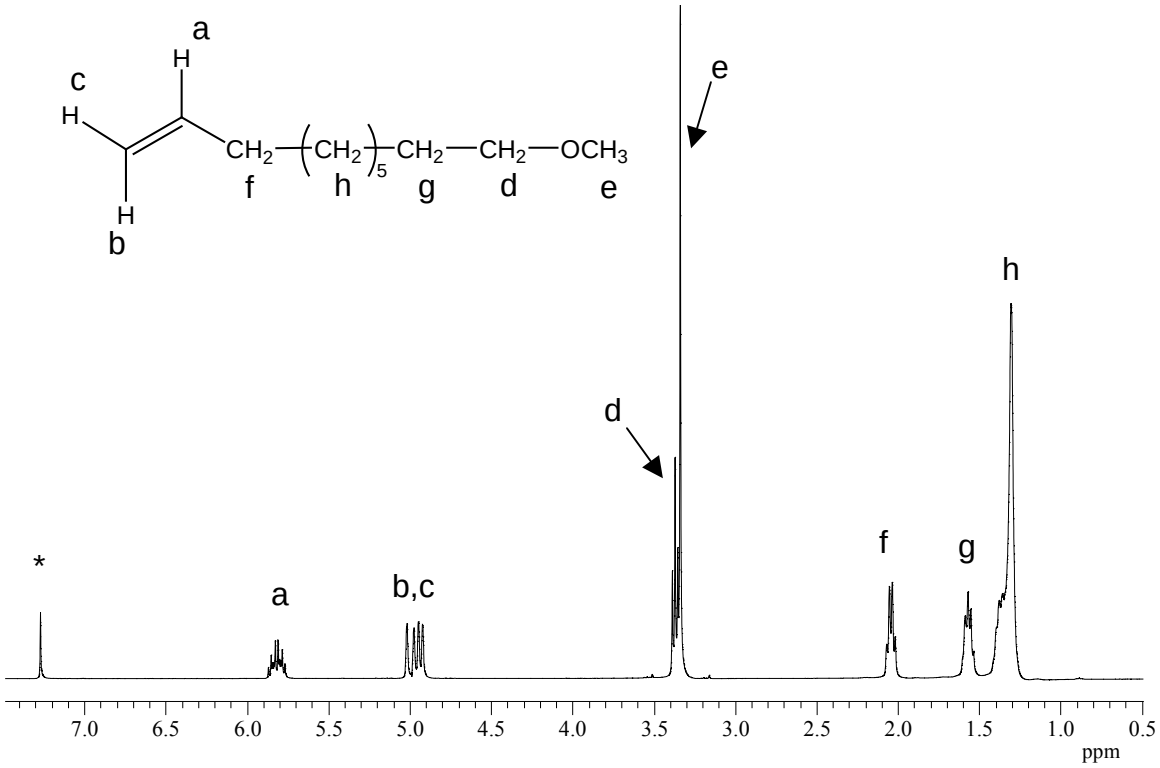

Figure 24. ^{1}H NMR spectrum (400 MHz, *$CDCl_3$) of methoxydecene **A**.

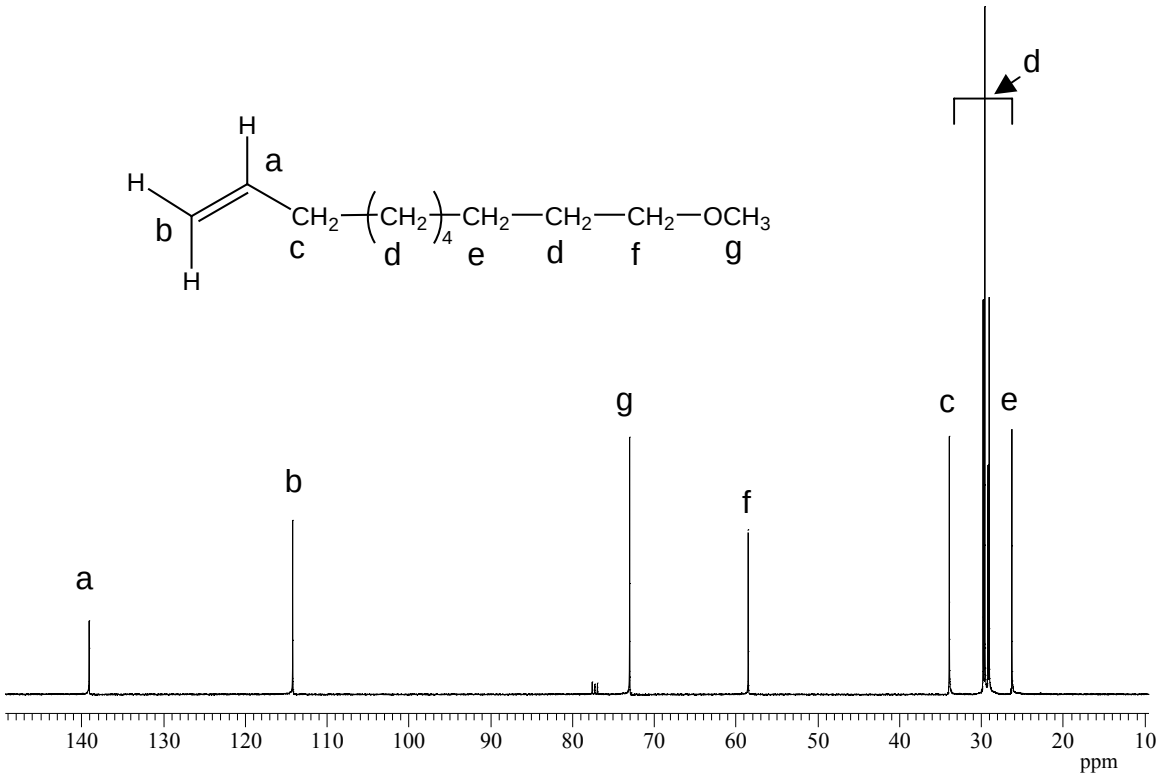

Figure 25. ^{13}C NMR (100 MHz, *$CDCl_3$) spectrum of methoxydecene **A**.

Table 1. ^{1}H NMR (400 MHz, $CDCl_3$) values for methoxydecene **A**.

^{1}H	*δ ppm*[a]
CH_2=C***H***$(CH_2)_8OCH_3$	5.73(5.81)
C***H***$_2$=CH$(CH_2)_8OCH_3$	4.91(4.99)
C***H***$_2$=CH$(CH_2)_8OCH_3$	4.85(4.93)
CH_2=CH$(CH_2)_7$C***H***$_2OCH_3$	3.29(3.36)
CH_2=CH$(CH_2)_7CH_2OC$***H***$_3$	3.26(3.33)
CH_2=CH(C***H***$_2)_7CH_2OCH_3$	1.98(2.02)
CH_2=CH(C***H***$_2)_7CH_2OCH_3$	1.51(1.57)
CH_2=CH(C***H***$_2)_7CH_2OCH_3$	1.25(1.30)

[a]Literature values in parentheses run on a 500 MHz NMR.[7]

Table 2. ^{13}C NMR (100 MHz, $CDCl_3$) values for methoxydecene **A**.

^{13}C	*δ ppm*[a]
CH_2=***C***H$(CH_2)_8OCH_3$	139.0(140.3)
CH$_2$=CH$(CH_2)_8OCH_3$	114.2(114.6)
CH_2=CH$(CH_2)_8O$***C***H_3	73.0(73.4)
CH_2=CH$(CH_2)_7$***C***H$_2OCH_3$	58.5(61.0)
CH_2=CH(***C***H$_2)_7CH_2OCH_3$	33.9(34.4)
CH_2=CH(***C***H$_2)_7CH_2OCH_3$	29.8(30.1)
CH_2=CH(***C***H$_2)_7CH_2OCH_3$	29.5, 29.2, 29.2[b], 29.0 (29.9, 29.8, 29.5, 29.3)
CH_2=CH(***C***H$_2)_7CH_2OCH_3$	26.2(26.6)

[a]Literature values in parentheses run at 125 MHz.[7] [b]Peak is overlapping and not resolved at 100 MHz in contrast to literature value at 125 MHz.

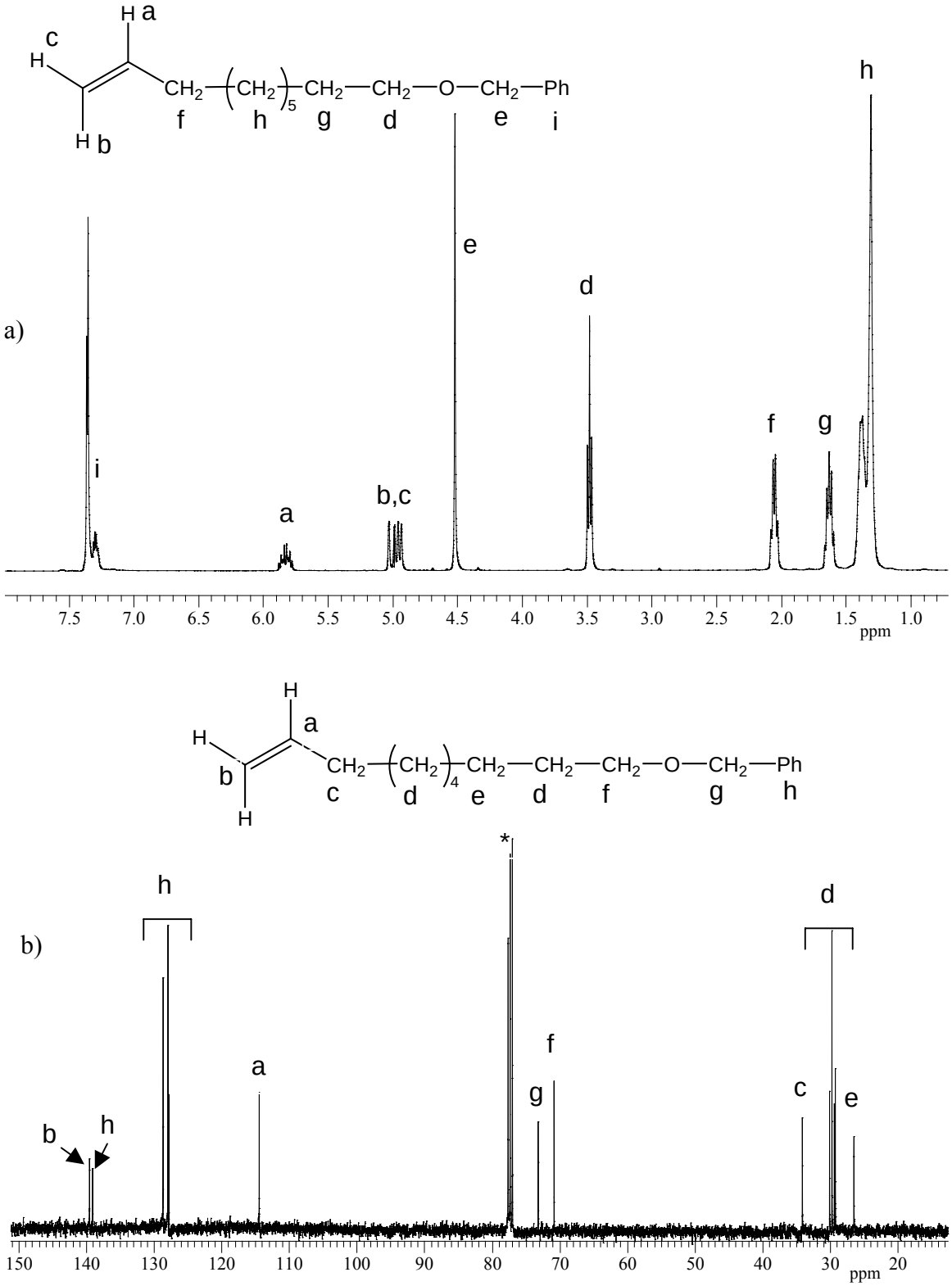

Figure 26. a) ^{1}H NMR spectrum (400 MHz, *$CDCl_3$) of benzyloxydecene **B** and b) ^{13}C NMR spectrum (100 MHz, $CDCl_3$) of benzyloxydecene **B**.

Table 3. ^{1}H NMR (400 MHz, $CDCl_3$) values for benzyloxydecene **B**.

^{1}H	*δ ppm*[a]
CH_2=CH$(CH_2)_8OCH_2$***Ph***	7.40-7.22(7.40-7.18)
CH_2=C***H***$(CH_2)_8OCH_2$Ph	5.83(5.80)
C***H***$_2$=CH$(CH_2)_8OCH_2$Ph	5.01(4.99)
C***H***$_2$=CH$(CH_2)_8OCH_2$Ph	4.94(4.92)
CH_2=CH$(CH_2)_7CH_2OC$***H***$_2$Ph	4.52(4.48)
CH_2=CH$(CH_2)_7C$***H***$_2OCH_2$Ph	3.48(3.45)
CH_2=CH$(C$***H***$_2)_7CH_2OCH_2$Ph	2.05(2.03)
CH_2=CH$(C$***H***$_2)_7CH_2OCH_2$Ph	1.63(1.61)
CH_2=CH$(C$***H***$_2)_7CH_2OCH_2$Ph	1.35(1.30)

[a]Literature values in parentheses run on a 300 MHz NMR.[8]

Table 4. ^{13}C NMR (100 MHz, $CDCl_3$) values for benzyloxydecene **B**.

^{13}C	δ ppm[a]
CH_2=***C***H$(CH_2)_8OCH_2Ph$	139.4(139.1)
$CH_2=CH(CH_2)_8OCH_2$***Ph***	139.0,128.6,127.8, 127.7 (138.8,128.3,127.6,127.5)
C$H_2=CH(CH_2)_8OCH_2Ph$	114.3(114.2)
$CH_2=CH(CH_2)_7CH_2O$***C***H_2Ph	73.1(72.9)
$CH_2=CH($***C***$H_2)_7$***C***H_2OCH_2Ph	70.7(70.5)
$CH_2=CH($***C***$H_2)_7CH_2OCH_2Ph$	34.0(33.9)
$CH_2=CH($***C***$H_2)_7CH_2OCH_2Ph$	30.0, 29.6, 29.3, 29.1 (29.8, 29.4, 29.1, 28.9)
$CH_2=CH($***C***$H_2)_7CH_2OCH_2Ph$	26.4(26.2)

[a]Literature values in parentheses run at 75 MHz.[8]

Also, shown below in Figure 27 is a sample ^1H NMR spectrum of monomer **A** with Cp_2ZrMe_2 in C_6D_6. This protocol was utilized for all newly synthesized monomers to test for trace hydroxyl impurities (i.e. water, unreacted alcohol). The monomer is combined with a deficiency (5 or 10 :1 molar ratio) of the OH-sensitive Cp_2ZrMe_2 in C_6D_6. For all monomers **A**-**E**, no cleavage of the Zr-Me bonds in Cp_2ZrMe_2 was observed as indicated by the absences of new resonances in the Cp (δ 5.74 for $(Cp_2ZrMe)_2O$), or in the methyl regions (δ 0.24 for CH_4) of the spectra. In addition, persistence of the Zr-Me resonance of Cp_2ZrMe_2 (-0.14 ppm) confirmed no hydroxyl impurities within the monomers.

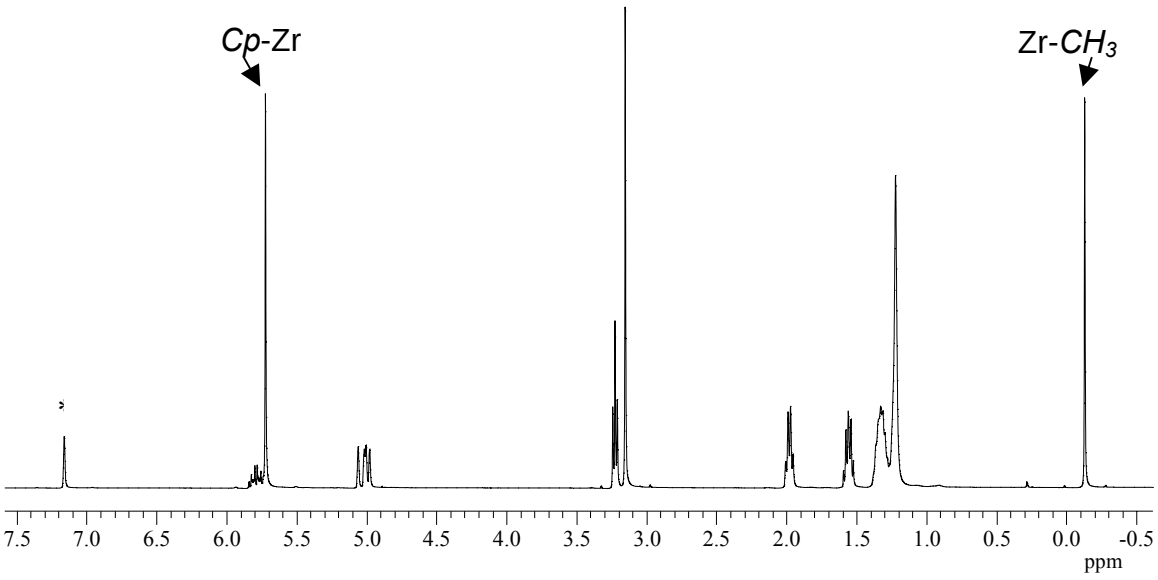

Figure 27. Sample ^{1}H NMR spectrum (400 MHz, *C_6D_6) of (5:1) methoxydecene **A** to Cp_2ZrMe_2.

3.2.1.2 Synthesis of 10-Trityloxydecene (C)

The synthesis of monomer **C** (10-trityloxydecene), a compound not prepared previously, was attempted by the method described in Section **3.2.1.1**; however, poor yields (< 40 %) were obtained. An alternate route was attempted, shown in Equation 11. Degassed 9-decen-1-ol was refluxed with trityl chloride and pyridine overnight to afford, after filtration of the pyridinium salt, $[C_6H_5NH][Cl]$, work up and purification via alumina column treatment , a viscous clear oil in 60 % yield.

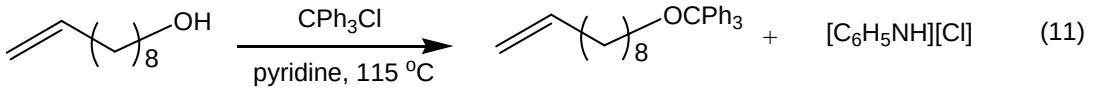

(11)

The ^{1}H and ^{13}C NMR spectra of this new monomer are given in Figures 28a and 29, as well as the chemical shift information for each in Tables 5 and 6. ^{1}H and ^{13}C NMR

assignments were based upon chemical shifts of known similar compounds such as 9-decen-1-ol and monomer **B**, in addition with values obtained from known literature for a trityl and/or phenyl ether resonances.[8a,b,12] In addition, monomer **C** was further verified by elemental analysis. As it can be seen, new phenyl peaks are evident at δ 7.48 -7.25 as well as a highly shielded methylene triplet at δ 3.08, when compared to the methylene unit next to OH in 9-decen-1-ol (δ 3.62). Also, given in Figure 28b is the ^{1}H NMR spectrum of monomer **C** with Cp_2ZrMe_2 in C_6D_6 to test for trace hydroxyl impurities (i.e. water, unreacted alcohol). The spectrum shows no cleavage of the Zr-Me bonds in Cp_2ZrMe_2 and/or new Cp resonances indicating that monomer **C** was indeed free of hydroxyl impurities.

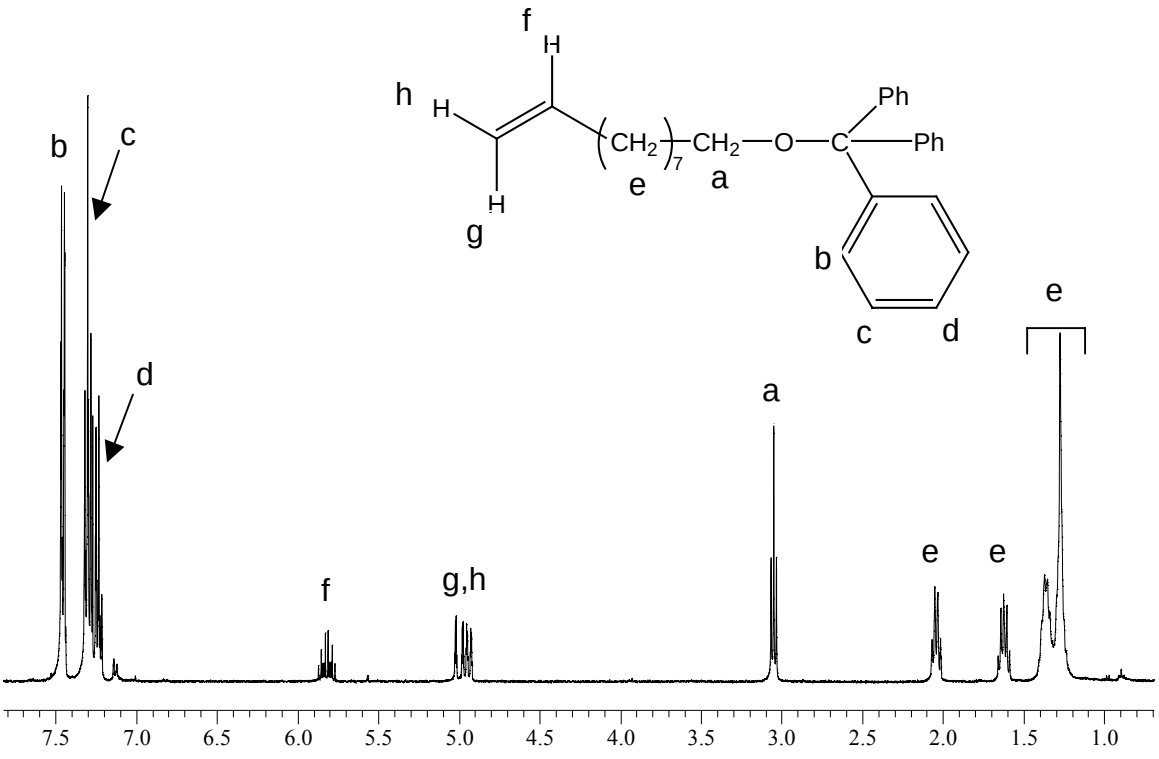

Figure 28a. ^{1}H NMR spectrum (500 MHz, $CDCl_3$) of trityloxydecene **C**.

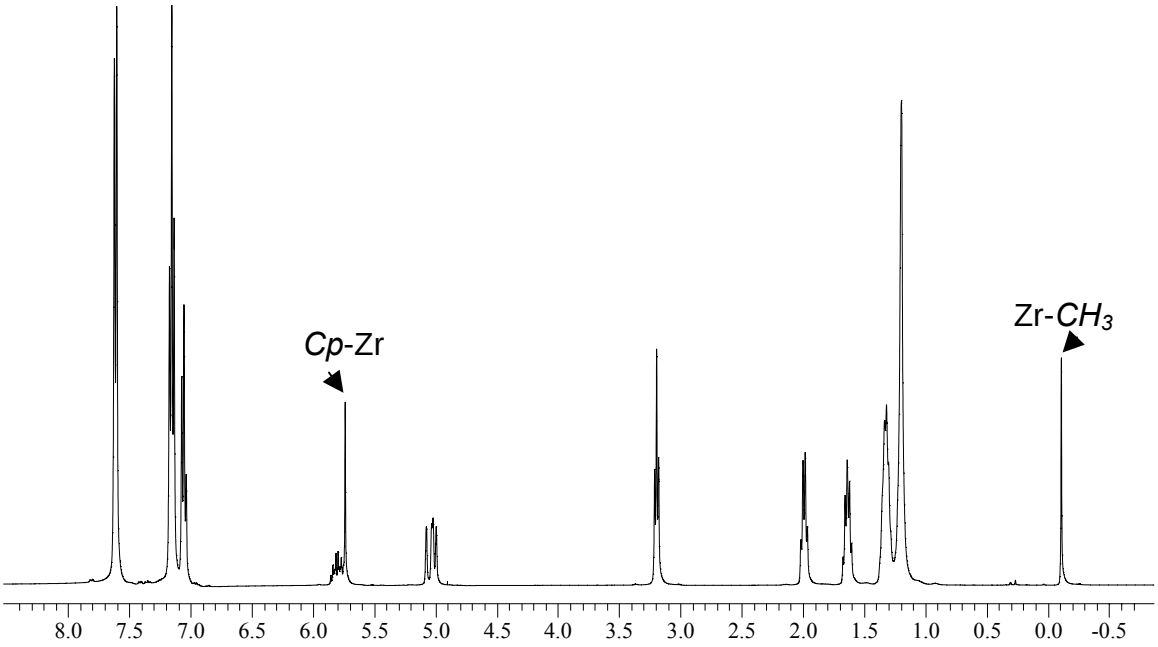

Figure 28b. ^{1}H NMR spectrum (400 MHz, C_6D_6) of (10:1) trityloxydecene **C** to Cp_2ZrMe_2.

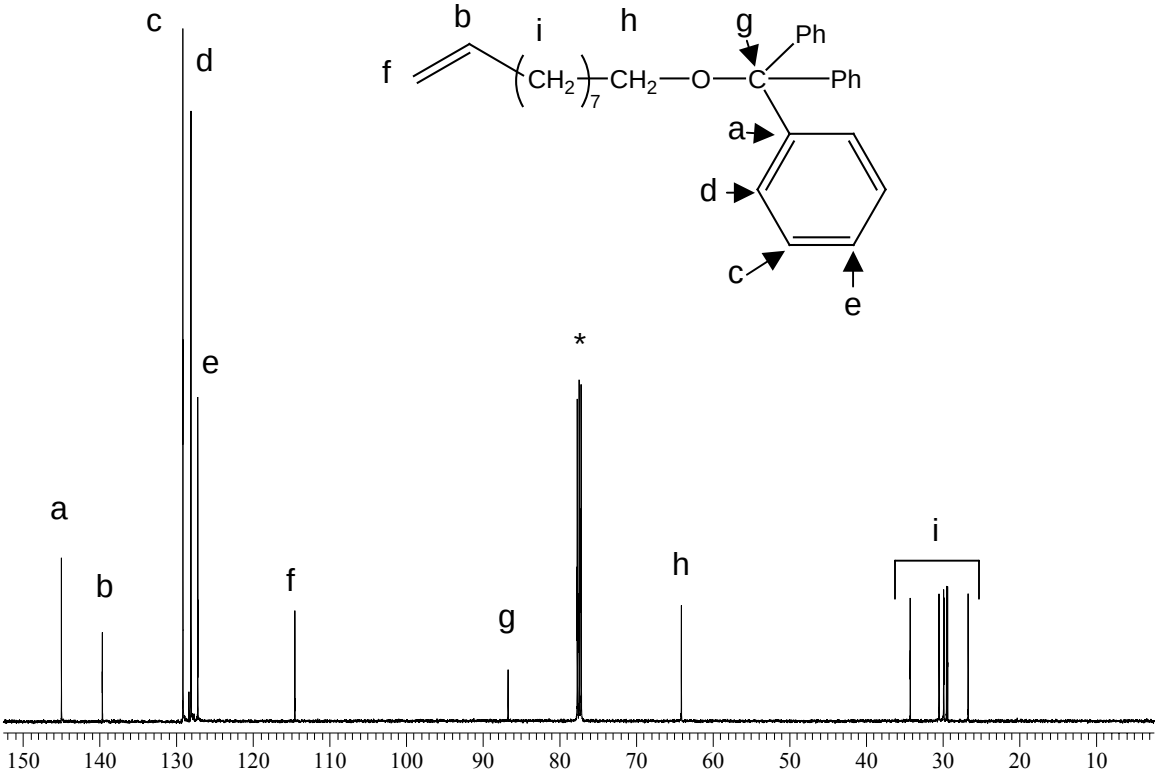

Figure 29. ^{13}C NMR spectrum (125 MHz, *$CDCl_3$) of trityloxydecene **C**.

Table 5. ^{1}H NMR (500 MHz, $CDCl_3$) data of trityloxydecene **C**.

^{1}H	δ, multiplicity, integration
Ph (*ortho*-***H***)	(7.48, d, 2H)
Ph (*meta*-***H***)	(7.32, t, 2H)
Ph (*para*-***H***)	(7.25, t, 1H)
CH_2=C***H***$(CH_2)_8OCPh_3$	(5.84, dddd, 1H)
C***H***$_2$=CH$(CH_2)_8OCPh_3$	(5.02, d, 1H)
C***H***$_2$=CH$(CH_2)_8OCPh_3$	(4.96, d, 1H)
CH_2=CH$(CH_2)_7$C***H***$_2OCPh_3$	(3.08, t, 2H)
CH_2=CH(C***H***$_2)_7CH_2OCPh_3$	(2.06, m, 2H)
CH_2=CH(C***H***$_2)_7CH_2OCPh_3$	(1.65, m, 2H)
CH_2=CH(C***H***$_2)_7CH_2OCPh_3$	(1.34, m, 10H)

Table 6. ^{13}C NMR (125 MHz, $CDCl_3$) data for trityloxydecene **C**.

^{13}C	*δ ppm*
Ph (*ipso*-***C***)	145.0
CH_2=***C***H$(CH_2)_8OCPh_3$	139.6
Ph (*meta*-***C***)	129.1
Ph (*ortho*-***C***)	128.2
Ph (*para*-***C***)	127.2
CH_2=CH$(CH_2)_8OCPh_3$	114.5
CH_2=CH$(CH_2)_8$O***C***Ph_3	86.7
CH_2=CH$(CH_2)_7$***C***H_2OCPh_3	64.1
CH_2=CH(***C***$H_2)_7CH_2OCPh_3$	34.2
CH_2=CH(***C***$H_2)_7CH_2OCPh_3$	30.4
CH_2=CH(***C***$H_2)_7CH_2OCPh_3$	29.9
CH_2=CH(***C***$H_2)_7CH_2OCPh_3$	29.8
CH_2=CH(***C***$H_2)_7CH_2OCPh_3$	29.5
CH_2=CH(***C***$H_2)_7CH_2OCPh_3$	29.3
CH_2=CH(***C***$H_2)_7CH_2OCPh_3$	26.7

3.2.1.3 Synthesis of 10-Trimethylsilyoxydecene (D)

The synthesis of monomer **D** (10-trimethylsilyoxydecene) was achieved by the method outlined by Azizi and Saidi.[9a] This method was chosen due to its efficiency, speed of reaction and solvent free conditions. The procedure utilizes hexamethyldisilazane (HMDS), a compound frequently used for the silylation of hydroxyl compounds[9b] , and lithium perchlorate, a catalyst that was found to enhance the silylation power of HMDS[9a]. The reaction is shown in Equation 12.

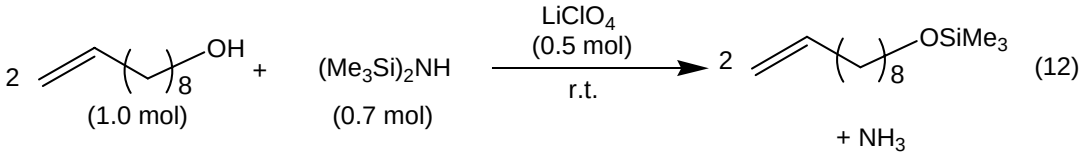

As mentioned above, the silylation power of HMDS is low and the reaction is believed to follow a SN_2-type pathway with attack of the oxygen of the alcohol at the silicon center and simultaneous breaking of the silicon-nitrogen bond. Subsequent deprotonation of the coordinated alcohol leads to one molecule of monomer **D**. The second silyl group can go on to further react with more alcohol and form another molecule of monomer **D** and ammonia gas (Scheme 30).[9c] This pathway generally involves high temperatures and the yields are poor. However, this reaction was found to proceed at room temperature and with high yields in the presence of $LiClO_4$ as described by Azizi and Saidi.[9a] The particular role of the $LiClO_4$ in this reaction was not reported.

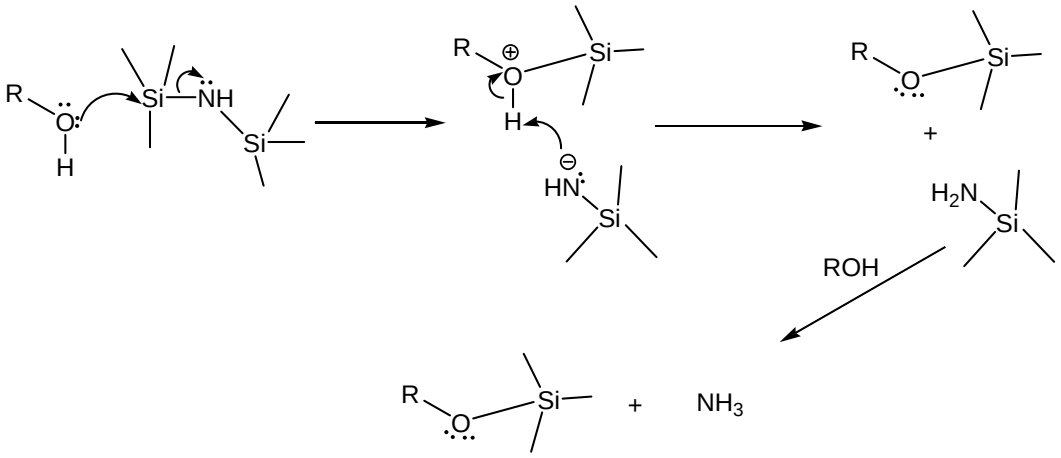

Scheme 30. Mechanism of formation of a silyl ether with HMDS in the presence of heat.

Therefore, this solventless reaction involved combining 9-decen-1-ol (1 mol) with HMDS (0.7 mol) and lithium perchlorate (0.5 mol), and allowing the mixture to stir overnight. The byproduct of the reaction was ammonia gas, and the catalyst $LiClO_4$ was recovered by filtration, after the product was dissolved in methylene chloride. After removal of the methylene chloride, the crude product **D** was dissolved in hexanes and purified (as with all monomers **A-D**) by passing through a 5 - 6 cm activated alumina column under argon. The product isolated after hexane removal was a colourless liquid and the yield of the reaction was high (89 %). The ^{1}H and ^{13}C NMR spectra of monomer **D** are shown in Figures 30 and 31 and the numerical data and assignments are given in Tables 7 and 8. The ^{1}H and ^{13}C NMR assignments were based upon chemical shifts of similar known compounds such as 9-decen-1-ol, in addition with literature values for trimethylsilyl ether resonances.[8a,b,12] In the ^{1}H NMR, in addition to the expected resonances as in monomers **A** – **C**, it can be seen that the triplet of the methylene protons next to the oxygen resonates at δ 3.55, and the methyl protons on the silyl group are at δ 0.9. The ^{13}C NMR data are consistent with the structure of monomer **D**, especially the

presence of the single peak at δ 62.8 (-CH_2-O-$SiMe_3$) and the peak at δ -0.33 (-CH_2-O-SiMe_3), which signify successful protection with a trimethylsilyl group. In addition, a high resolution mass spectrum was obtained for monomer **D** and compared very well with the theoretical prediction ($M + H^+$, calc. 229.1909, found 229.1904). Despite several attempts, a satisfactory elemental analysis for this monomer could not be obtained (calculated C: 68.35, H: 12.36, found C: 65.70, H: 11.42). Also shown in Figure 32 is the monomer **D** with Cp_2ZrMe_2, demonstrating no cleavage of the Zr-Me bonds in Cp_2ZrMe_2 and/or new Cp resonances indicating that monomer **D** was indeed free of hydroxyl impurities.

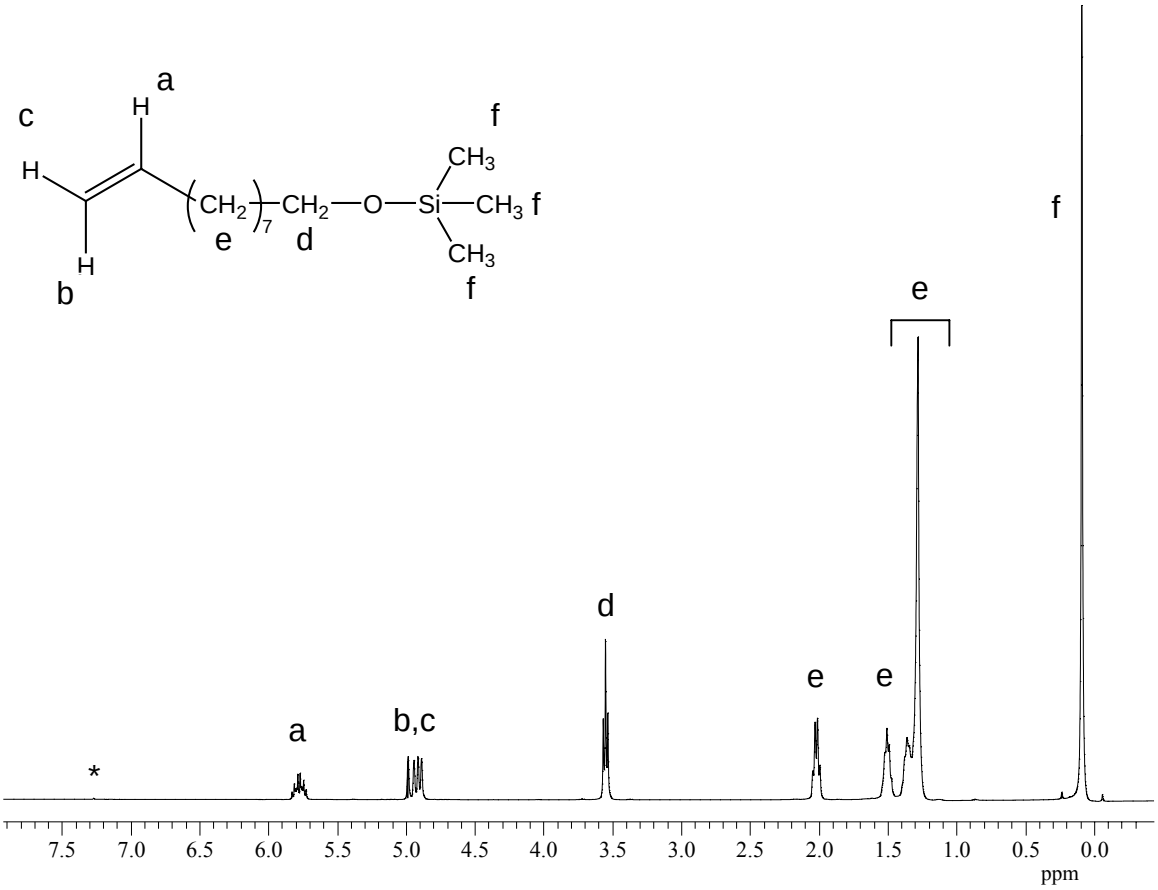

Figure 30. ^{1}H NMR spectrum (400 MHz, *$CDCl_3$) of trimethylsilyloxydecene **D**.

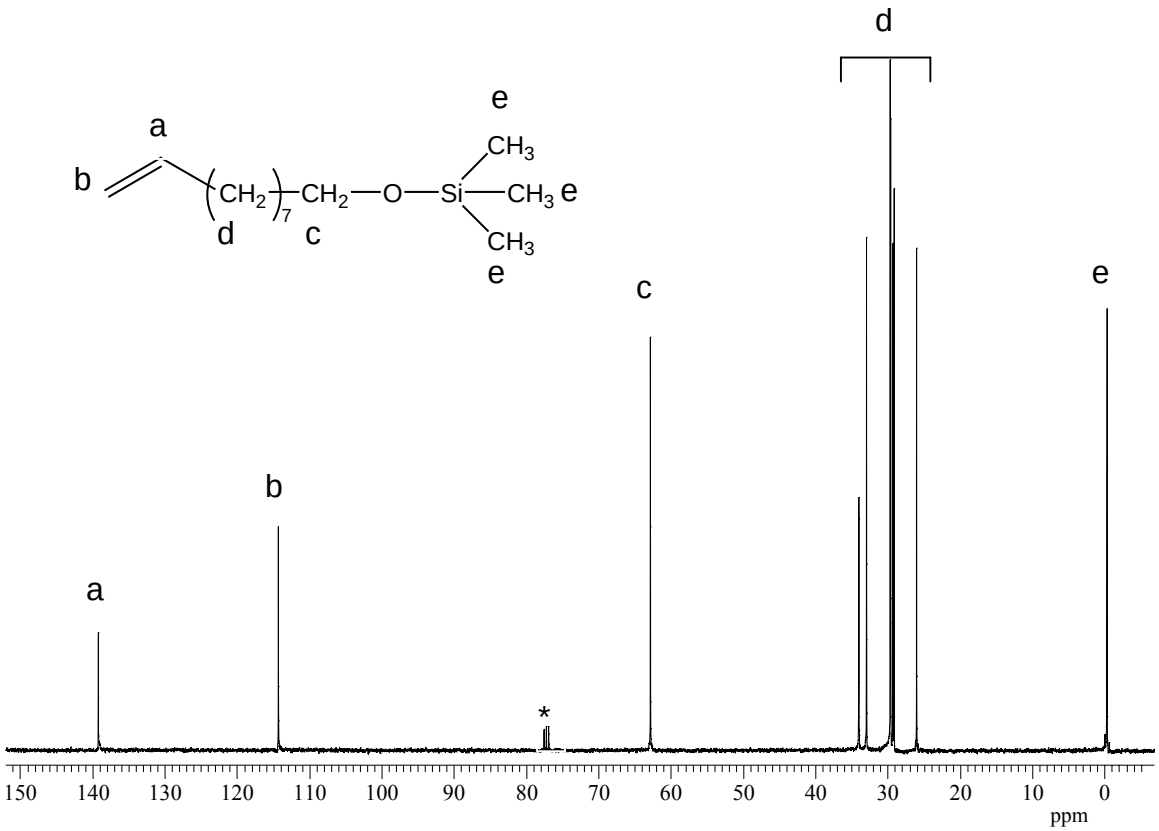

Figure 31. ^{13}C NMR spectrum (100 MHz, *$CDCl_3$) of trimethylsilyloxydecene **D**.

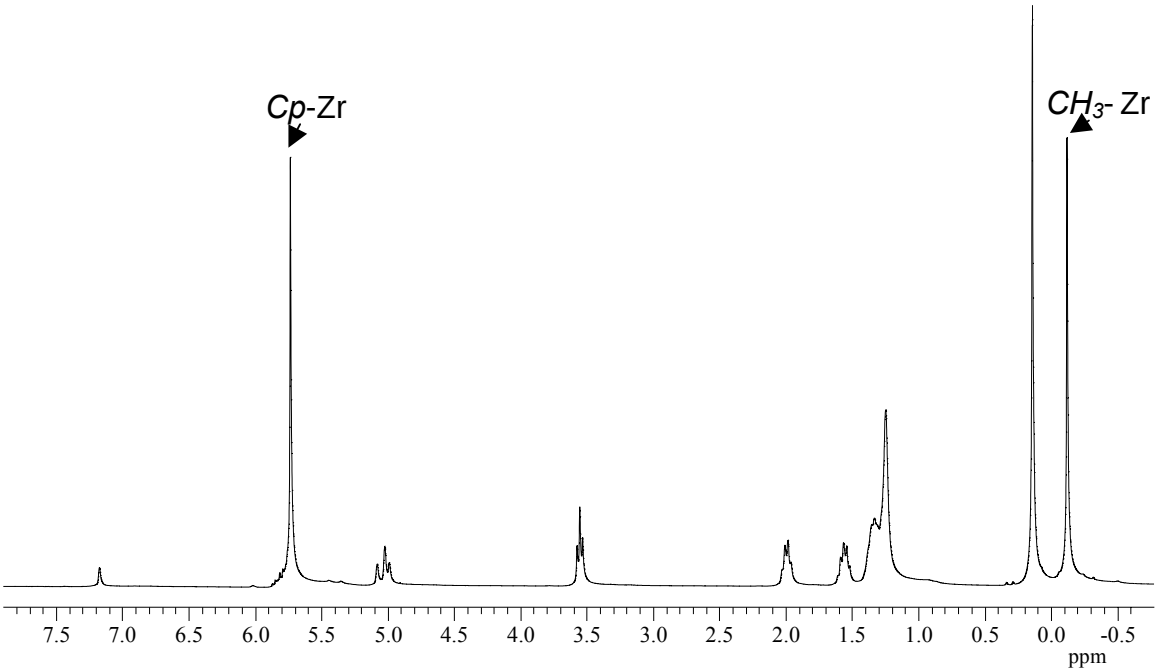

Figure 32. ^{1}H NMR spectrum (300 MHz, *C_6D_6) of (5:1) monomer **D** to Cp_2ZrMe_2.

Table 7. ^{1}H NMR (400 MHz, $CDCl_3$) data of trimethylsilyloxydecene **D**.

^{1}H	δ, multiplicity, integration
$CH_2=C\boldsymbol{H}(CH_2)_8OSiMe_3$	(5.78, dddd, 1H)
$C\boldsymbol{H}_2=CH(CH_2)_8OSiMe_3$	(4.96, d, 1H)
$C\boldsymbol{H}_2=CH(CH_2)_8OSiMe_3$	(4.90, d, 1H)
$CH_2=CH(CH_2)_7C\boldsymbol{H}_2OSiMe_3$	(3.55, t, 2H)
$CH_2=CH(C\boldsymbol{H}_2)_7CH_2OSiMe_3$	(2.02, m, 2H)
$CH_2=CH(C\boldsymbol{H}_2)_7CH_2OSiMe_3$	(1.50, m, 2H)
$CH_2=CH(C\boldsymbol{H}_2)_7CH_2OSiMe_3$	(1.32, m, 10H)
$CH_2=CH(CH_2)_7CH_2OSi\boldsymbol{Me}_3$	(0.90, s, 9H)

Table 8. ^{13}C NMR (100 MHz, $CDCl_3$) data for trimethylsilyoxydecene **D**.

^{13}C	*ppm*
$CH_2=\boldsymbol{C}H(CH_2)_8OSiMe_3$	139.3
$\boldsymbol{C}H_2=CH(CH_2)_8OSiMe_3$	114.4
$CH_2=CH(CH_2)_7\boldsymbol{C}H_2OSiMe_3$	62.9
$CH_2=CH(\boldsymbol{C}H_2)_7CH_2OSiMe_3$	34.1
$CH_2=CH(\boldsymbol{C}H_2)_7CH_2OSiMe_3$	33.0
$CH_2=CH(\boldsymbol{C}H_2)_7CH_2OSiMe_3$	29.8
$CH_2=CH(\boldsymbol{C}H_2)_7CH_2OSiMe_3$	29.7
$CH_2=CH(\boldsymbol{C}H_2)_7CH_2OSiMe_3$	29.2
$CH_2=CH(\boldsymbol{C}H_2)_7CH_2OSiMe_3$	26.1
$CH_2=CH(CH_2)_7CH_2OSi\boldsymbol{Me}_3$	-0.24

3.2.1.4 Synthesis of 10-Triphenylsilyoxydecene (E)

The synthesis of monomer **E** (10-triphenylsilyloxydecene) was accomplished using the method outlined by Piers *et al.*,[10a] who reported several successful silylation reactions with a variety of other alcohols.[10b,c] Therefore, it was tested and found that this method was an effective silylating route for 9-decen-1-ol. This synthetic route involves using trispentafluoroborane, $B(C_6F_5)_3$, as a catalyst for the effective dehydrogenative silylation of the alcohol. The reaction for this synthesis is shown in Equation 13. The byproduct of this reaction was hydrogen gas.

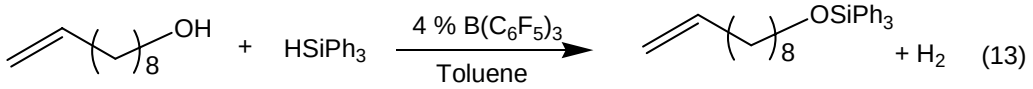

The mechanism of this reaction was discussed by Piers *et al.* and it was found that the key step was the dissociation of the borane-alcohol in order for the borane to interact with the R_3SiH and effect silation of the alcohol (Scheme 31).[10a]

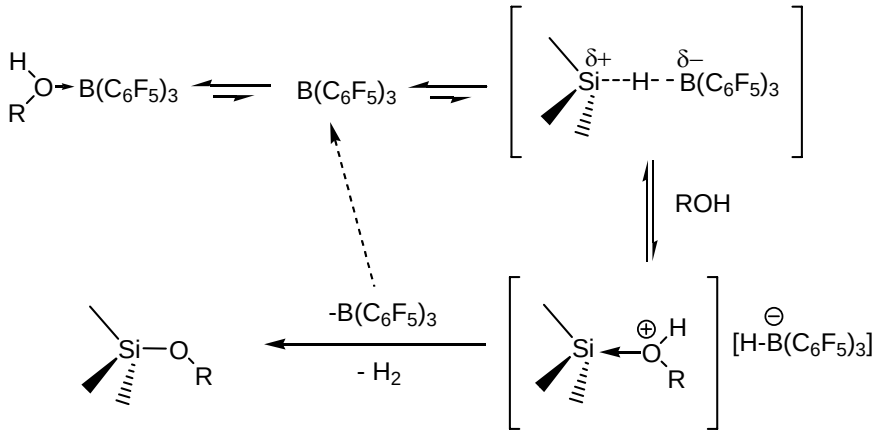

Scheme 31. Proposed mechanism of silylation of an alcohol using $B(C_6F_5)_3$.

This proposed mechanism stems from previous extensive work that Piers had done with hydrosilation of carbonyl functions.[10b,c] It was found that combining a catalytic amount of $B(C_6F_5)_3$ with triphenylsilane and 9-decen-1-ol generates the monomer **E** as a viscous, colourless oil in good yields (80 %). Prior to large scale reaction of monomer **E**, the reaction was monitored by ^1H NMR spectroscopy by observing the disappearance of the starting material and generation of product. Allyl alcohol has been silylated by Piers *et al.* and the time frame was found to be 72 h at room temperature and this procedure was used as a guide.[10a] It was found that for monomer **E**, the reaction was complete after 68 h at room temperature. After dissolving monomer **E** in hexanes, passing it through an activated alumina column to remove any residual impurities, and eventual removal of hexanes overnight, the monomer **E** was characterized by ^1H and ^{13}C NMR spectroscopy, high resolution mass spectrometry and elemental analysis. The ^1H and ^{13}C NMR spectra of monomer **E** are shown in Figures 33 and 34 and the numerical data are shown in Tables 9 and 10. The ^1H and ^{13}C NMR assignments were based upon chemical shifts of known similar compounds such as 9-decen-1-ol, in addition with values obtained from known literature for triphenylsilyl ether resonances.[8a,b,12]

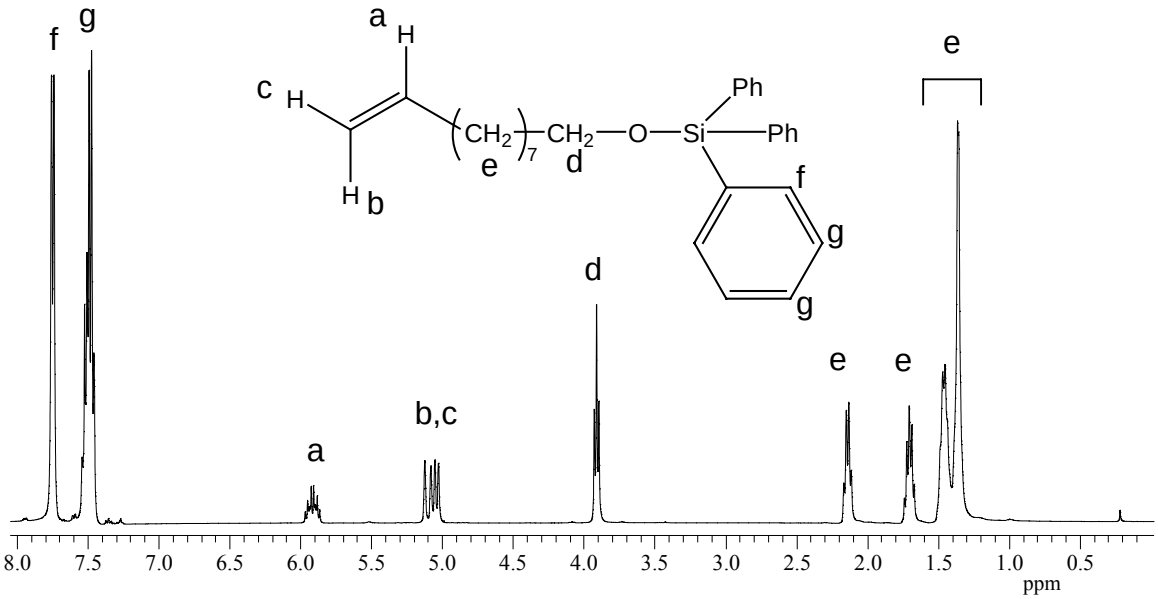

Figure 33. ^{1}H NMR spectrum (400 MHz, $CDCl_3$) of monomer **E**.

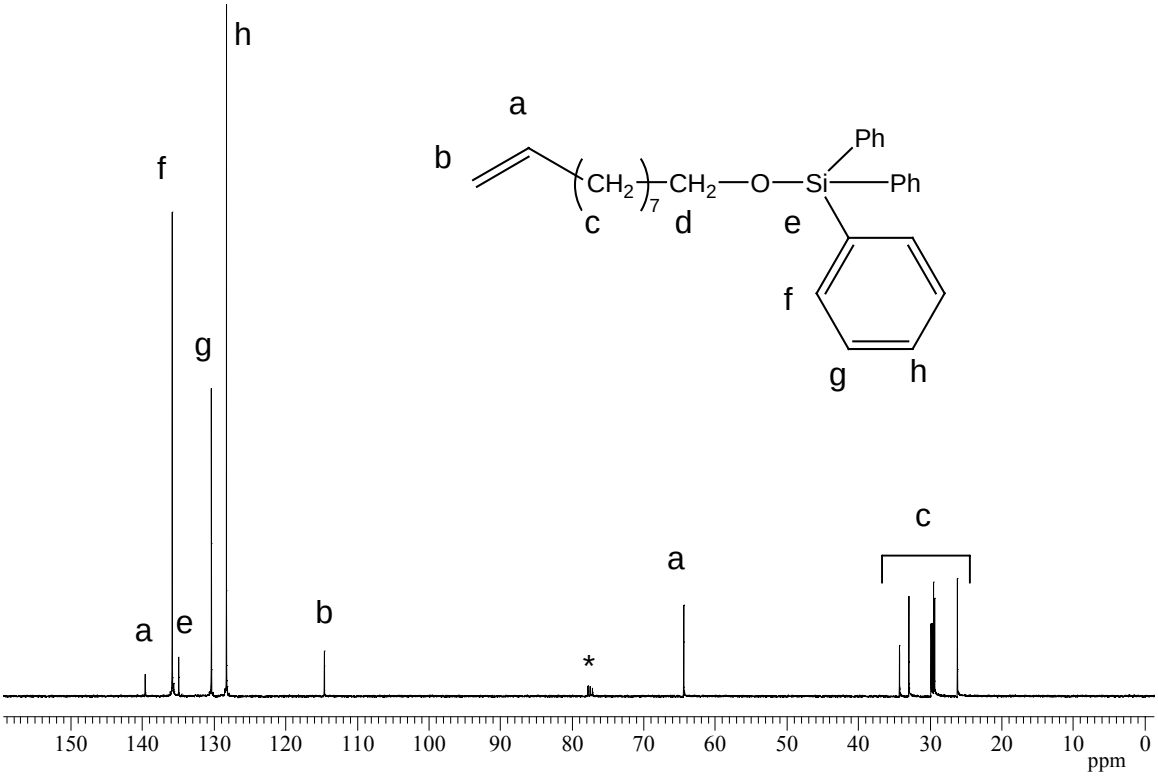

Figure 34. ^{13}C NMR spectrum (100 MHz, *$CDCl_3$) of monomer **E.**

Table 9. ^{1}H NMR (400 MHz, $CDCl_3$) data of triphenylsilyloxydecene **E**.

^{1}H	δ, multiplicity, integration
Ph (ortho-***H***)	(7.75, d 6H)
Ph (meta,para-***H***)	(7.63-7.43, m, 9H)
CH_2=C***H***$(CH_2)_8OSiPh_3$	(5.92, dddd, 1H)
C***H***$_2$=CH$(CH_2)_8OSiPh_3$	(5.10, br d, 1H)
C***H***$_2$=CH$(CH_2)_8OSiPh_3$	(5.04, br d, 1H)
CH_2=CH$(CH_2)_7$C***H***$_2OSiPh_3$	(3.91, t, 2H)
CH_2=CH(C***H***$_2)_7CH_2OSiPh_3$	(2.14, m, 2H)
CH_2=CH(C***H***$_2)_7CH_2OSiPh_3$	(1.70, m, 2H)
CH_2=CH(C***H***$_2)_7CH_2OSiPh_3$	(1.40, m, 10H)

Table 10. ^{13}C NMR (100 MHz, $CDCl_3$) data for triphenylsilyoxydecene **E**.

^{13}C	*ppm*
CH_2=***C***H$(CH_2)_8OSiPh_3$	139.6
Si***Ph***$_3$ (*meta*-***C***)	135.8
Si***Ph***$_3$ (*ipso*-***C***)	134.9
Si***Ph***$_3$ (*ortho*-***C***)	130.3
Si***Ph***$_3$ (*para*-***C***)	128.2
CH_2=CH$(CH_2)_8OSiPh_3$	114.6
CH_2=CH$(CH_2)_7$***C***H_2OSiPh_3	64.4
CH_2=CH(***C***$H_2)_7CH_2OSiPh_3$	34.2, 32.9, 29.8, 29.7, 29.5, 29.3, 26.2

As it can be seen in Figure 33, the phenyl peaks are present at δ 7.79 – 7.43 on the silicon and the methylene protons next to the oxygen are more deshielded (δ 3.91) than that in ordinary 9-decen-1-ol. This can be attributed to the significant decrease of the electron density on the oxygen, by electron delocalization between oxygen and silicon through pπ – dπ interaction. Also shown in Figure 35 is the monomer **E** with Cp_2ZrMe_2 demonstrating no cleavage of the Zr-Me bonds in Cp_2ZrMe_2 and/or new Cp resonances indicating that monomer **E** was indeed free of hydroxyl impurities.

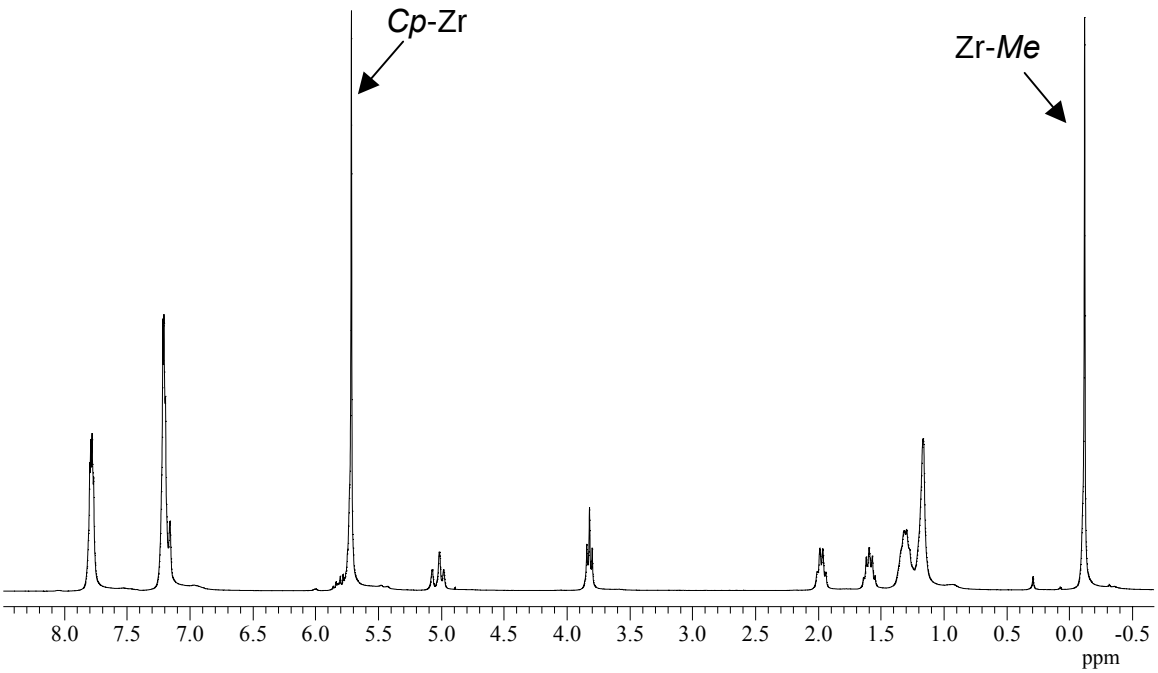

Figure 35. ^{1}H NMR spectrum (300 MHz, C_6D_6) of monomer **E** with Cp_2ZrMe_2.

3.2.1.5 Synthesis of *n*-decyl methyl ether (F)

The synthesis of *n*-decyl methyl ether **F** was achieved using the same procedure as in Equation 10, but using *n*-decyl alcohol, to afford a clear oil in 67 % yield (Equation 14).

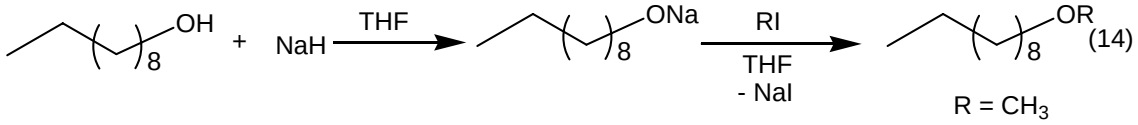

The ^{1}H NMR of the spectrum is shown in Figure 36. The triplet of the –C*H*$_2$OMe can be seen at δ 3.38, while the singlet for the methoxy is at δ 3.34. The multiplets for the methylene protons at δ 1.58 and 1.28 and the methyl end group at δ 0.89. This compound was synthesized for a copolymerization study to be discussed later (Section **3.2.3.4**).

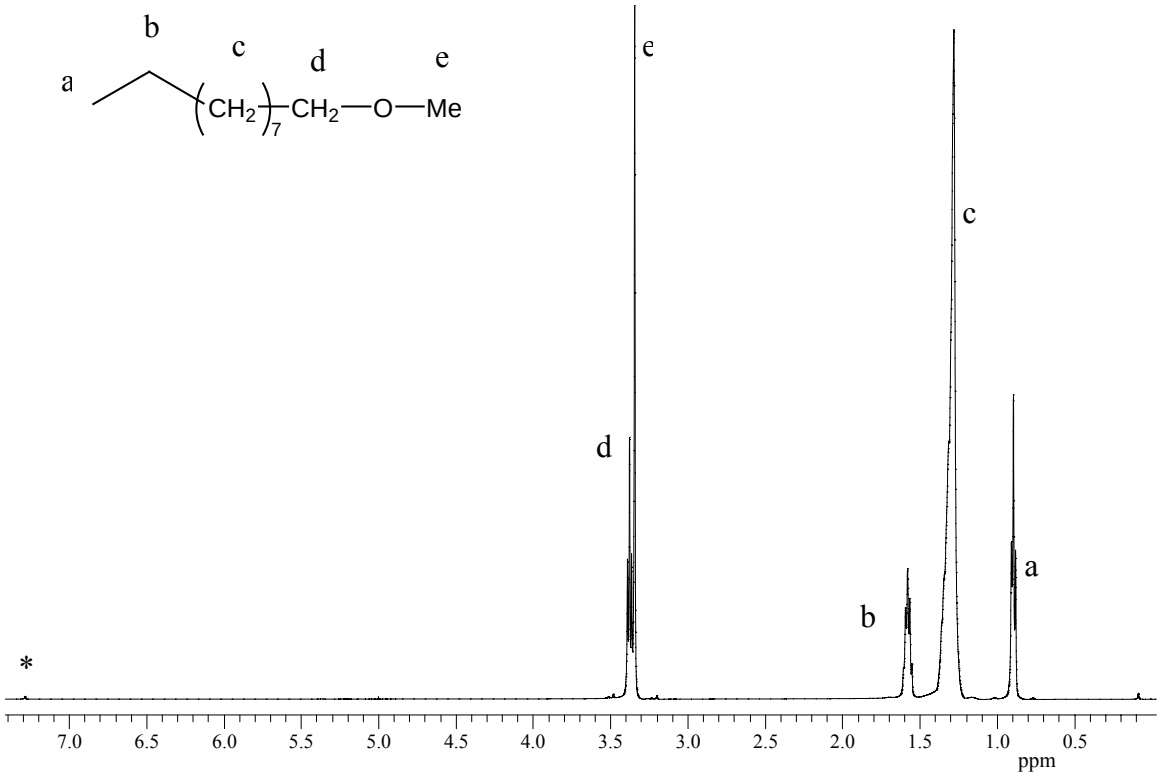

Figure 36. ^{1}H NMR spectrum (500 MHz, *$CDCl_3$) of *n*-decyl methyl ether **F**.

3.2.2 Homopolymerization Studies of Polar Monomers A – D

In an attempt to analyze the homopolymerization behaviour of the synthesized protected polar monomers **A – D** with potential early metal metallocene catalyst systems, an NMR study was undertaken. This study was anticipated to yield insight as to how future experiments involving copolymerization studies with ethylene and propylene may be approached, as well as information as to how the polar monomers interact with an early metal catalyst. In each case discussed below and for simplicity of the ^{1}H NMR spectrum, the catalyst system used was the *in situ* generated zwitterionic compound **G**, $[Cp_2ZrMe][MeB(C_6F_5)_3]$. This compound was synthesized by adding a solution of Cp_2ZrMe_2 in chlorobenzene-d_5 to a solution of $B(C_6F_5)_3$ in chlorobenzene-d_5 and shaking the solution vigorously. The $B(C_6F_5)_3$ abstracts a methyl group from the Cp_2ZrMe_2 to form the zwitterionic compound **G**, which contains a bridging μ-methyl as shown in Scheme 32.

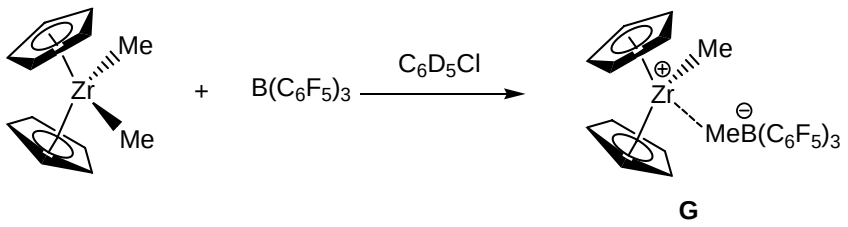

Scheme 32. Formation of zwitterionic compound **G** in C_6D_5Cl.

To this catalyst system **G** were added 5 equivalents of the desired polar monomer **A – D** and the ^{1}H NMR was monitored over time up to 48 h at room temperature. The solvent of choice for these reactions was either chlorobenzene-d_5 or methylene chloride-d_2, mainly to ensure the reaction products remained in solution. Dissolving the

zwitterionic compound in chlorobenzene-d_5 or methylene chloride-d_2 affords yellow solutions, and after addition of the polar monomers **A – D**, each solution turned orange and remained orange for the duration of the experiment with no visible precipitate. Figure 37 shows the ^{1}H NMR spectra of the reaction of **G** with 5 equivalents of monomer **A**. As can be seen in Figure 37, the top spectrum is of monomer **A** in C_6D_5Cl and the second spectrum is of **G** in C_6D_5Cl. The latter spectrum contains three resonances at δ 5.91 (Cp), 0.46 (Zr-*Me*) and 0.32 (*Me*B(C_6F_5)$_3$). The broad peak at δ 0.32 was consistent with the μ-methyl on the counteranion bridging to the metal center.[13]

When solutions of **A** and **G** were combined, the spectrum at 0 min shows a new Cp resonance at δ 5.95 and a new Zr-*Me* resonance at δ 0.58, and disappearance of the broad peak at δ 0.32, indicating displacement of the counteranion from zirconium. The protons of the methyl group of the free counteranion are believed to be at δ 1.1. The vacant site on the metal is probably occupied by the oxygen of the monomer **A**, and this is justified by the exchange broadening of the –C*H*$_2$-O-CH$_3$ triplet at δ 3.25 and methoxy group singlet (–CH$_2$-O-C*H*$_3$) at δ 3.16 (Scheme 33).

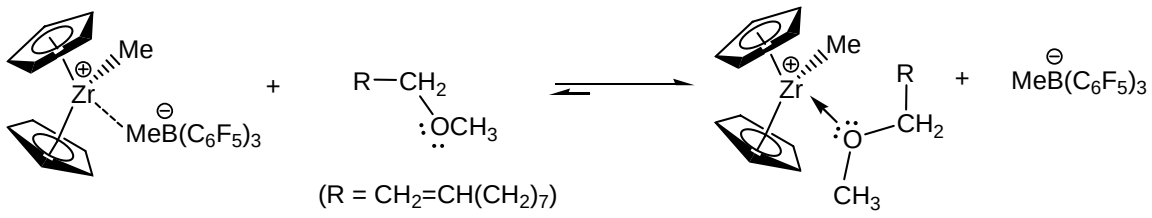

Scheme 33. Coordination of the polar monomer to compound **G**.

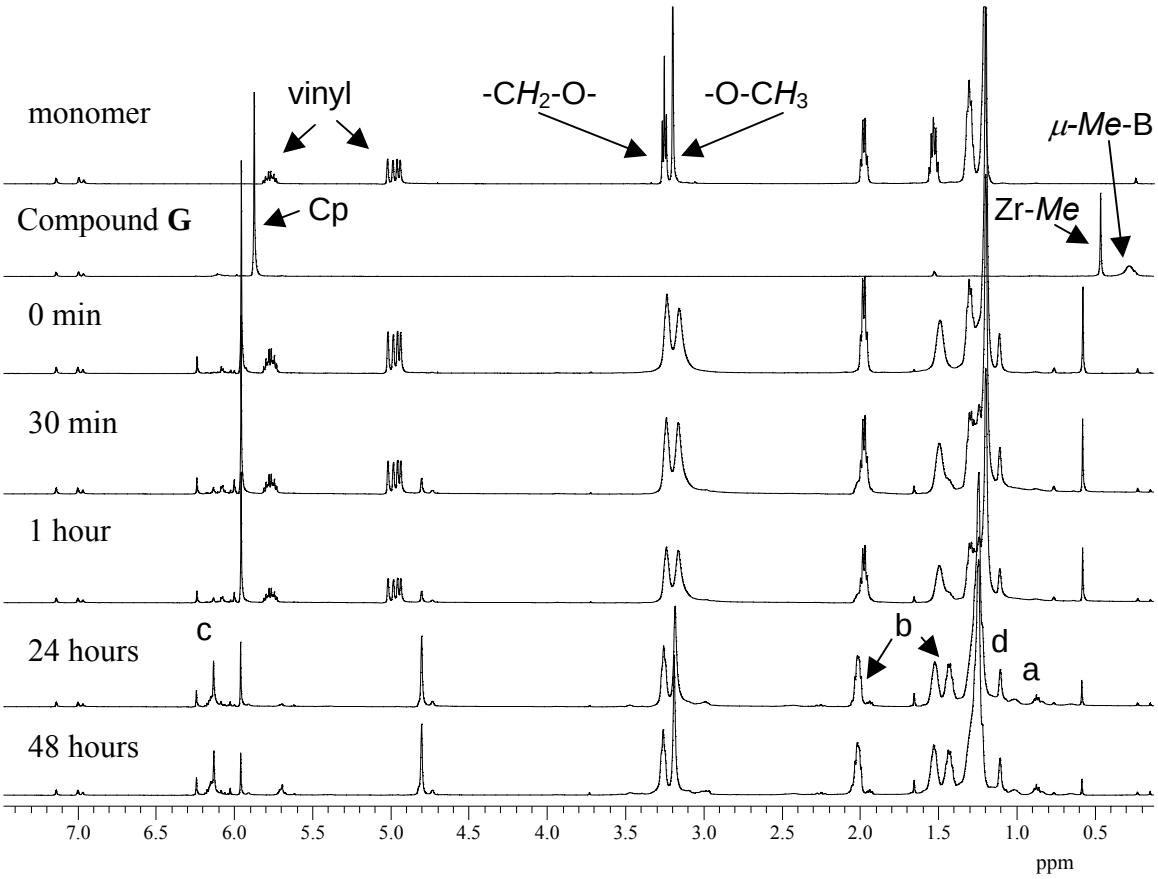

Figure 37. Stacked plots (500 MHz, C_6D_5Cl) of monomer disappearance with time for 5 equiv. of monomer **A** (methoxydecene) with **G** (a - new methyl peak, b – new methylene peak, c – new Cp peaks, d – free counteranion).

In addition, the vinyl protons are unchanged, signifying no coordination of the vinyl group to the metal. Therefore, the new Cp and Zr-*Me* protons can be attributed to the new oxygen bound monomer to the metal center. Interestingly, as the time elapses to 1 h and eventually 24 and 48 h, the vinyl resonances disappear, new Cp resonances emerge (from δ 6.24 – 6.00), the methoxydecene triplet and singlet sharpen slightly, a new methylene peak occurs at δ 1.44 and the Zr-*Me* resonance weakens. All these spectral changes suggest the possible formation of oligomers with time. Especially, the disappearance of the vinyl protons, a new methylene peak at δ 1.44 and a barely visible triplet at δ 0.87, which could be a methyl group on an oligomer chain end, all support this finding. Despite

these observations over long periods of time, initial spectra analysis shows the methoxydecene to be a poor protecting group, as seen by broadening of methoxy region of the spectra and coordination to the metal center. Given enough time, however, a reaction takes place. Large scale reactions involving **A** and **G** resulted in the isolation of a yellowish sticky wax. The identification of this material was attempted via electrospray mass spectrometry and MALDI-TOF, but no isotopic pattern consistent with oligomers of this monomer were identified.

Similar experiments with other monomers resulted in some interesting outcomes. Monomer **B**, with the benzyl protecting group, resulted in spectra that are consistent with a reaction taking place (Figure 38), as in Figure 37. However, broadening of the triplet next to oxygen at δ 3.49 is not significant as in Figure 37 with monomer **A**, indicating the benzyl group could be potentially an effective protecting group. The vinyl resonances largely disappear within 1 h, in contrast to that in Figure 37 with monomer **A**, where 24 h were needed for the vinyl resonances to disappear. The disappearance of the Zr-Me resonance at δ 0.52 in Figure 38 seems to be slower than that in Figure 37 at greater reaction times as evident by observing the intensity of each singlet at 24 h. The free counteranion peak may be at δ 1.1 (as in Figure 37), but it is obscured by the dominant peak at δ 1.3. Furthermore, as in Figure 37, the spectra in Figure 38 show new Cp resonances (δ 6.70 to 6.40), new methylene peaks (region from δ 2.1 to 1.7) and possible new methyl resonances at ~ δ 0.86. Again, large scale reactions and characterization by electrospray mass spectrometry and MALDI-TOF of the isolated product resulted in no identifiable isotopic patterns consistent with oligomers of monomer **B**. As it was confirmed by Figures 37 and 38, the vinyl groups do disappear with time indicating

possible oligomer formation. This system is too complicated to completely assign due to unidentifiable side reactions and/or presence of unforeseen impurities.

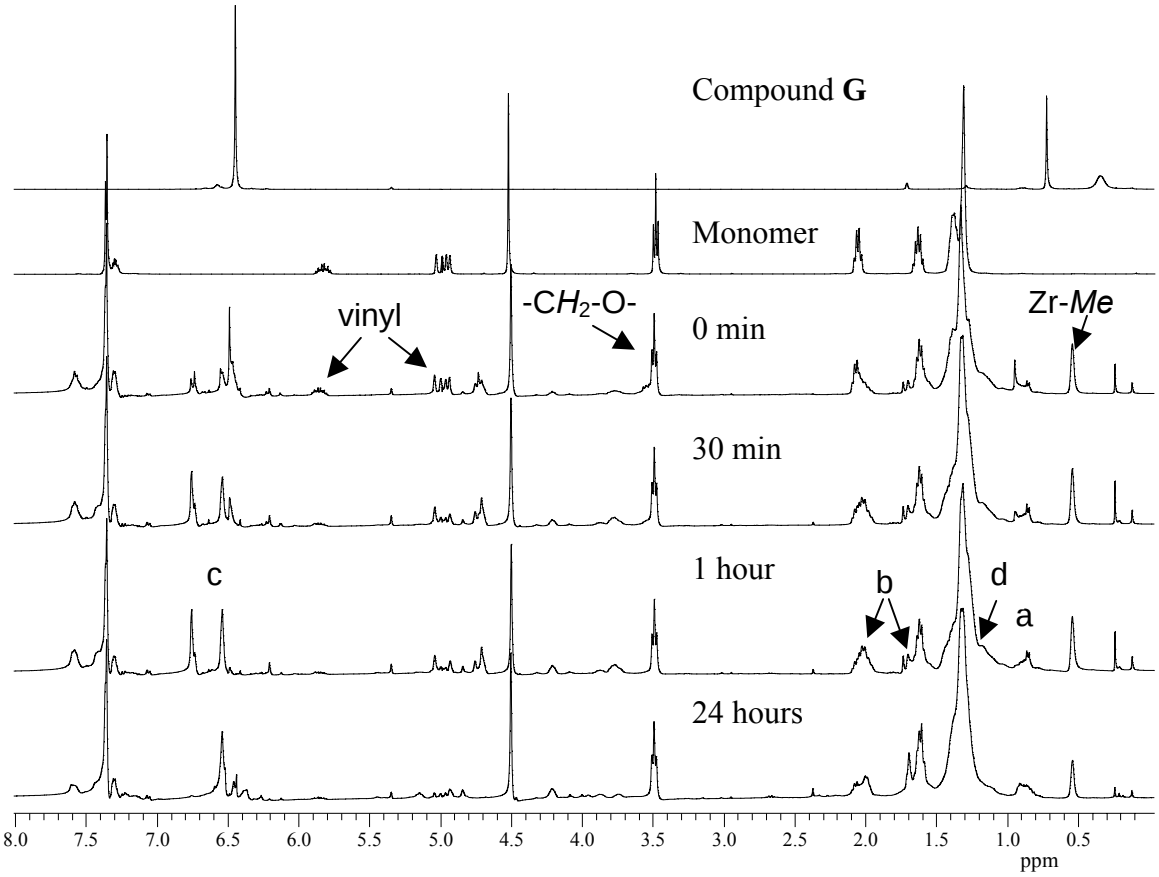

Figure 38. Stacked plots (400 MHz, CD_2Cl_2) of monomer disappearance with time for 5 equiv. of monomer **B** (benzyloxydecene) with **G** (a – new methyl, b – new methylene, c – new Cp, d – possible free counteranion peak).

Looking ahead for when the bulkier monomers **C** – **E** were to be used, we expected similar or better results. NMR studies with monomers **C** – **E** gave results that were surprising (Figures 39-41). While monomers **A** and **B** showed the *complete* disappearance of resonances in the vinyl region (δ 4.70-6.00) within at least 24 h, this was not the case for monomers **C** – **E**, for which the vinyl resonances weakened little. Figure 39 shows the spectra for the reaction of **G** with monomer **D**. As seen in Figure 39,

the complete disappearance of the vinyl region with time was not observed even after 24 h. However, new resonances were observed in the methylene region (δ 2.1 to 1.7) and methyl region (δ 0.86) consistent with some formation of possible oligomers.

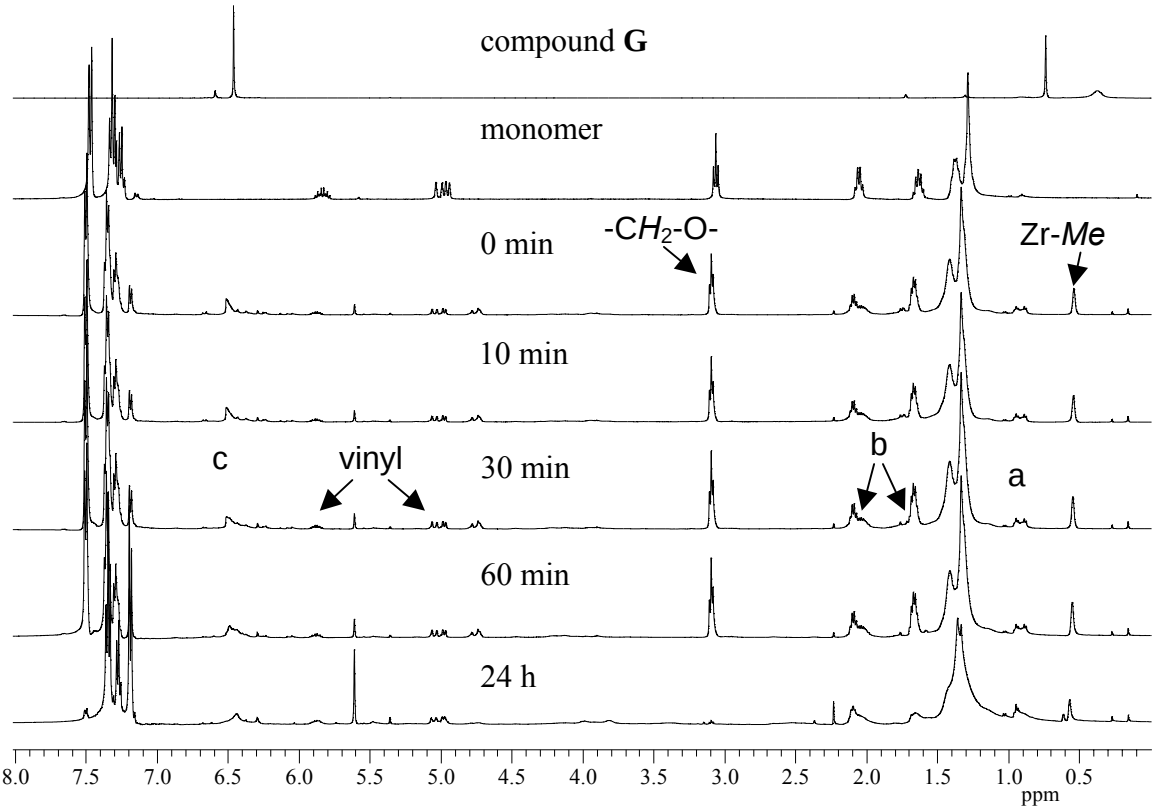

Figure 39. Stacked plots (500 MHz, CD_2Cl_2) of monomer disappearance with time for 5 e.q. trityloxydecene **C** with **G** (a – new methyl, b – new methylene, c – new Cp).

In addition, there was no broadening of the methylene resonance next to the oxygen of the trityl group, signifying that the trityl group was an effective protecting group.

In contrast, Figure 40 shows that the resonances in the vinyl region of the spectrum of monomer **D** remained largely unchanged, although some oligomerization occurred as indicated by the broadening in the methylene (δ 2.1 to 1.7) and methyl regions (δ 0.86) of each spectrum. Again, there was no broadening of the methylene protons next to the trimethyl protecting group, demonstrating that the trimethylsilyl group

was also an effective protecting group. Lastly, monomer **E** in Figure 41 shows similar results to that of the trityl protecting group in Figure 39 with regards to the vinyl region (δ 4.70 to 6.00) containing resonances even after 24 hr. Also evidence for oligomers were seen in the methylene and methyl regions as in Figure 39. Interestingly, the methylene next to the oxygen was broader than those for monomers **C** and **D**. This observation suggests that some interaction of the oxygen on the monomer could exist with the metal center.

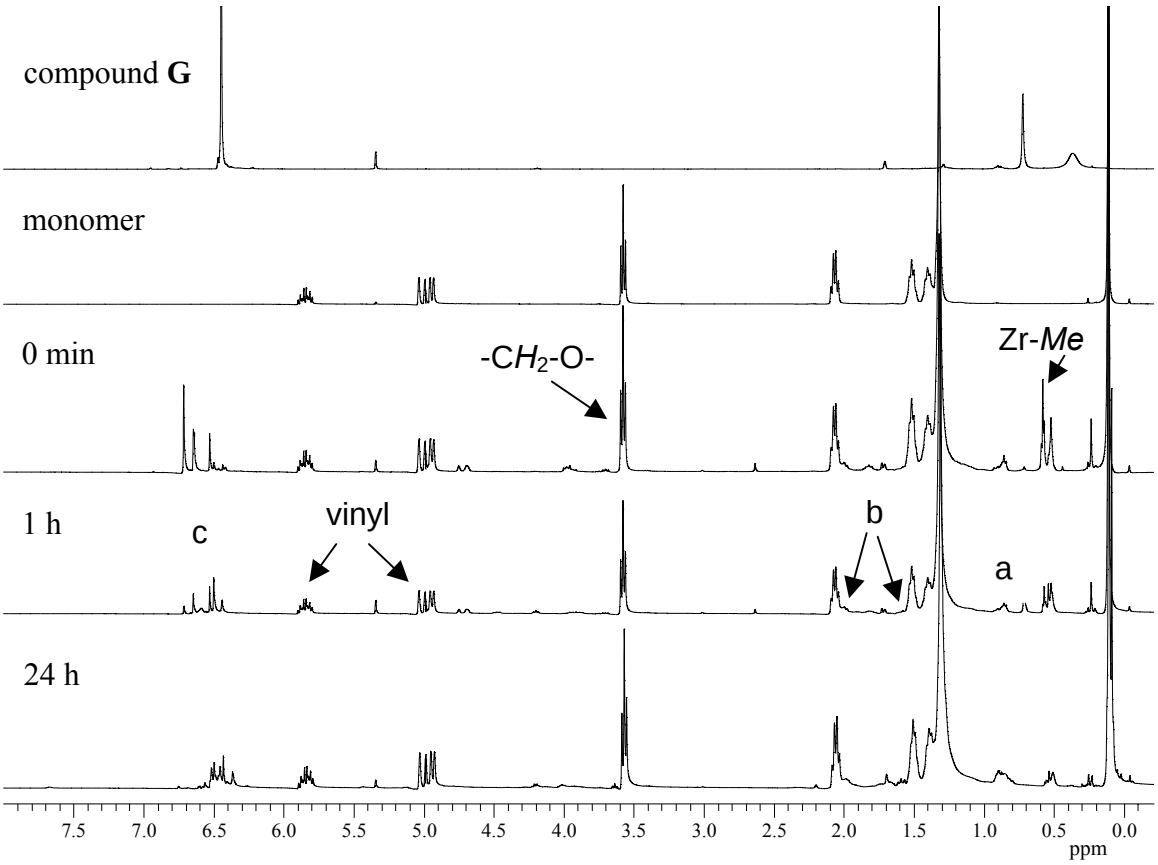

Figure 40. Stacked plots (400 MHz, CD_2Cl_2) of monomer disappearance with time for 5 equiv. of monomer **D** (trimethylsiloxydecene) with **G** (a – new methyl, b – new methylene, c – new Cp).

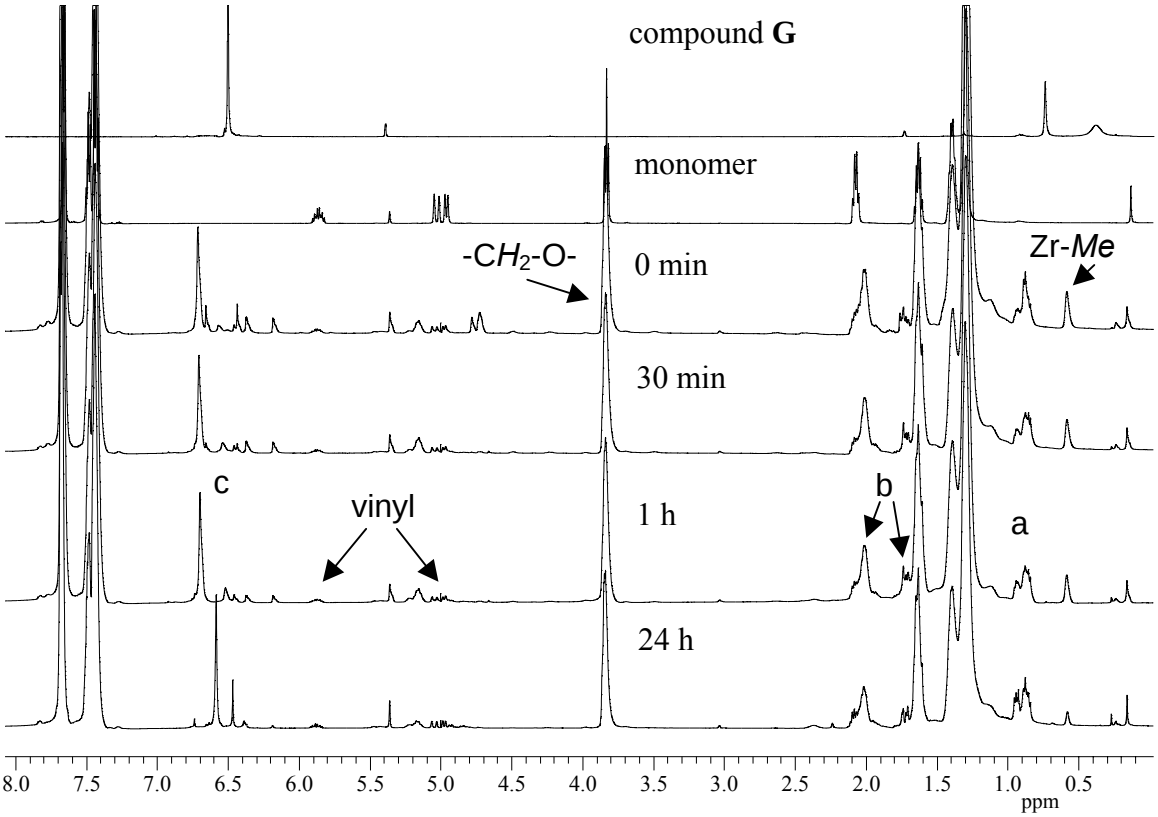

Figure 41. Stacked plots (500 MHz, CD_2Cl_2) of monomer disappearance with time for 5 equiv. of monomer **E** (triphenylsiloxydecene) with **G** (a – new methyl, b – new methylene, c – new Cp).

Therefore, even with little evidence of homopolymerization or oligomerization occurring with these bulkier monomers **C** - **E**, attempts to copolymerize these monomers with olefins could prove to be effective if reaction conditions (e.g. cocatalyst, solvent, etc.) and mode of polar monomer addition are examined.

In summary, the above NMR experiments involving monomers **A** – **E** displayed considerable variance in the regions of δ 0 – 1.2 and in the Cp regions (δ 6 – 7). These major differences make it difficult to ascertain the outcome of future co- and homopolymerization attempts. However, the monomer **A** system gave some useful initial

information regarding the Cp, Zr-Me and B-Me resonances, as well as how the monomer reacts over time.

3.2.3 Copolymerization Studies of Polar Monomers A – D

After examining homopolymerization attempts and interactions of the chosen monomers **A** – **D** with a simple early metal catalyst system (Section **3.2.2**), our next focus was the investigation and development of methodologies for the incorporation of polar monomers into polyolefins, particularly polyethylene and polypropylene. We chose to work initially with ethers of 9-decen-1-ol. Previous researchers[14a] have found that higher incorporations of polar monomers are generally achieved with monomers containing chains longer than C_6 (such as 10-undecen-1-ol), possibly because of the greater separation of the polar functionality from the C=C bond,[14a,b] and 9-decen-1-ol is also relatively inexpensive. To assess the effectiveness of various groups as masking agents for the hydroxyl group, we chose to work with monomers **A – D**, as these encompass a range of steric requirements and would address the hypothesis that bulkier substituents would hinder ether oxygen coordination and thus would inhibit copolymerization the least.

Our initial study involved copolymerizations with ethylene and propylene using *rac*-Et(Ind)$_2$ZrCl$_2$, an excellent catalyst for the homopolymerization of ethylene and the isospecific polymerization of propylene to isotactic polypropylene (*i*-PP).[15] We utilized two copolymerization procedures, one in which an ethylene or propylene saturated toluene solution of *rac*-Et(Ind)$_2$ZrCl$_2$ and polar monomer was activated by addition of

MAO, and an alternative procedure in which we added the polar monomer 5 minutes *after* activating the solution of ethylene or propylene with precatalyst *rac*-$C_2H_4(Ind)_2ZrCl_2$ with MAO. Initiation of homopolymerization processes is often slower than propagation,[16] so we thought it might be desirable to induce chain growth before addition of polar monomer. Although the latter procedure resulted in some polyethylene or isotactic polypropylene forming in the reaction mixtures, the new copolymers were found to be sufficiently soluble that they could be readily separated from the relatively insoluble polyethylene or isotactic polypropylene. In each copolymerization attempt, ethylene or propylene was continuously fed into the reaction mixture until termination of the reaction.

The concentrations of ethylene or propylene in each reaction mixture were calculated using an equation developed by Ferreira *et al.*,[17a] where Henry's Law and continuous flow of olefin monomer are taken into account (Equation 14, 15).

$$[E] = p_e \times 1.74 \times 10^{-3}\, e^{(1278.6/T)} \qquad (14)$$

$$[P] = p_p \times 7.67 \times 10^{-6}\, e^{(3452.3/T)} \qquad (15)$$

where [E] is the concentration of ethylene and [P] is the concentration of propylene in toluene (mol/L); p_e is the pressure of ethylene (1 atm) and p_p is the pressure of propylene (1 atm); and T is the absolute temperature (in Kelvin). Therefore, the concentration of ethylene was 0.134 M and of propylene was 0.959 M, both at 1 atm, 21 ^oC in toluene as solvent. However, as the temperatures of the polymerization reaction mixtures rose to about 60 ^oC, the alkene concentrations decreased as the reactions proceeded. Therefore,

the initial concentrations would have decreased to 0.081 M ethylene, 0.242 M for propylene, when temperatures reached 60 ^{o}C.

Each copolymerization reaction was quenched with acidified ethanol to destroy the active catalyst and residual MAO, and the resulting mixture was stirred overnight to ensure complete MAO quenching as the polymeric products precipitated. Each copolymer reaction mixture was filtered and the solid products were dried in a vacuum oven overnight at 60 ^{o}C. The copolymers were characterized by ^{1}H and ^{13}C NMR in the desired deuterated chlorinated solvent (e.g. TCE-d_2) or solvent mixtures (*o*-dichlorobenzene (ODCB)/C_6D_6) either at room or high temperatures, depending on the solubilities of the resulting copolymers. The ^{1}H NMR spectrum of each copolymer sample was used to determine the mole percent incorporation of polar monomer in each copolymer. The integration intensities of the methylene resonances next to the oxygen in all polar comonomers (which all resonated at δ3 – 4) were compared to those of the backbone methylene resonances of the polyethylene or polypropylene (~ δ1.4) and expressed as a percentage. For the copolymer studies involving polypropylene and 1-hexene (section **3.2.3.3**), the ^{13}C NMR spectrum of each copolymer was used to calculate the mole percent incorporation of 1-hexene, since the ^{1}H NMR contained overlapping resonances.

The results of the ethylene and propylene copolymerization reactions initiated at 21 °C will be discussed below.

3.2.3.1 Copolymerization Studies of Polar Monomers A – E with Ethylene

The general reaction scheme for copolymerization of polar monomers **A** – **E** with ethylene is shown in Equation 16.

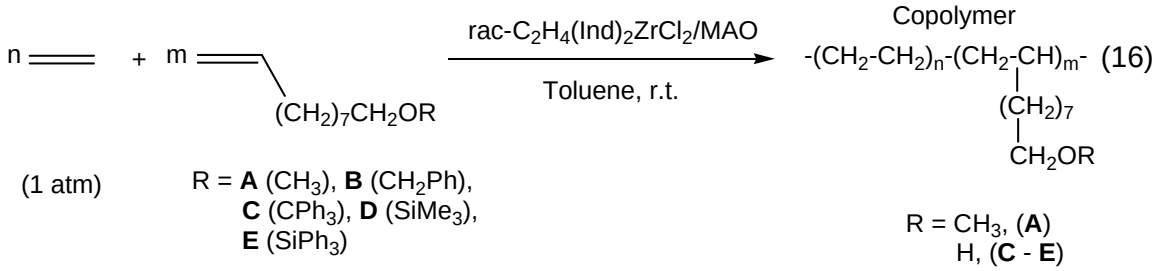

(16)

Figure 42 is a representative ^{1}H NMR spectrum of the copolymer obtained from ethylene copolymerization with monomer **A**. Figure 43 is a representative example of the copolymers from ethylene copolymerization with monomers **C** – **E.** As it can be seen in Figure 42, the methoxy group is left untouched in the final polymer, even after workup. This is unique for monomer **A**, however, as all other monomers **C** - **E** produce hydroxyl containing copolymer materials after work up (Figure 43). The chemical shift of the broadened methylene group in Figure 42 is at δ 3.43 (–C*H*$_2$-O-CH$_3$, triplet) and that of the methoxy group is at 3.37 (–CH$_2$-O-C*H*$_3$, singlet). These values are in good agreement with the literature, where a similar copolymer of ethylene with 10-undecenyl methyl ether has chemical shifts at δ 3.33 (triplet) and δ 3.27 (singlet).[17b] The main chain polyethylene (–C*H*$_2$-)$_n$ resonance occurs at δ 1.38, as well as the polymer methyl end group at δ 0.98, which was used for the calculation of number average molecular weight, M_n.

In Figure 43, the methylene protons next to the hydroxyl group occurs at δ 3.69 (consistent with literature[17b] data of a similar copolymer of ethylene and 10-undecen-1-o1 of δ 3.58) but all the remaining signals due to the polymer main chain and polymer end

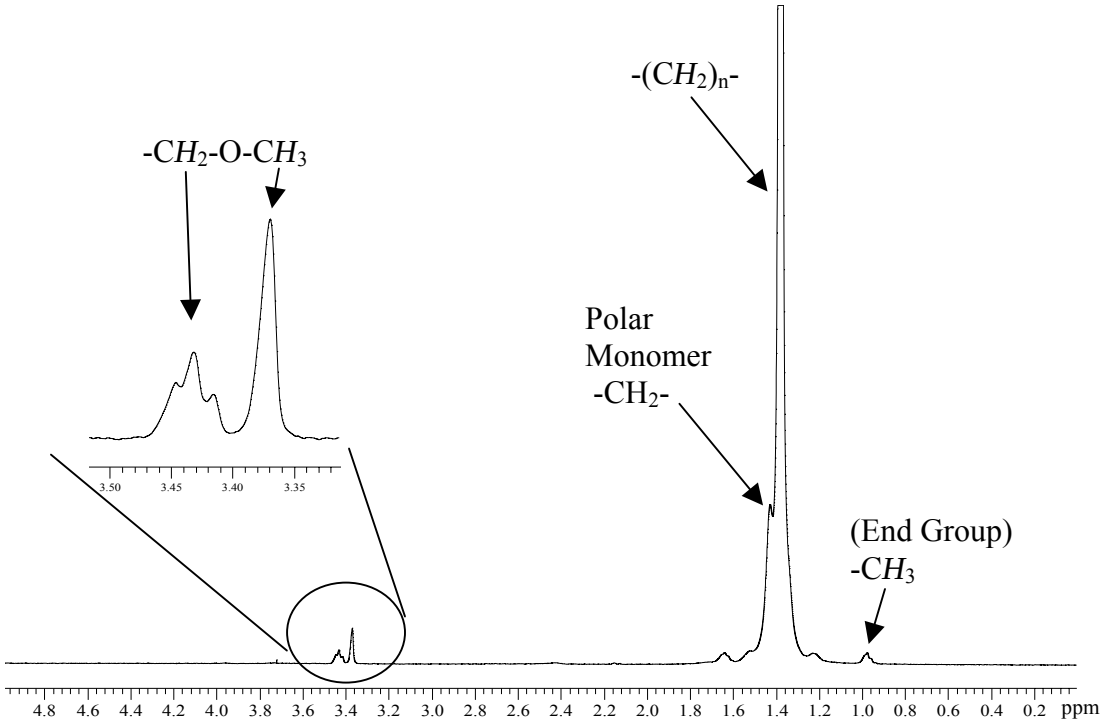

Figure 42. Representative ^{1}H NMR spectrum (400 MHz, TCE-d_2, 120 ^{o}C) of the isolated copolymer of experiment 1.

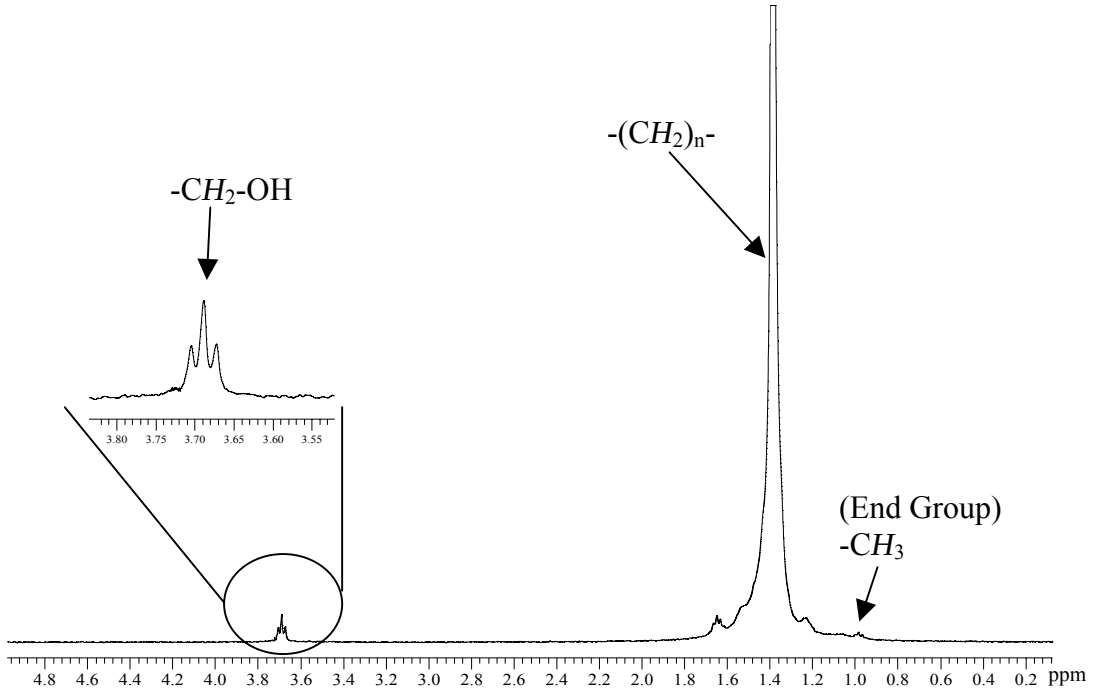

Figure 43. Representative ^{1}H NMR spectrum (400 MHz, TCE-d_2, 120 ^{o}C) of the isolated copolymer of experiment 7.

groups are similar to those in Figure 42.

As can be seen from Table 11 (Experiments 1-9), copolymerization reactions involving ethylene invariably resulted in low degrees of incorporation (0.004 – 1.2 %) of polar comonomers, whether the catalyst was activated in the presence of comonomer or prior to comonomer addition. Monomer **B** is not reported because *no* incorporations were observed in spite of numerous attempts. These incorporation values are lower than literature values where 10-undecen-1-ol with the same catalyst are used (0.7 - 3.6 %).[17b] However, the reaction conditions are different in the literature; with high MAO ratios of 4000:1 and higher ethylene pressures up to 1.5 atm.

Table 11. Copolymerizations of Ethylene with Polar Monomers $CH_2=CH(CH_2)_7CH_2OR$ (R = Me, $PhCH_2$, Ph_3C, Me_3Si, Ph_3Si) using the catalyst *rac*-$C_2H_4(Ind)_2ZrCl_2$/MAO.

Run	Comonomer	Activator Type[c]	Yield (g)	Incorp. (mol %)	T_m[d] (^oC)	M_n[a]
1	$CH_2=CH(CH_2)_8OMe$	MAO-10	2.0	0.12	128	2170
2[b]	$CH_2=CH(CH_2)_8OMe$	MAO-10	1.7	0.93	123	4520
3	$CH_2=CH(CH_2)_8OCPh_3$	MAO-10	2.5	0.004	128	2870
4[b]	$CH_2=CH(CH_2)_8OCPh_3$	MAO-10	1.6	1.1	112, 126	11500
5	$CH_2=CH(CH_2)_8OCPh_3$	MAO-10	1.6	0.1	106, 130	25410
6	$CH_2=CH(CH_2)_8OSiMe_3$	MAO-69	2.8	0.4	129	51000
7[b]	$CH_2=CH(CH_2)_8OSiMe_3$	MAO-69	1.3	1.2	121	8660
8	$CH_2=CH(CH_2)_8OSiPh_3$	MAO-69	3.0	0.2	127	6820
9[b]	$CH_2=CH(CH_2)_8OSiPh_3$	MAO-69	4.1	0.1	126	5360

[a] Calculated from integrating polymer end group ($-CH_3$, Figure 42, 43) relative to main chain polymer resonance.[b] Precatalyst and polar monomer premixed and MAO added last.[c] MAO-10 is Aldrich 10 % wt. solution in toluene; MAO-69 is Akzo Nobel 6.9 % wt. in toluene.[d] 5.00 ^oC/min ramping.

It would seem that none of the polar comonomers can compete effectively with the relatively small ethylene molecule and, as a result, the resulting low degrees of branching are reflected in values of T_m which are all very similar to that of high density polyethylene (120 – 130 ^oC).[18] The number average molecular weights (M_n) of the copolymers in Table 11 varied from 2170 to 51000, where the M_n values were consistently high with the trityl protecting group monomer **C**. This suggests that the trityl protecting group was effective in preventing catalyst poisoning, however, the existence of two T_m values suggests that a homogeneous copolymer was not achieved, but more likely two homopolymers were obtained. Since the low degrees of incorporation of polar monomers rendered comparisons of little value, we continued with propylene copolymers.

It should be noted that different MAO supplies were used during the course of this ethylene study due to availability issues, Aldrich (10 % wt.) and Akzo Nobel (6.9 % wt.). Since polar monomer incorporations were low and use of different MAO bottles resulted in little change in the percent incorporations, we moved on to studies with propylene. However, it will be shown later (Section **3.2.3.5**) that different MAO batches and the aging of MAO played a role in the percent incorporations for propylene copolymerizations.

3.2.3.2 Copolymerization Studies of Polar Monomers A – E with Propylene

As the results of the ethylene copolymerization were not as hoped, it was hoped that the use of propylene monomer would be more promising due to a few key reasons. Firstly, propylene is a bulkier monomer than ethylene and may not be as effective a

competitor for the catalyst coordination site. Hence, the polar monomers may compete better for insertion. Secondly, stereoregular polymers and copolymers can be made (e.g. isotactic) using the appropriate catalyst, with propylene, and therefore interesting and potentially useful materials with improved properties may result with the incorporation of a functional group into these already useful materials. The general scheme for the propylene polymerizations is shown in Equation 17.

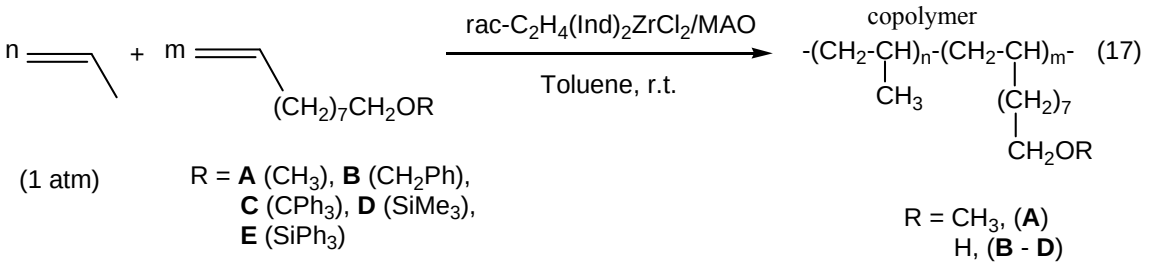

In Table 12, the results of copolymerization experiments involving propylene are shown; all polymerizations were repeated at least twice (as shown) and all products were, where possible, characterized by ^{1}H and ^{13}C NMR spectroscopy, IR spectroscopy and differential scanning calorimetry (DSC). The MAO used for these data collections were from Aldrich (10 wt % in toluene) and each run was done using the same bottle of MAO. The ^{1}H NMR spectra of copolymers **A1** (Figure 44, solvent-ODCB/C_6D_6) and **A2** exhibited the triplets expected for the OCH_2 groups and the singlets expected for the terminal OMe groups, at δ 3.37 and 3.34, respectively. In addition, resonances characteristic of isotactic polypropylene[19a] at δ 1.72, 1.40 and 0.87 are also obvious. The resonances of the long chains of the polar monomer are obscured by the much stronger resonances of the polypropylene chains.

Table 12. Copolymerizations of Propylene with Polar Monomers $CH_2=CH(CH_2)_7CH_2OR$ (R = Me, $PhCH_2$, Ph_3C, Me_3Si, Ph_3Si) using the catalyst system *rac*-$C_2H_4(Ind)_2ZrCl_2$/MAO-10.

Run	Comonomer[c] (100 equiv.)	Product IDs	Time (min)	Yield (g)	Mol % incorp.	T_m (^oC)	M_n[a]
10	None	**S1**	30	3.9	-	120	900
11	None	**S2**	30	3.7	-	118	1188
12	$CH_2=CH(CH_2)_8OMe$	**A1**	30	2.6	2.0	127	6342
13	$CH_2=CH(CH_2)_8OMe$	**A2**	30	3.0	1.7	126	4687
14	$CH_2=CH(CH_2)_8OCH_2Ph$	**B1**	30	4.6	0.5	128	3087
15	$CH_2=CH(CH_2)_8OCH_2Ph$	**B2**	30	5.2	0.2	124	2520
16	$CH_2=CH(CH_2)_8OCPh_3$	**C1**	30	4.2	0.4	121	1008
17	$CH_2=CH(CH_2)_8OCPh_3$	**C2**	30	4.1	0.5	123	953
18	$CH_2=CH(CH_2)_8OSiMe_3$	**D1**	30	2.7	0.9	128	5817
19	$CH_2=CH(CH_2)_8OSiMe_3$	**D2**	30	2.8	0.7	128	7123
20	$CH_2=CH(CH_2)_8OSiPh_3$	**E1**	30	4.9	-	121	1340
21	$CH_2=CH(CH_2)_8OSiPh_3$	**E2**	30	4.9	-	118	1596
22[b]	$CH_2=CH(CH_2)_8OSiMe_3$	**D3**	30	1.9	0.4	96	1957
23[b]	$CH_2=CH(CH_2)_8OSiMe_3$	**D4**	30	2.0	0.3	102	2160
24[b]	$CH_2=CH(CH_2)_8OSiPh_3$	**E3**	30	3.0	-	n.t.	1503
25[b]	$CH_2=CH(CH_2)_8OSiPh_3$	**E4**	30	3.0	-	n.t.	1457

[a]Calculated from integrating polymer end group (vinylidene group at ~ δ 4.7) relative to main chain polymer resonance.[b] Copolymerization performed at 60 ^oC. n.t.- no transition (i.e. amorphous). [c]Increasing polar monomer to 500 equivalents resulted in *no* incorporation of polar monomer and only homopolymer. MAO-10 was Aldrich (10 wt % in toluene) using same batch (i.e. bottle).

Copolymers (**B** – **D**) exhibit very similar spectra to that shown in Figure 44 but, following work-up, the spectra of the copolymers exhibit only a triplet attributable to the –CH_2OH group and indicative of only hydroxyl end groups and cleavage of the protecting group. Representative ^{1}H NMR spectra for copolymers **B** – **D** are shown in Figures 45 – 47. Table 13 shows the chemical shifts of the methylene resonance in the polar monomer next to the oxygen in the each of the copolymers **B** – **D** as well as the chemical shift data for the propylene resonances in the specified solvent used.

Table 13. Chemical Shift Values (δ) for Copolymers **B** – **D**.

Copolymer	*Polar Monomer (-CH_2-OH)*	*Polypropylene (-CH-)*	*Polypropylene (-CH_2-)*	*Polypropylene (-CH_3)*
[a]**B1**	3.52	1.50	1.15	0.81
[a]**B2**	3.59	1.56	1.19	0.85
[a]**C1**	3.61	1.61	1.21	0.85
[a]**C2**	3.57	1.66	1.28	0.89
[b]**D1**	3.60	1.72	1.40	0.95
[b]**D2**	3.59	1.73	1.39	0.98

[a]400 MHz, TCE-d_2 at 120 ^{o}C.
[b]400 MHz, ODCB/C_6D_6 at 80 ^{o}C.

Copolymers **B1** (Figure 41) and **B2** (benzyl protecting group) gave incorporations of polar monomer that were low (up to 0.5 mol %) and similar mole percent incorporations were obtained for copolymers **C1** and **C2** (trityl protecting group). These results suggest that bulkier protecting groups do not promote more incorporation of polar monomer within the polypropylene. The results for copolymers **D1** and **D2** (trimethylsilyl protecting group) gave slightly higher incorporations (up to 0.9 mol %) and disappointing results were obtained for products **E1** and **E2**, where essentially homopolymers were isolated. Comparing with literature data for incorporation of similar long chain polar monomers (e.g. 1-undecen-1-ol), values from 3.6 mol % up to 37 mol % were obtained.[19b] It can be seen that the data collected in this study were not as high as the

literature values. However, it should be noted that this study utilized reaction conditions that were less demanding (e.g. lower pressures and temperatures and MAO ratios were four times higher in literature values[19b]). The data in Table 13 were consistent with the literature,[19b] where the methylene protons next to the oxygen resonated at approximately δ 3.5 - 3.6. The propylene backbone resonances were consistent, but the NMR solvent and temperature can greatly affect the chemical shift values of the copolymer (cf. TCE-d_2 and ODCB/C_6D_6 propylene resonances). Lastly, in an effort to determine if more polar monomer incorporation could be achieved, experiment runs 22 – 25 were done at a higher starting temperature (60 ^oC). The products **D3** and **D4** obtained were copolymers (up to 0.4 mol %), however the incorporations were actually lower than those done at 21 ^oC. Clearly, increasing the temperature for this particular system did not increase the polar monomer content. This phenomenon was further evident in products **E3** and **E4** where only homopolymer was isolated.

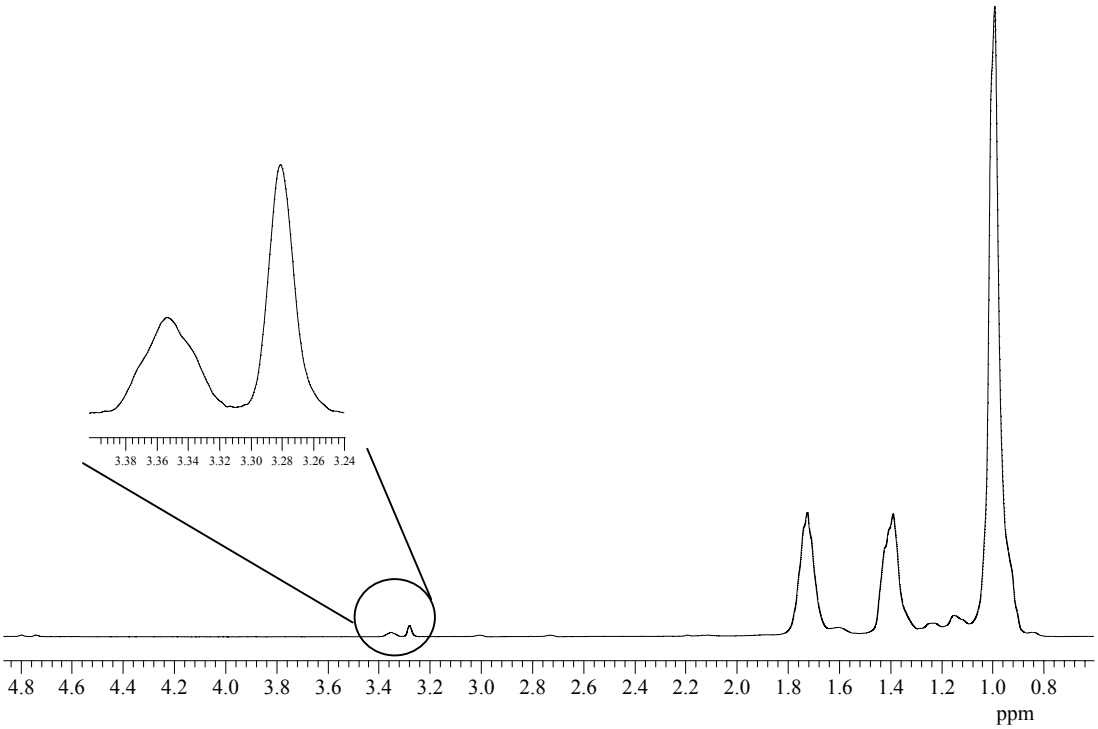

Figure 44. ^1H NMR spectrum (400 MHz, ODCB/C_6D_6, 80 ^oC) of copolymer **A1**.

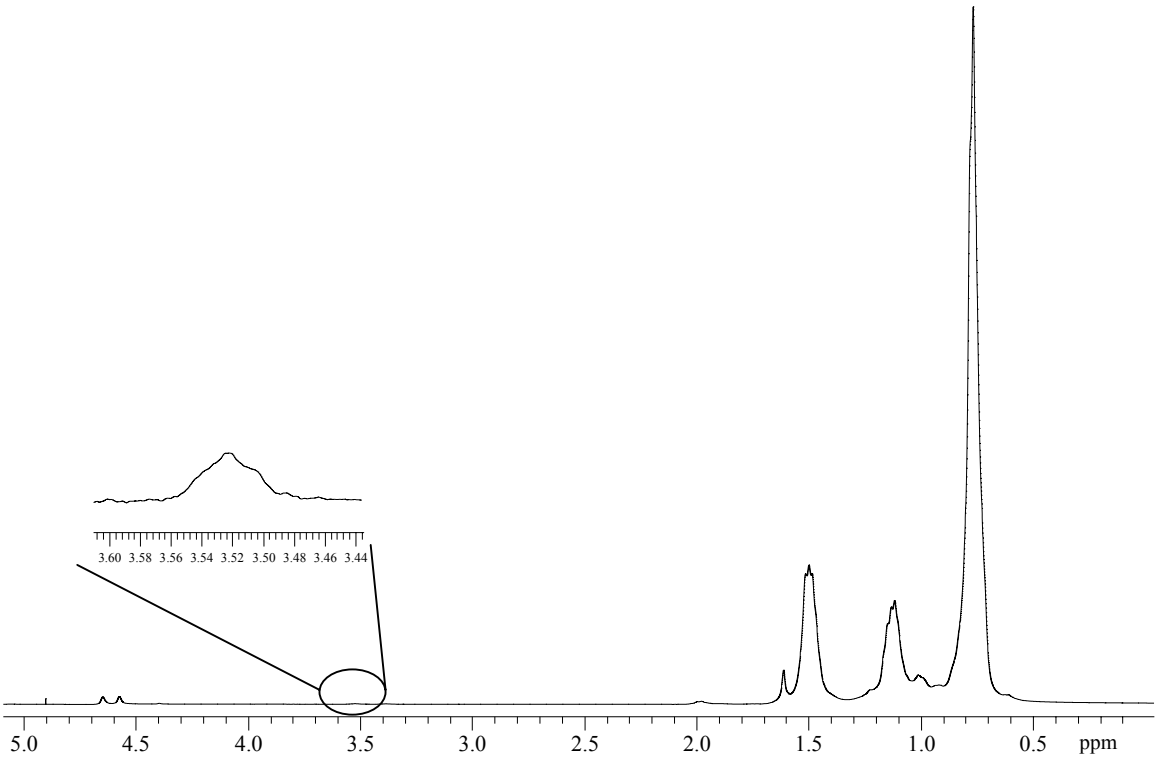

Figure 45. ^{1}H NMR spectrum (400 MHz, TCE-d_2, 120 ^{o}C) of copolymer **B1**.

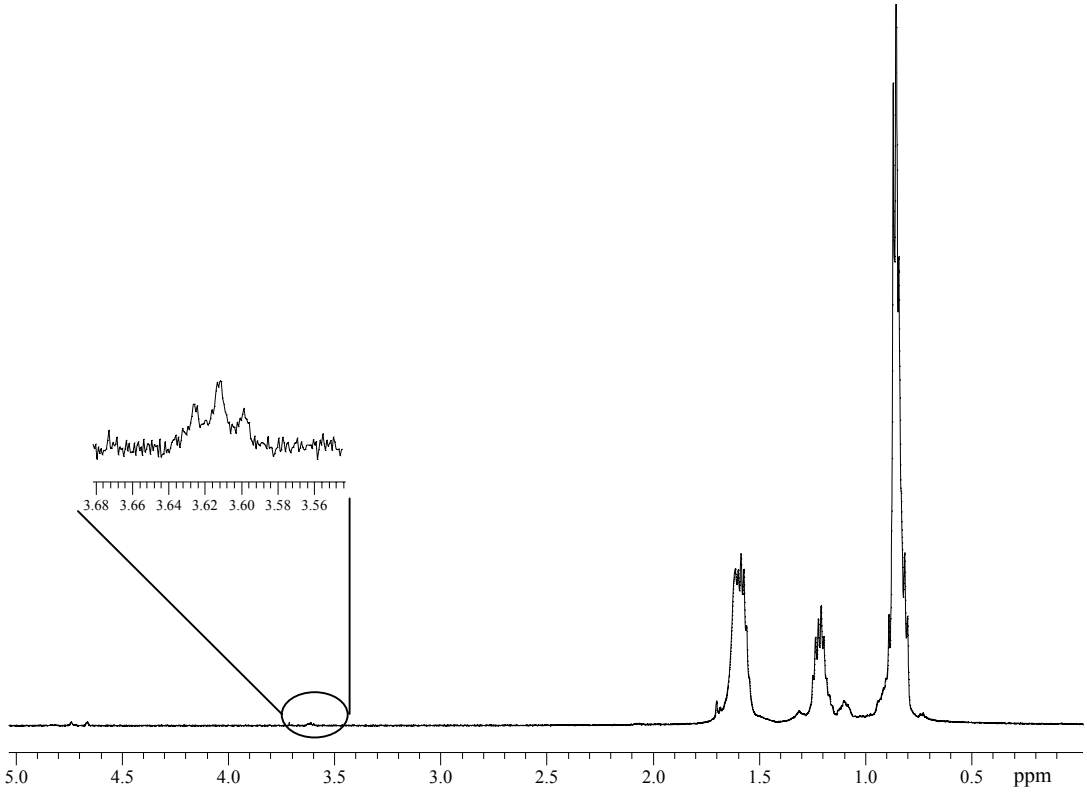

Figure 46. ^{1}H NMR spectrum (400 MHz, TCE-d_2, 120 ^{o}C) of copolymer **C1**.

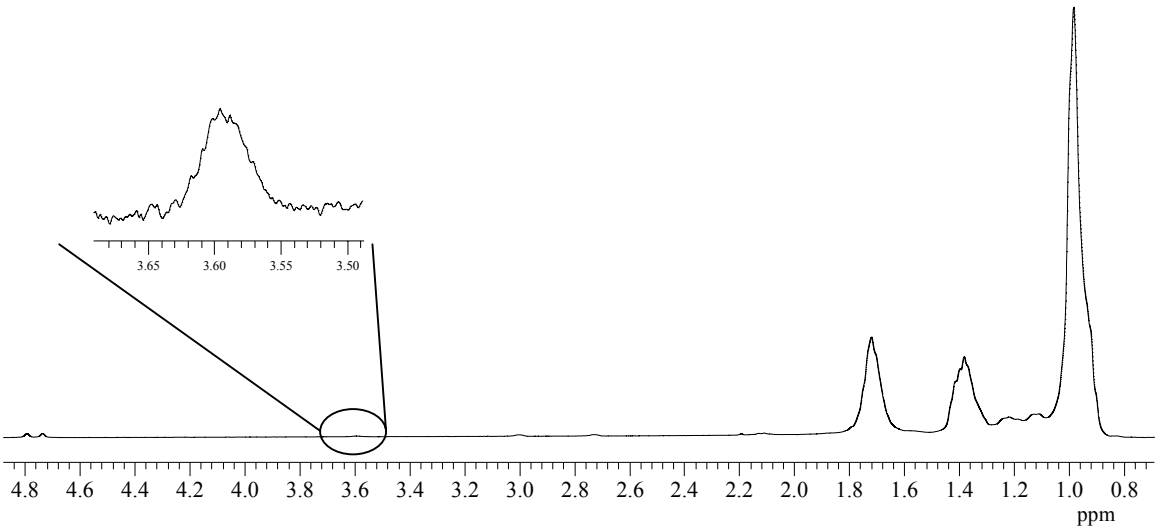

Figure 47. ^{1}H NMR spectrum (400 MHz, ODCB/C_6D_6, 80 ^{o}C) of copolymer **D1**.

The ^{13}C NMR spectra of copolymers (**A** - **D**) exhibit resonances with chemical shifts consistent with there being copolymers. For example, for copolymer (**D2**) (Figure 48), there are three major peaks of the isotactic propylene backbone at δ 47.1, 29.5 and 23.3 and for the polar monomer at δ 44.5, 34.6, 31.9, 31.5, 31.2, 27.6, 27.0 and 26.0. These peak assignments were based on literature assignments of similar copolymers, and with further verification via examination of the polypropylene homopolymer and polar monomer ^{13}C resonances.[20a] The peak at δ 64.8 is diagnostic of the –C*H*$_2$OH of the polar monomer end, signifying incorporation and effective protecting group scission. Also, vinylidene end groups for the copolymer are observed, as indicated in Figure 48. This vinylidene end group is a typical result of chain transfer reactions involving catalyst $C_2H_4(Ind)_2ZrCl_2$ under similar reaction conditions (i.e. toluene, r.t, 1 atm propylene).[20b] For copolymer **A1** (where polar monomer ends are methoxy groups), two resonances are evident at δ 58.6 and 73.2, corresponding to the –C*H*$_2$OCH$_3$ and –CH$_2$OC*H*$_3$ groups respectively.

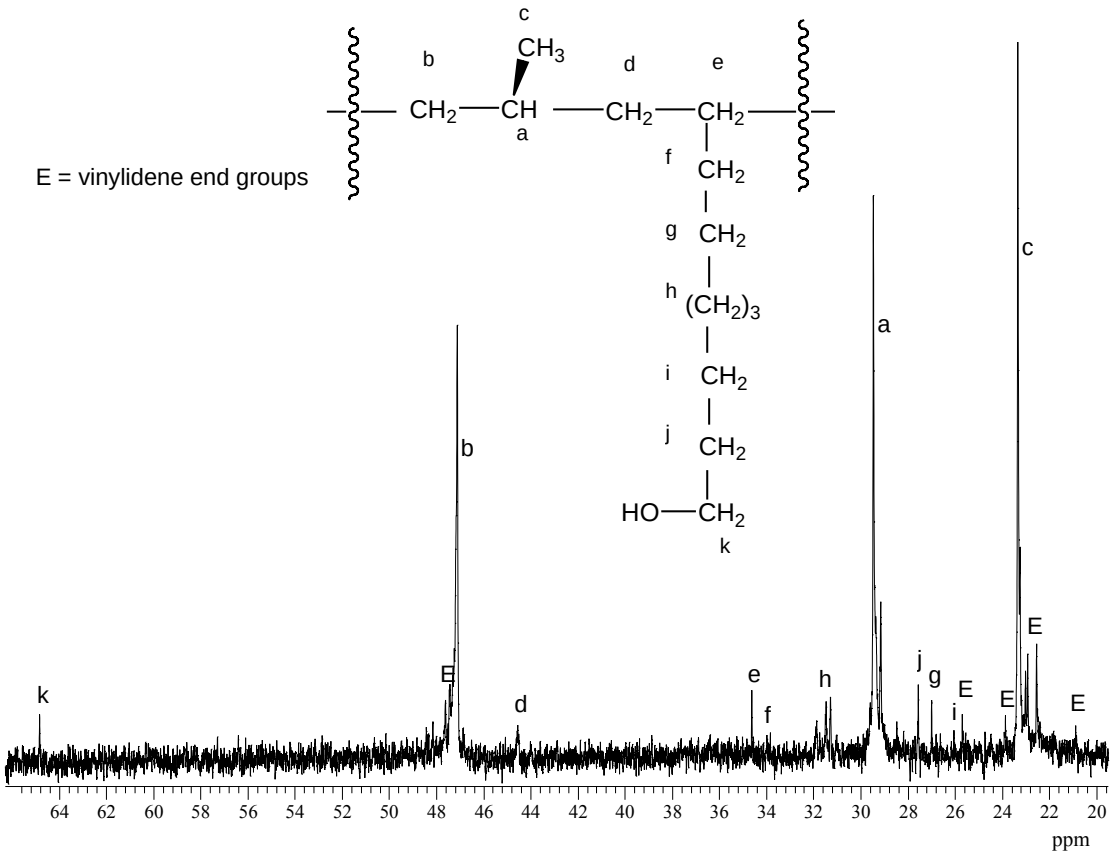

Figure 48. ^{13}C NMR spectrum (500 MHz, TCE-d_2) of copolymer **D**.

The infrared spectra (IR) of copolymers (**A** - **D)** were prepared using a chloroform solution of each copolymer and producing a film on a KBr disk by allowing the solvent to evaporate. The IR of copolymers **A1** and **A2** (with methoxy groups) exhibited the characteristic C-H stretches of the polypropylene backbone at 2950-2840 cm^{-1}, in addition to C-H bending modes at 1457 and 1376 cm^{-1}.[21] In addition to these peaks, bands at 1120-1017 cm^{-1} (C-O stretch) could be seen. For copolymers (**B** - **D)** (where hydroxyl groups are confirmed present), a distinct broad peak can be seen at approximately 3400 cm^{-1} due to hydrogen bonding within the copolymer (Figure 49).

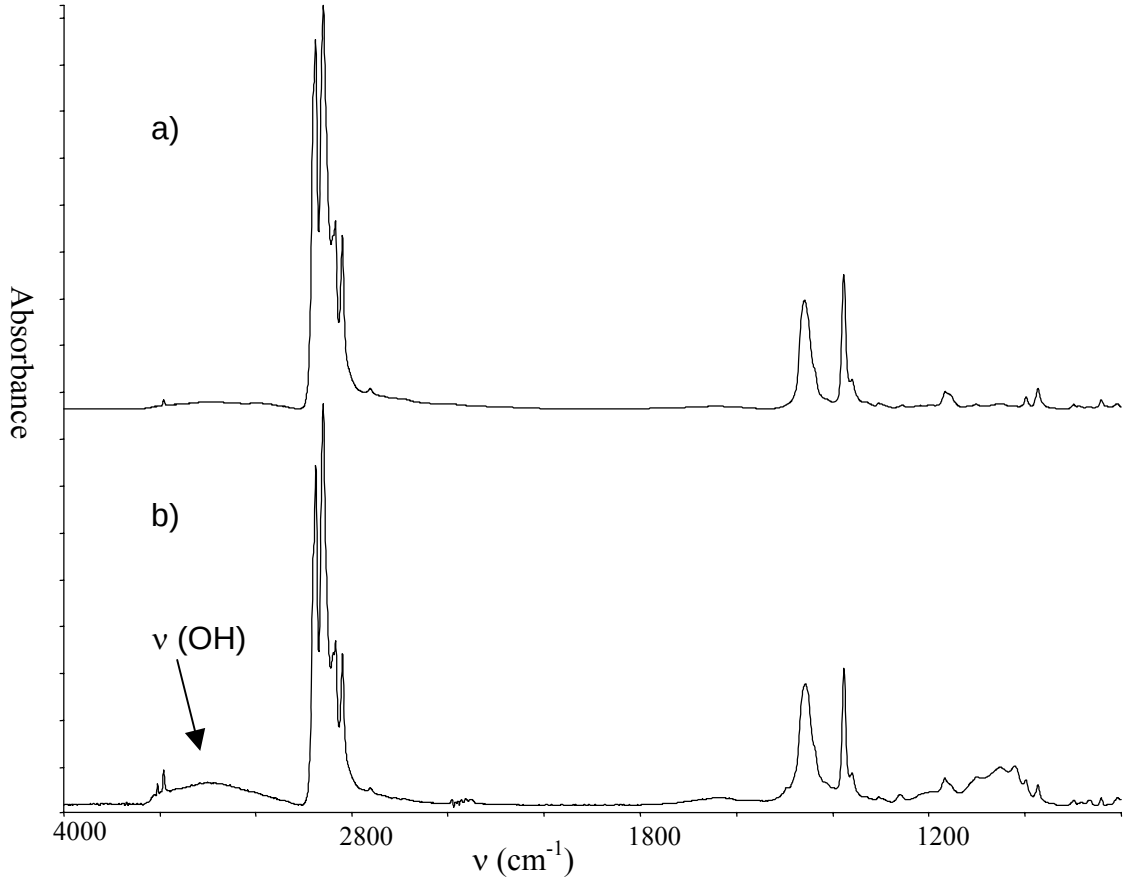

Figure 49. Absorbance infrared spectra (films) of a) pure polypropylene and b) copolymer **D1**.

The melting temperature (T_m) of copolymers **A** – **D** and homopolymers **E** were analyzed by DSC to determine the physical properties of the new materials. The pure isotactic polypropylene synthesized in this study had a T_m between 118 and 120 ^oC. This T_m range was lower than a typical T_m value for isotactic polypropylene (approximately 170 ^oC). This lower T_m could be explained by examining the polymerization conditions (i.e. low propylene pressures, low MAO ratios, etc.). Typical isotactic polypropylene reaction conditions required more demanding conditions to achieve higher T_m values (i.e.

high propylene pressures, high MAO content, etc).[22] Copolymers (**A - D)** gave some interesting results. Copolymers **A1** and **A2** (R = OMe) gave *slightly* higher T_m values (127 and 126 ^oC, respectively) than pure isotactic polypropylene when polar monomer incorporations were the highest (2.0 % and 1.7 %). As the polar monomer incorporation decreased (runs 15 - 17) so did the T_m. A possible reason for the decrease in T_m could be rationalized by the very little incorporation of polar monomer does not contribute to the overall copolymer properties, and therefore the crystalline domains within the copolymer would resemble that of ordinary isotactic polypropylene. For copolymers **D1** and **D2**, what is seen is that an increase in T_m occurs for incorporations of 0.7 to 0.9 % (run 18 (128 ^oC), run 19 (128 ^oC)) of polar monomer. This could be explained by possible hydrogen bonding dominating at this level of incorporation (> 0.5 %). Interestingly, the copolymerizations run at 60 ^oC (runs 22 – 25) with the silyl polar monomers showed that copolymer **D3** and **D4** had significant lower T_m values (96 ^oC and 102 ^oC, respectively). This could be attributed to the fact that starting at higher copolymerization temperatures affects the tacticity of the resulting copolymer, and hence the degree of crystal packing within the material (Figure 50). Interestingly, the materials obtained for products **E1 - E4** were not copolymers as indicated by *no* mole percent incorporation and *no* thermal transitions (i.e. amorphous polymers) were seen by DSC. The product yields of **E1** – **E4** were amongst the highest, showing that the triphenylsilyl group was an effective protecting group to prevent catalyst deactivation. However, the monomer **E** was a poor competitor versus propylene for monomer coordination and insertion and the result was poor incorporations.

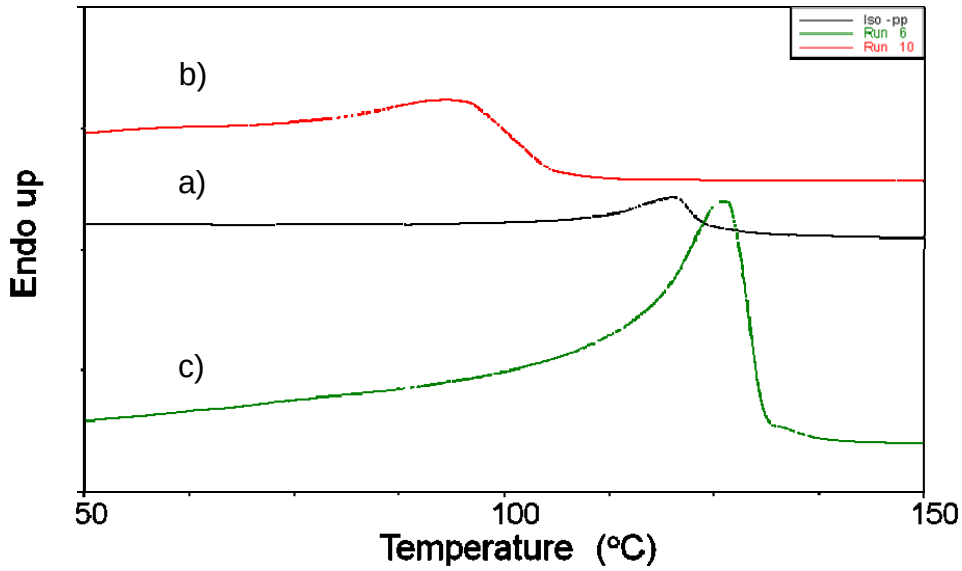

Figure 50. DSC traces of a) pure polypropylene **S2** (118 °C), b) copolymer **D3** (96 °C, 0.4 % incorporation) and c) copolymer **D1** (128 °C, 0.9 % incorporation).

The molecular weights of copolymers (**A** – **D**) were moderate under the mild copolymerization conditions. Typically, large MAO/Zr ratios (e.g. 4000/1), high pressures (> 5 atm), high temperatures (60 °C) and long reaction times (up to 24 hr) are employed in attempting copolymerizations of polar monomers with olefins.[23] In this study, the MAO/Zr ratio is low (1000/1), the propylene pressure is 1 atm, the reactions are started at 21 °C and are carried out for short reaction times (up to 30 min). Therefore, upon analysis of the molecular weights in Table 12, the results appeared promising. Longer reaction times (> 30 min) were attempted, but did not result in much higher molecular weights or yields of the resulting copolymers. In addition, the T_m of the copolymers at longer reaction times were not significantly different from those reactions done at 30 min. The highest molecular weight was that of copolymer **A1** (run 12, M_n ~ 6.3 kg/mol). When the copolymerizations were started at higher temperatures (runs 22 -

23), a severe drop in molecular weight occurred (*cf*. run 18 (5817 g/mol) and run 22 (1953 g/mol)). This could be attributed to faster catalyst deactivation and/or side reactions (such as chain transfer to MAO).

The highest degrees of polar monomer incorporation were achieved with the methoxy comonomers **A1** and **A2** (2.0 mol % , 1.7 mol %, respectively) and the next closest was the trimethylsilyl comonomer **D1** (0.9 mol %), while the trityl (runs 16, 17) and triphenylsilyl (runs 20, 21) comonomers, containing much more steric hindrance near the ether oxygen, gave lower degrees of incorporation or none at all. This is an unexpected result as it would seem the bulkier alkyl/aryl protecting groups (as in comonomers **B**, **C** or **E**) would lead to the best incorporation of polar monomer (i.e. making catalyst deactivation more difficult). Perhaps competition for the vacant site on the catalyst was more effective for the smaller propylene molecule, during copolymerization, than the longer, and in some cases more bulkier, polar comonomers. This explanation helps to rationalize why the comonomer **A** had the largest incorporation into polypropylene since it is perhaps small enough to diffuse to the active catalyst center. The copolymerization attempts at higher temperatures (runs 22 – 25) were done to see if an increase in temperature could aid the bulkier comonomer to effectively compete with the propylene unit. Unfortunately, no noticeable increase in percent incorporation was observed in each case.

Another important observation was made in the course of these copolymerization studies regarding MAO use as an activator. Preliminary results with polar monomers **A** – **D** and propylene copolymerizations using an Aldrich MAO bottle (10 wt % in toluene) that had been aged (i.e. opened, sealed and stored at 4 ^{o}C for months) revealed, in some

cases, higher polar monomer incorporations into polypropylene (Table 14). Repetition of the same abovementioned experiments done with a new, unopened Aldrich MAO bottle (as in Table 12) gave incorporations that were lower than the aged MAO. Indeed some of the parameters were different such as reaction time and number of equivalents of polar monomer (e.g. for monomer **A**, a longer reaction time was used, 90 min), but in the case of monomer **D**, where the reaction conditions were the same, a greater than 4 fold increase in incorporation was seen with old MAO. Additionally, the reactions started at higher temperatures (60 ^{o}C) shown in Table 14 (runs 32 and 33) gave polar monomer incorporations (1.8 mol % for **D**, 1.4 mol % for **E**) whereas *no* incorporation was seen for the studies down with the new MAO (Table 12). Numerous attempts to try and reproduce the initial preliminary results in Table 14 were unsuccessful. These interesting observations lead to subsequent studies where aliquots from a new bottle of MAO were subjected to a series of pretreatments to see if the aging of MAO affects the polar monomer incorporation into polypropylene under these copolymerization conditions. These MAO pretreatments will be discussed in section **3.2.3.5**.

Table 14. Preliminary results of the copolymerization of propylene with polar monomers **A** – **E** using catalyst *rac*-Et(Ind)$_2$ZrCl$_2$ with aged MAO.[a]

Run	Comonomer (equiv.)	Time (min)	Yield (g)	mol % Incorp.	T_m (^oC)	M_n[b]
26	-	30	3.3	-	124	5459
27	**A** (100)	90	6.8	4.8	132	3150
28	**B** (100)	60	4.6	1.1	128	4696
29	**C** (50)	45	3.7	0.5	124	5645
30	**D** (100)	30	1.2	4.6	131	2805
31	**E** (100)	30	6.5	0.7	114	1936
32[c]	**D** (100)	30	1.1	1.8	107	2768
33[c]	**E** (100)	30	1.0	1.4	108	2079

[a]All copolymerizations were done at least twice and the average values are shown. [b]Determined by ^{1}H NMR end group analysis. [c]Copolymerizations performed at 60 ^{o}C.

3.2.3.3 Copolymerization Studies of 1-Hexene with Propylene

In order to ascertain the extent to which incorporation of a long chain 1-alkene was actually possible, in the absence of competing OR moieties, copolymerization studies were also carried out with 1-hexene. We find that 1-hexene is incorporated to the extent of 1.7-13.0 mol %, depending on reaction conditions and order of addition of the MAO (Table 15). The experiments in Table 15 were designed to encompass all the previous copolymerization reaction conditions in Table 12, such as the order of addition of polar monomer. The temperature of each copolymerization in Table 15 was monitored.

It was found the temperatures reached a maximum temperature change (ΔT) of 40 (i.e. a maximum temperature of 60 ^{o}C was reached from the initial 21 ^{o}C).

Table 15. Propylene copolymerizations with 1-hexene using *rac*-$C_2H_4(Ind)_2ZrCl_2$/MAO in toluene. (catalyst:hexane:MAO) →(1:100:1000). Reaction times all 20 min.

Run	Comonomer (equiv.)	Yield (g)	Mol % Incorp.[b]	T_m (^{o}C)	M_n[a]	ΔT[e] (^{o}C)
34	-	2.53	-	120	2780	<40
35[c]	1-Hexene (100)	4.38	2.9	106	2366	<40
36[d]	1-Hexene (100)	4.03	1.7	127	1089	<40
37[c]	1-Hexene (500)	4.00	9.1	n.t	2184	<40
38[d]	1-Hexene (500)	4.67	13.0	n.t	1592	<40

[a]calculated from integrating olefinic polymer end group relative to main chain peak of polymer. [b]calculated from ^{13}C NMR by integrating *polymer main chain CH_3* resonance with *butane branch CH_3*. [c]precatalyst and hexene premixed and MAO added last. [d]Hexene added 5 mins after MAO addition. n.t – no transition. [e]Final maximum temperature – initial temperature.

As it can be seen, the reaction times were only for 20 min (in contrast to 30 min). All of the copolymerizations began to cool after 20 min, suggesting that polymerization had ceased because of catalyst deactivation. The results in Table 15 were each done once, but the results were comparable to each other despite whether the polar monomer was added before or 5 min after the MAO addition (cf. run 35 and 36; cf. run 37 and 38). Comparing the results in Table 12 to those in Table 15, it can be seen that the levels of incorporation of 1-hexene (1.7 – 2.9 mol %) into polypropylene are most comparable to monomer **A** (1.7 – 2.0 mol %) and monomer **D** (0.7 – 0.9 mol %) and less to the monomers **B** and **C** (range from 0.3 to 0.5 mol %). Therefore, both CH_2=$CH(CH_2)_7CH_2OMe$ and

CH_2=CH$(CH_2)_7CH_2OSiMe_3$ may be incorporated to a similar degree or more than is 1-hexene under the same conditions. Figure 51 shows a typical ^{1}H NMR spectrum of the propylene-hexene copolymer and Figure 52 shows a typical ^{13}C NMR spectrum. The ^{1}H NMR is not very informative due to the overlapping of resonances, but propylene (P) resonances at δ 1.72, 1.40 and 0.87 are obvious, while less obvious are some of the 1-hexene (H) resonances at δ 1.1 and 1.2 (others are obscured by overlapping). In addition, vinylidene peaks (V) are evident at δ 4.81 and 4.74 due to chain transfer reactions.

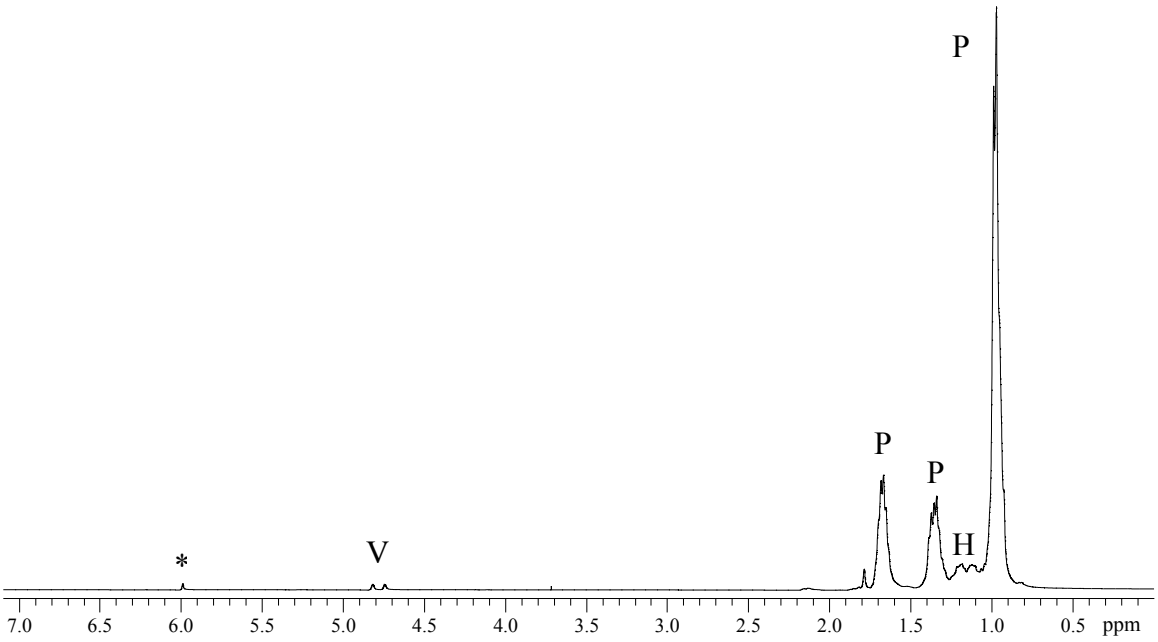

Figure 51. High temperature ^{1}H NMR spectrum (400 MHz, TCE-d_2, 120 ^{o}C) of a copolymer of polypropylene with 2.9 % of 1-hexene.

The ^{13}C NMR spectrum in Figure 52 was used to calculate the mole percent of 1-hexene units incorporated within a copolymer of polypropylene and 1-hexene by a method developed by Kissin and Brandolini.[24] This method utilizes peak areas (Equations 19 – 21) of regions in the ^{13}C spectrum and quantifies the amount of propylene [P], 1-hexene

[H] and total monomer [P] + [H] in the sample. A simple ratio of [H] to total monomer [P] + [H] times 100 % , yields the percent 1-hexene content.

$$[P] = (46.0 – 48.9 \text{ ppm}) + 0.5(44.0 – 44.5 \text{ ppm}) \quad (19)$$

$$[H] = (23.4 – 23.5 \text{ ppm}) + (33.6 – 33.9 \text{ ppm}) + (35.4 – 35.7 \text{ ppm}) \quad (20)$$

$$[P] + [H] = (28 – 30 \text{ ppm}) \quad (21)$$

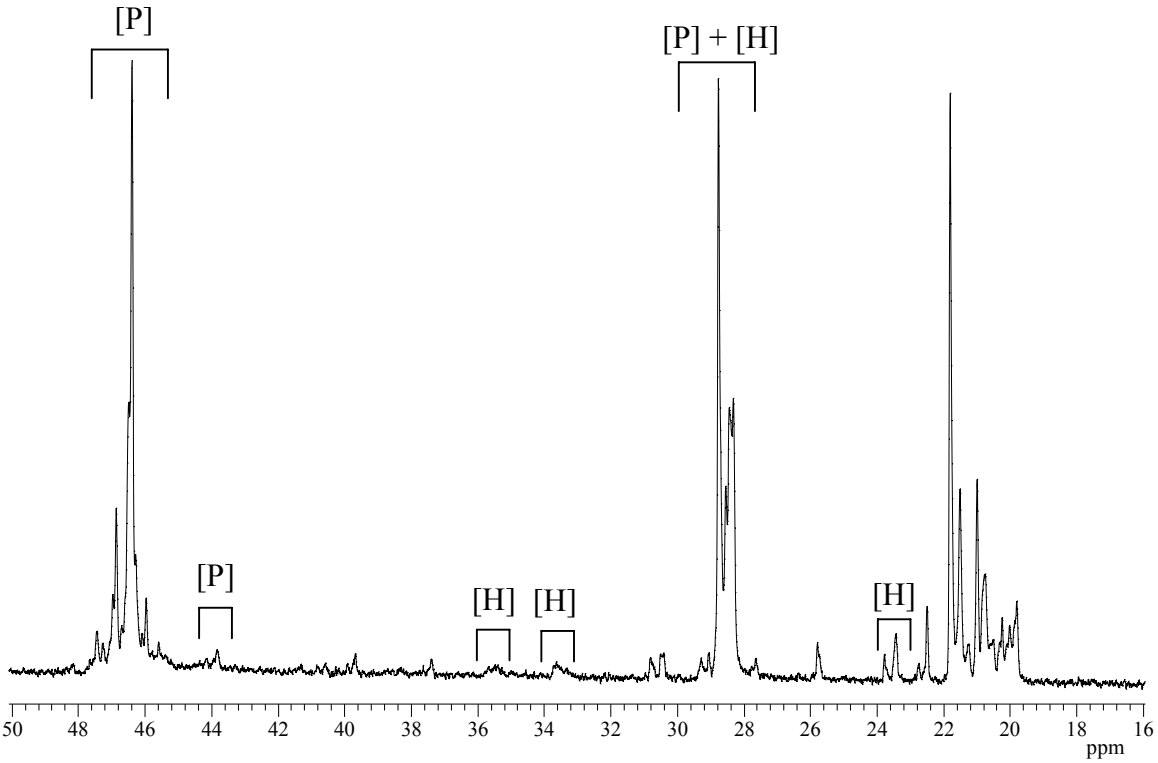

Figure 52. High temperature ^{13}C NMR spectrum (400 MHz, ODCB/C_6D_6, 80 ^oC) of a copolymer of polypropylene with 13.0 % of 1-hexene.

In Table 15, the results of the propylene – 1-hexene copolymerizations (each done once) show the yields are comparable to those in Table 11 and the molar incorporations of 1-hexene for runs 35 and 36 are 2.9 and 1.7 %, respectively. These reaction conditions are

similar to all previous polar monomers studies (Table 12), especially run 36, where 100 equivalents of polar monomer were added. These values show that polar monomer incorporation rival that of nonpolar 1-hexene and in the one case is in fact improved (comonomer **A1**). As a further test, we increased the amount of 1-hexene 5-fold (runs 37 and 38) and much higher incorporations occurred without catalyst deactivation. When this was attempted with the polar monomers **A** – **E**, no copolymer was obtained in each case (Table 12, see footnote). The T_m values decreased in value (run 35, 106 ^{O}C) compared to blank run 34 (no 1-hexene, 120 ^{o}C). This decrease can be attributed to the random incorporation of C_4 branches along the polymer chain, which tends to affect crystallinity within the polymer. However, in run 36, the crystallinity increases (127 ^{o}C) and this could be possibly due to the mode of addition (i.e. after 5 min). In runs 37 and 38, the mole percents are high enough to disrupt the crystalline domain of the copolymer main chain to the point where crystallinity is not detected.

3.2.3.4 Copolymerization Studies of 1-Hexene with Propylene in the presence of *n*-Decyl Methyl Ether F.

In light of all the results so far, no correlation was found between degree of incorporation of the decenyl ethers with steric requirement of the series of R groups; the highest degrees of incorporation for the comonomers CH_2=CH$(CH_2)_7CH_2OR$ were obtained when R = Me and Me_3Si, the lowest when R = Ph_3C, $PhCH_2$ and Ph_3Si. To better understand these findings, a study was done to see the effect that a saturated ether (such as n-decyl ether) might have on incorporations and copolymerization results. It is

tentatively proposed that the presence of a not too sterically encumbered ether group may be important because it might be able to maneuver itself into the spaces in between the bulky MAO-based counteranions and the catalytic site on zirconium, eventually binding weakly to the latter. Once anion-cation separation has been achieved, the olefinic ether can perhaps exchange ends such that the C=C bond coordinates and migratory insertion can ensue. Such a process may be less available to the non-polar 1-hexene and to the much bulkier phenyl-containing ethers. This hypothesis was tested by carrying out propylene-1-hexene copolymerizations in the presence of the long chain, saturated *n*-decyl methyl ether. Table 16 shows the results of propylene-1-hexene copolymerization in the presence of 100 equivalents of *n*-decyl methyl ether.

Table 16. Propylene copolymerizations with 1-hexene in the presence of 100 equiv. of decyl ether. Reaction times all 20 min.

Run	Comonomer (equiv.)	Yield (g)	Mol % Incorp.[b]	T_m (^oC)	M_n[a]	ΔT[e] (^oC)
39[c]	1-Hexene (100)	1.11	5.1	118	1.4×10^4	<20
40[d]	1-Hexene (100)	1.29	6.5	122	1.5×10^4	<20
41[c]	1-Hexene (500)	1.03	20	n.d.	6426	<20
42[d]	1-Hexene (500)	1.32	18	n.d.	2449	<20

[a]calculated from integrating polymer end group relative to main chain peak of polymer. [b]calculated from ^{13}C NMR by integrating *polymer main chain* CH_3 resonance with *butane branch* CH_3. [c]precatalyst and hexene premixed and MAO added last. [d]Hexene added 5 mins after MAO addition. n.d. – not detected. [e]Final maximum temperature – initial temperature.

As it can be seen in Table 16 (each done once), the mole percent incorporations increased significantly for all runs 39 to 42 by at least 1.5 times for runs 39 and 40 (*cf*. runs 35 and

36, Table 7) and a maximum of up to 20 mol % for run 41 was obtained when higher equivalents of 1-hexene were used (*cf*. 9.1 mol %, Table 14). In addition, higher molecular weights were obtained (up to 1.5 x 10^4 g/mol) and the T_m values are not detected when we achieve incorporations of up to 18 mol %.

The temperature of each copolymerization in Table 16 was monitored. It was found the temperatures reached a maximum temperature change of 20 (i.e. a maximum temperature of 40 ^oC was reached from the initial 21 ^oC). These temperature values in the presence of decyl ether are lower than in the absence of ether, where temperatures of the copolymerization reached average values up to 60 ^oC (i.e. $\Delta T \sim 40$, Table 14). These results conform to the initial hypothesis that an unhindered saturated ether can indeed allow for more comonomer incorporation to occur with the polymer main chain.

3.2.3.5 MAO Effects on the Copolymerization Studies of Propylene with Polar Monomers

As discussed in section **3.2.3.2**, some issues regarding MAO batches from the current supplier (Aldrich) were observed. Depending on the MAO batched used (i.e. an aged bottle (MAO-I) versus a new, unopened bottle (MAO-II)), the propylene – polar monomer copolymerization results varied. Table 17 summarizes the results of some comparable copolymerization runs using the two different types of MAO, seen previously in Tables 11 and 13. As mentioned in section 3.2.3.2, there are some clear differences seen with monomer **D** when comparing runs 18 and 19 in Table 17, with run 30. More than a four fold increase in incorporation was seen with the aged MAO-I than with the

new MAO-II. Similarly, monomer **E** (runs 20 and 21 in Table 17) shows no incorporation with MAO-II, whereas when using MAO-I, 0.7 mol % was seen.

Table 17. Comparsions of new methylaluminoxane (MAO-I) and aged methylaluminoxane (MAO-II) in the copolymerization studies of propylene-with polar monomers.

Run	MAO Type	Comonomer (equiv.)	Time (min)	Yield (g)	mol % Incorp.	T_m (^oC)	M_n[a]
18	MAO-II	**D1** (100)	30	2.7	0.9	128	5817
19	MAO-II	**D2** (100)	30	2.8	0.7	128	7123
30	MAO-I	**D** (100)	30	1.2	4.6	131	2805
20	MAO-II	**E1** (100)	30	4.9	-	121	1340
21	MAO-II	**E2** (100)	30	4.9	-	118	1596
31	MAO-I	**E** (100)	30	6.5	0.7	114	1936
22[b]	MAO-II	**D3** (100)	30	1.9	0.4	96	1957
23[b]	MAO-II	**D4** (100)	30	2.0	0.3	102	2160
32[b]	MAO-I	**D** (100)	30	1.1	1.8	107	2768
24[b]	MAO-II	**E3** (100)	30	3.0	-	n.t.	1503
25[b]	MAO-II	**E4** (100)	30	3.0	-	n.t.	1457
33[b]	MAO-I	**E** (100)	30	1.0	1.4	108	2079

[a]Determined by ^1H NMR. [b]Copolymerizations performed at 60 ^oC.

Copolymerizations started at 60 ^oC (as seen in Table 17) also have some interesting differences. The monomer **D** with MAO-II resulted in incorporations of up to 0.4 mol %, whereas with aged MAO-I, an incorporation of up to 1.8 mol % was obtained. The

monomer **E** gave very interesting results as *no* incorporations were seen with runs 24 and 25 using MAO-II, however, using MAO-I, up to 1.4 mol % of incorporation of polar monomer was detected.

MAO differs from batch to batch as the amounts of residual trimethylaluminum (TMA) vary, and over periods of time (i.e. aging), the TMA ratios can change. In an attempt to determine the effects of aging MAO on our copolymerization studies, a study was undertaken where an aliquot from a new bottle of MAO (Aldrich, 10 % wt in toluene) was subjected to a series of pretreatments. These pretreatments were: 1) heating the MAO at 80 ^{o}C for 18 hr overnight, 2) pumping down the toluene solution of MAO to remove TMA, 3) adding 50 equivalents of oxygen to MAO and 4) adding 50 equivalents of water to the MAO. Once the MAO was modified in each of these ways, it was tested for its effectiveness in the copolymerization of propylene with selected polar monomers. The MAO typically used in the literature for co- and homopolymerization studies generally uses either MAO as received from the supplier (as a solution in toluene)[25] or modified MAO, containing no TMA (i.e. concentrating the MAO/toluene solution to dryness and then redissolving in toluene again)[26].

The relevant literature on MAO aging is very limited.[27] Tritto *et al.* described a detailed study of the effects of 'aging' MAO on ethylene polymerization results using three different types of MAO.[27a] The catalyst used was *rac*-Et(Ind)$_2$ZrCl$_2$. Tritto *et al.* found that the three types of MAO used (two from the same supplier and one 'aged' sample from a different supplier) affect the polymerization results significantly. They concluded that: a) reproducibility of polymerization results were difficult using the 3 different MAO batches, b) the 'aging' of MAO plays an important role in determining

polymerization activity and polymer molecular weights (M_w) and c) the amount of TMA in each MAO batch was significant, as excessive TMA could lower MAO molecular weights (via chain scission), which in turn could be less able to stabilize the active catalyst during polymerization (i.e. free TMA may interact with the active catalyst creating a dormant species).[27a] Stellbrink *et al.* has recently reported some observations regarding MAO stability over several months.[27b] It was found that MAO with time in toluene solution at room temperature lacks stability and forms a gel fraction and a solid material. However, they additionally found for their experiments that when the MAO was stored over a 8 month period at ~0 ^{o}C, it was stable with no gel fraction or precipitate being formed.[27b] The complexity of MAO is thus an issue, and below we have contributed our observations to the ongoing studies of the effects aging MAO on polymerization experiments. All experiments discussed here were done twice and the average values are given and compared to the values given in Table 12.

The first MAO 'aging' experiment was heating the MAO at 80 ^{o}C for 18 hr under argon, and then allowing it to cool. This experiment was done to mimic a situation where MAO that has been stored for months. Heating the MAO may be an approximate way to simulate and accelerate the aging process. In addition, it was possible to analyze whether the heating process alters MAO composition (e.g. TMA content) and its overall reactivity. This cooled batch of MAO (after heat treatment) was then added to activate the catalyst *rac*-Et(Ind)$_2$ZrCl$_2$ in the mixture of propylene and toluene, and then the selected monomer **D** (trimethylsiloxydecene) in toluene was added 5 min after MAO (treated with heat) addition. The ^{1}H NMR spectrum of the resulting copolymer is shown in Figure 53.

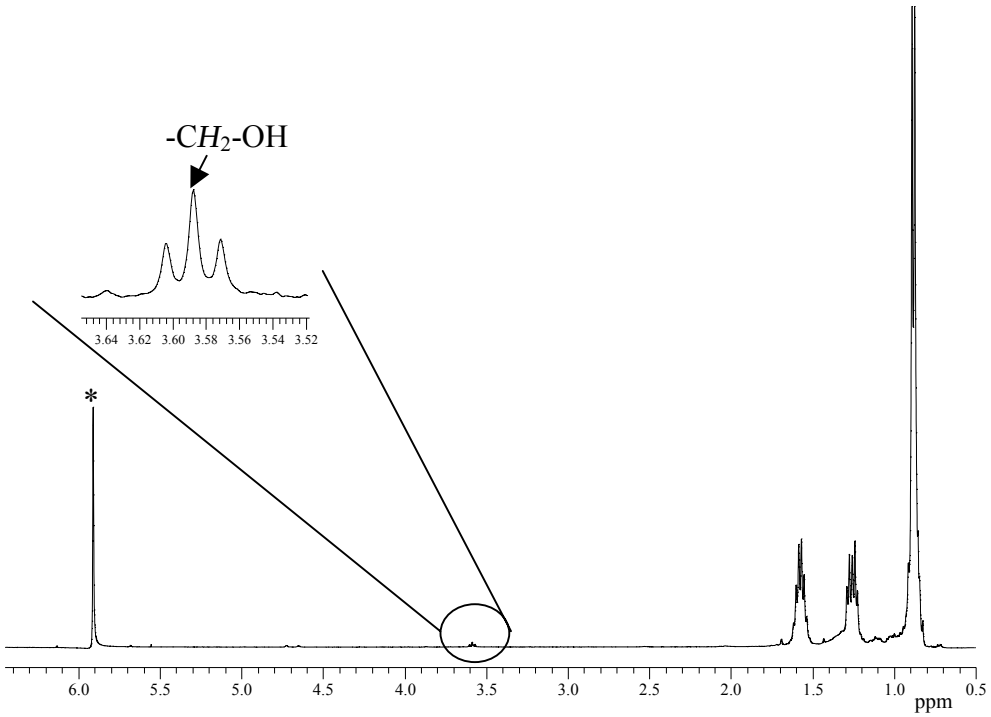

Figure 53. ^{1}H NMR spectrum (400 MHz, TCE-d_2, 120 ^{o}C) of the copolymer obtained from using pretreated MAO (heating 18 hr at 80 ^{o}C).

It was found that the average yield of copolymer was lower (~2.17 g) compared to the average value from Table 12 of ~2.8 g, but the degree of incorporation of polar monomer was on average 0.97 mol %, which was very similar to the average value of 0.8 mol % in Table 12. Although this outcome produced a difference in copolymer yield, the incorporation of polar monomer was not significantly different than when obtained with untreated MAO (Table 12). Therefore, there is some evidence that MAO pretreatment by heat can alter the yield of copolymer, but percent incorporation amounts of polar monomer within polypropylene seem unaffected. To our knowledge, the heating pretreatment of MAO and its subsequent use in copolymerization studies has not been reported.

The second MAO 'aging' experiment involved taking an aliquot of 10 wt % in toluene MAO and pumping down the solution to dryness to remove any residual free TMA. This procedure was done to eliminate the 'free' TMA in the MAO that could contribute to chain transfer reactions to aluminum and/or catalyst inhibition, which results in decreased catalyst activity and low polymer molecular weights. The resulting white MAO solid was then redissolved in toluene and then added to activate the catalyst *rac*-Et(Ind)$_2$ZrCl$_2$ in the mixture of propylene and toluene. The selected monomer **A** (methoxydecene) in toluene was then added 5 min after the MAO (redissolved solid) addition. The ^{1}H NMR spectrum of the resulting copolymer is shown in Figure 54.

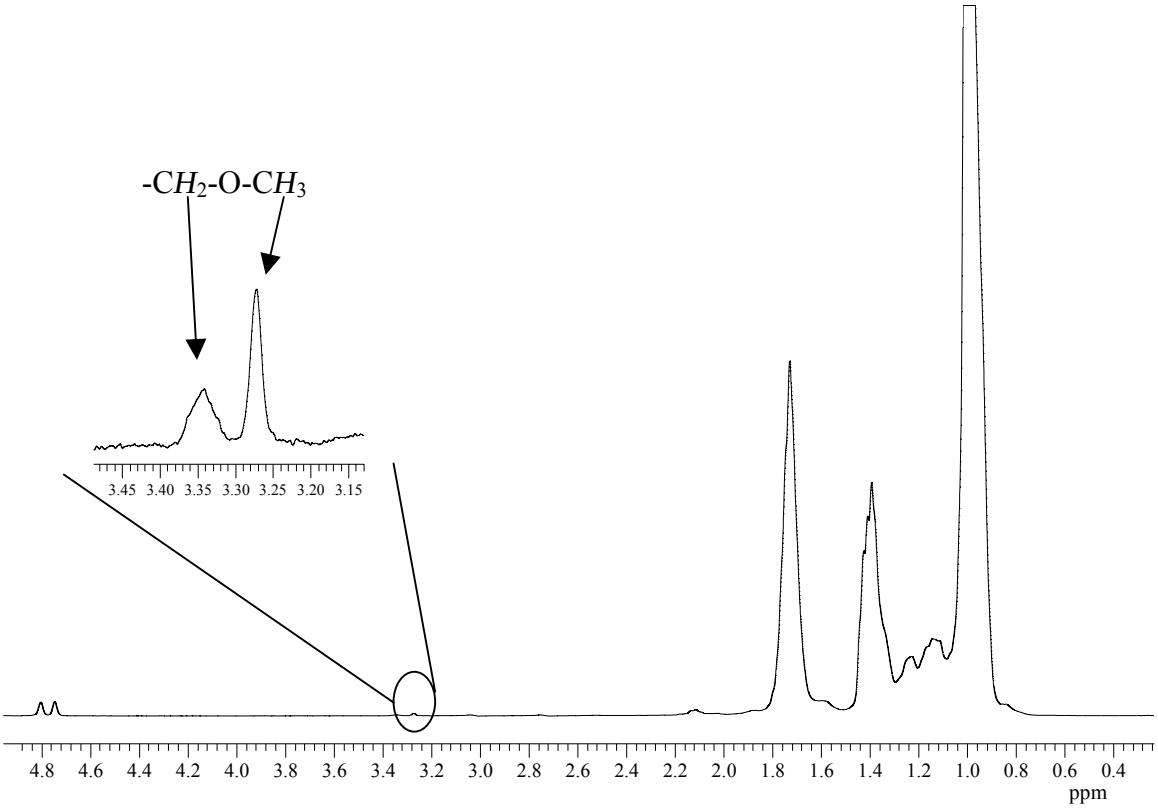

Figure 54. ^{1}H NMR spectrum (400 MHz, ODCB/C_6D_6, 80 ^{o}C) of the copolymer obtained from using pretreated MAO (evacuation overnight to remove residual TMA).

The average result of the experiment above gave a yield of copolymer of 1.40 g, which was less than the results in Table 12 (average value 2.8 g). The degree of polar monomer incorporation was significantly lower (0.17 mol %) than reported in Table 12 (1.8 mol %). Hence, the TMA plays an important role in aiding the effective masking of polar monomers and/or preventing catalyst deactivation. This trend has been shown in the literature.[19b, 26b, 28] For example, Hagihara has shown that when excess TMA was added to protected allyl monomers[26b] or 5-hexen-1-ol[28] in copolymerization studies with olefins, an increase in polar monomer content was seen in both cases.

The third MAO 'aging' experiment involved taking MAO and deliberately adding 50 equivalents of air (oxygen), with respect to the aluminum, and stirring the solution overnight under argon. The experiment was done to see if oxygen can alter the MAO composition in order to enhance percent incorporation behaviour without comprising activity. This MAO (treated with oxygen) was added to a solution containing the catalyst *rac*-Et(Ind)$_2$ZrCl$_2$, propylene and toluene, and then the selected monomer **D** (trimethylsilyoxydecene) was added 5 min after the MAO (treated with oxygen) addition. The ^{1}H NMR of the resulting copolymer is shown in Figure 55.

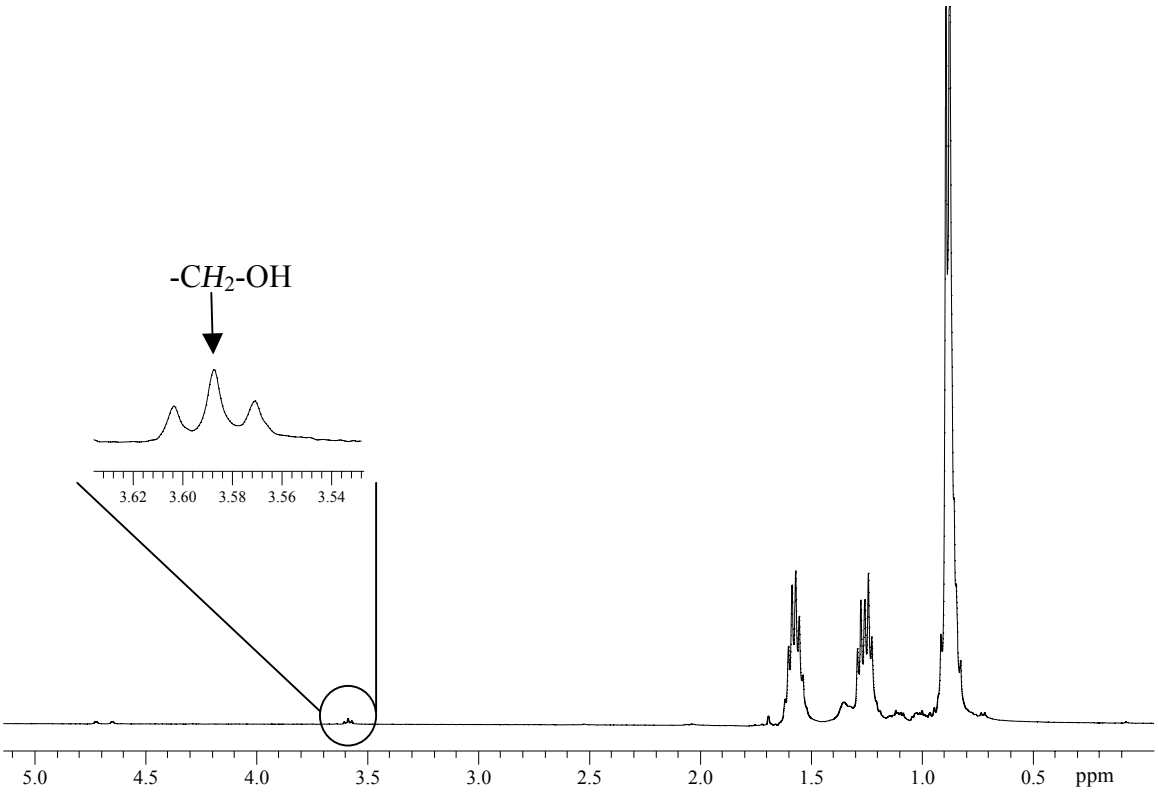

Figure 55. ^{1}H NMR spectrum (400 MHz, TCE-d_2, 120 ^{o}C) of the copolymer obtained from using pretreated MAO (adding 50 equiv. of oxygen).

The average result of this experiment gave a copolymer yield of ~2.5 g, which was similar to the results shown earlier in Table 12 (~2.7 g), and also the degree of polar monomer incorporation was very similar (0.83 mol %) to that reported in Table 12 (0.8 mol %). Hence, these results suggest that the addition of oxygen did not affect the outcome of the copolymer in terms of yield or degree of polar monomer incorporation. A possible reason is that the 1000 equivalents of MAO (treated with oxygen) was sufficient enough to efficiently scavenge the oxygen within the system. To our knowledge, this prior oxygen treatment of MAO followed by use in copolymerization studies has not been reported.

The fourth experiment involved taking MAO and deliberately adding 50 equivalents of water (H_2O) with respect to the aluminum. This experiment was done to see how adding excess water directly to the MAO followed by stirring overnight would alter the MAO composition. The free TMA in the MAO will react with the water to generate more MAO and methane. We were thus interested in how this would affect polar monomer incorporations. After stirring this solution overnight over argon, it was added to the catalyst *rac*-Et(Ind)$_2$ZrCl$_2$ in the mixture of propylene and toluene and the selected monomer **A** (methoxydecene) in toluene was added 5 min after MAO (treated with water) addition. The ^{1}H NMR of the copolymer is shown in Figure 56.

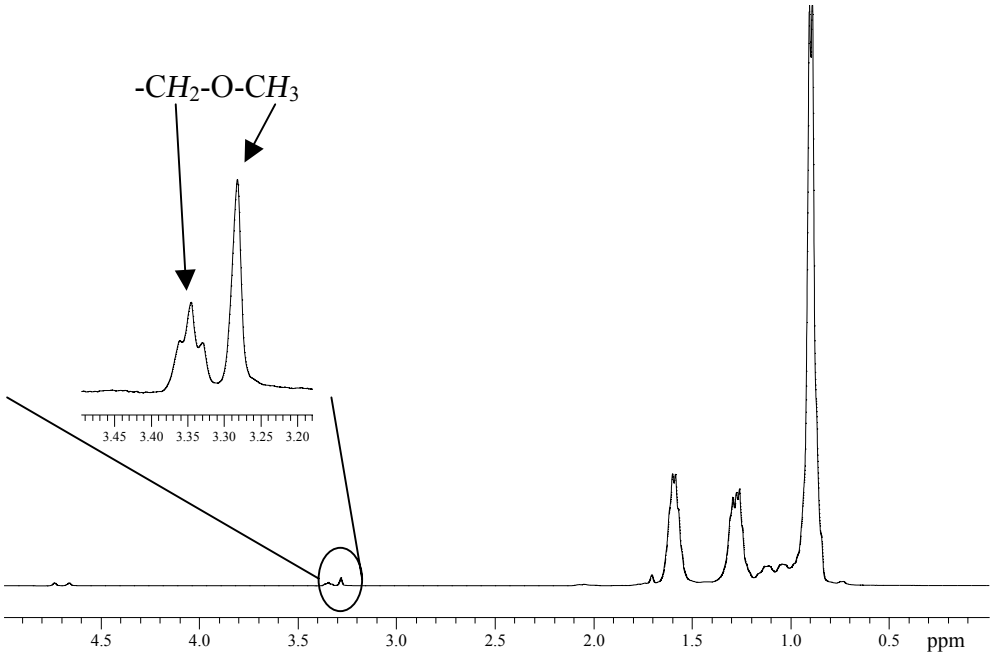

Figure 56. ^{1}H NMR spectrum (400 MHz, TCE-d$_2$, 120 ^{o}C) of the copolymer obtained from using pretreated MAO (adding 50 equiv. of water).

The average copolymer yield in this experiment was lower (~1.6 g) when compared to the average value in Table 12 of ~2.8 g, and the degree of monomer incorporation was also lower (0.7 mol %) compared to the average value of ~1.8 mol %. Here, the amount

of water does play an important role in determining polymer yields and polar monomer incorporations. A possible reason for this was that the water reacts with free residual TMA in the MAO, thereby creating more MAO and new aluminum-oxygen-methyl moieties. This reduction in TMA could decrease the further masking of the protected polar monomer, and therefore the polar monomer may be poisoning or inhibiting insertion at the active catalyst. To our knowledge, the deliberate prior addition of water to MAO, stirring overnight under argon followed by use in copolymerization studies, has not been reported.

Of the four experiments, three experiments have proved, to some extent, to affect the degree of incorporation. Heating MAO, removing TMA and water content all proved to contribute adversely in the copolymerization results, whereas added oxygen content proved to have little effect. Thus we were unable to rationalize the activity of the older MAO used, and conclude that MAO samples purchased are not necessarily identical.

3.2.3.6 Copolymerization Attempts using *rac*-Et(Ind)$_2$ZrMe$_2$/CPh$_3$B(C$_6$F$_5$)$_4$ Catalyst System for Propylene with Polar Monomers

Due to the complex issues that MAO can create in the propylene copolymerization studies mentioned above, a different approach to copolymer formation, other than MAO activation, was attempted. The catalyst system *rac*-Et(Ind)$_2$ZrMe$_2$/CPh$_3$B(C$_6$F$_5$)$_4$, which is analogous to the system *rac*-Et(Ind)$_2$ZrCl$_2$/MAO, but with a different activation pathway (Section **1.1.5.1**) and counteranion (i.e. B(C$_6$F$_5$)$_4^-$ versus ClMAO$^-$) was chosen as a possible alternate. The dimethylated version of the catalyst *rac*-Et(Ind)$_2$ZrCl$_2$ was synthesized as described in the literature.[29] The reaction of

the precatalyst *rac*-Et(Ind)$_2$ZrCl$_2$ with 2.05 equivalents of methyllithium in toluene, followed by filtration, concentration of the supernatant and cooling to -20 ^{o}C, resulted in the yellow product being isolated in 33 % yield (Equation 22a).

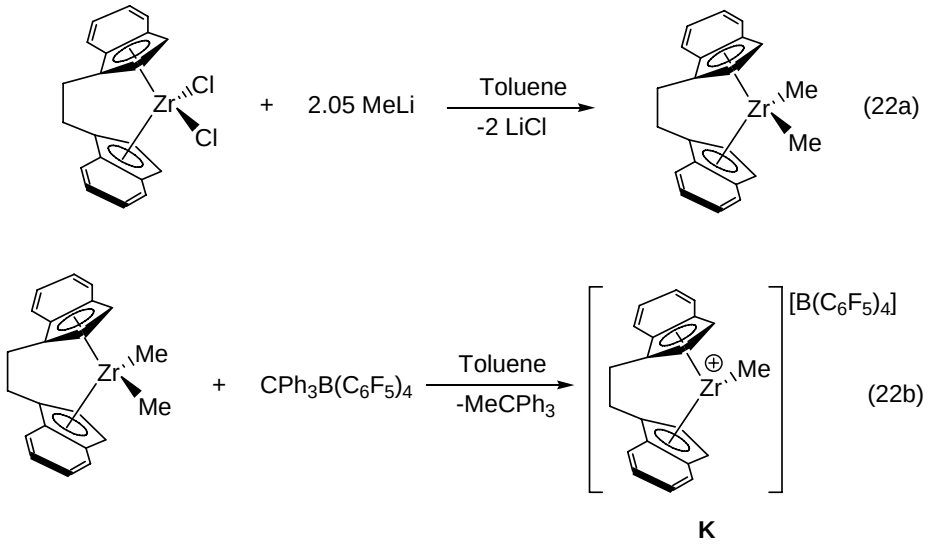

The ^{1}H NMR of this air sensitive precatalyst *rac*-Et(Ind)$_2$ZrMe$_2$ agrees well with the literature values.[29] Activation of this catalyst was achieved by reacting 1.0 equivalent of CPh$_3$B(C$_6$F$_5$)$_4$ with *rac*-Et(Ind)$_2$ZrMe$_2$ to form the ion pair [*rac*-Et(Ind)$_2$ZrMe][B(C$_6$F$_5$)$_4$] (**K**), which is the active catalyst (Equation 22b). As in all previously discussed propylene copolymerizations, the selected polar monomers **A** and **C** were added to the polymerization mixture after 5 min of activating the precatalyst. The results of these copolymerization tests (each done twice) were disappointing, with *no* polar monomer incorporations detected in either case of monomer **A** (Figure 57) and **C** (Figure 58). It can be seen in Figure 57 that no resonances in region of δ 3.43 and 3.37, corresponding to the triplet of –C*H*$_2$-OCH$_3$ and singlet for –CH$_2$-*OCH*$_3$, respectively, are seen. Similarly for monomer **C**, no resonance at δ 3.69 for the –C*H*$_2$-OH can be detected in Figure 58. The

only evident peaks seen in these spectra are for pure isotactic polypropylene. Therefore, it can be concluded that the use of MAO as a cocatalyst was a critical component for successful polar monomer incorporation into polypropylene under the reaction conditions of this study.

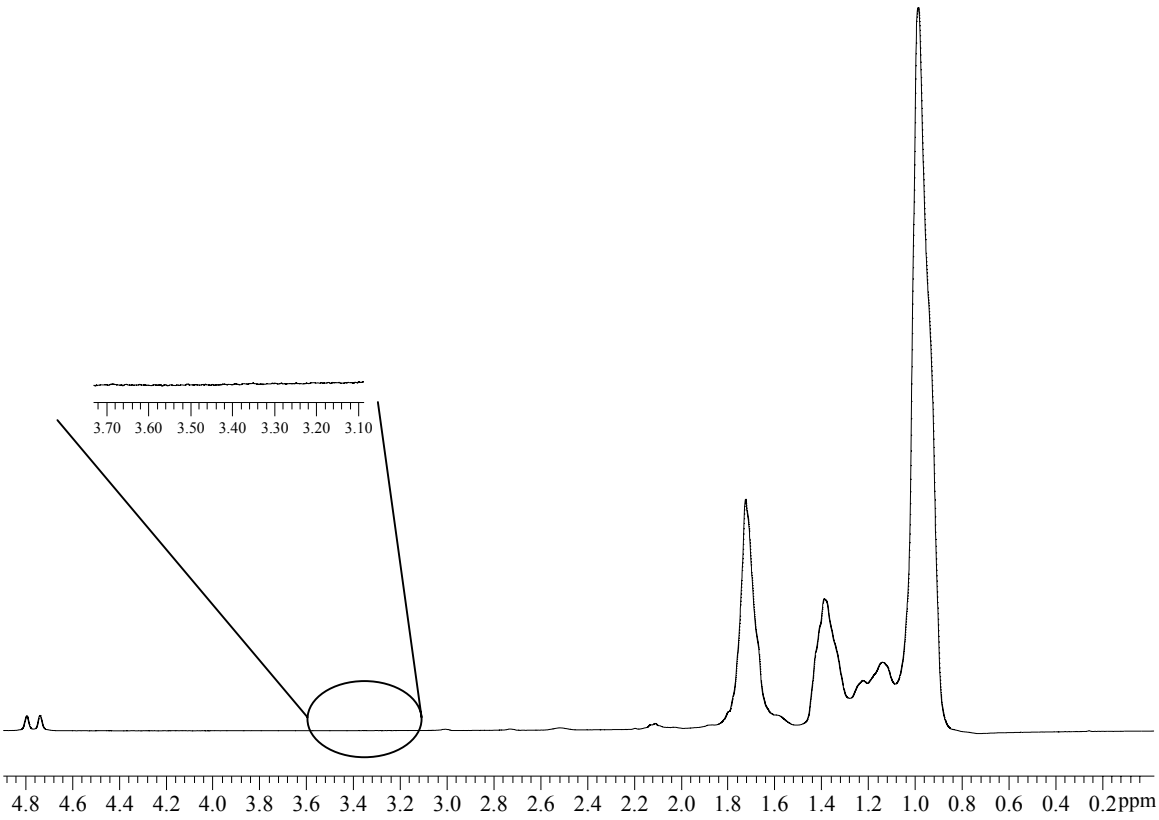

Figure 57. ^{1}H NMR spectrum of the product from the copolymerization reaction of propylene with monomer **A** (methoxydecene) with catalyst **K** (400 MHz, ODCB/C_6D_6, 80 ^{o}C).

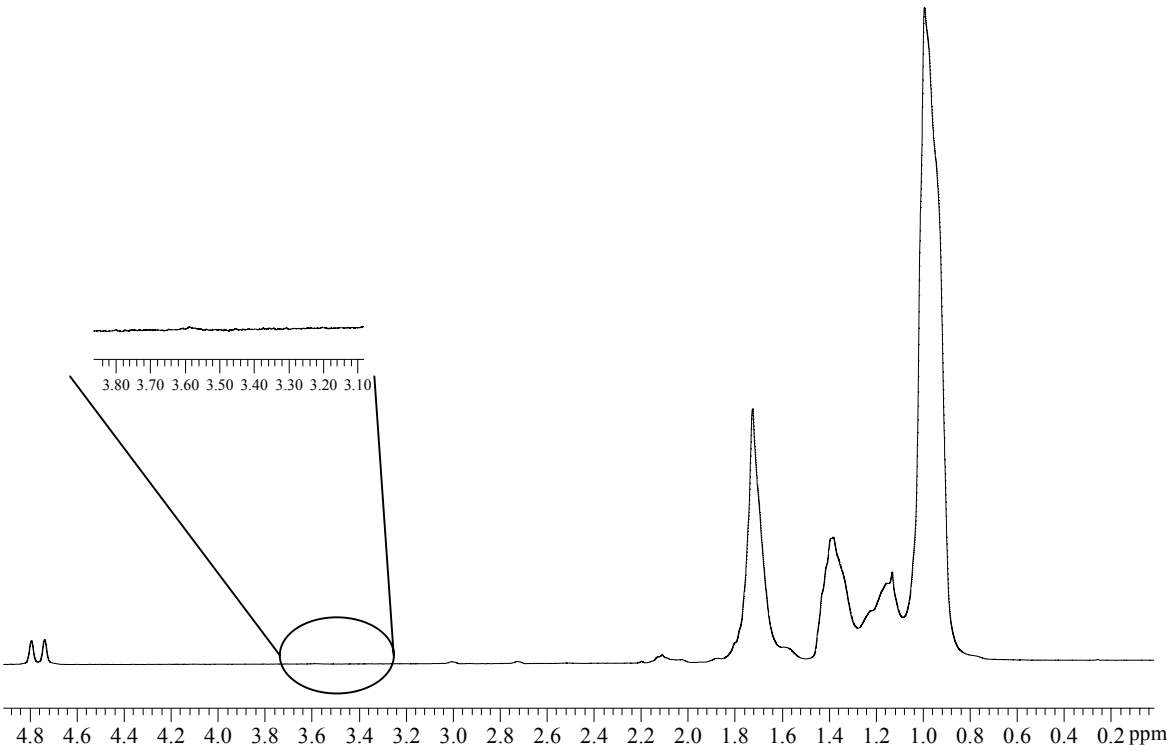

Figure 58. ^{1}H NMR spectrum of the product from the copolymerization reaction of propylene with monomer **C** (trityloxydecene) with catalyst **K** (400 MHz, ODCB/C_6D_6, 80 ^{o}C).

REFERENCES FOR CHAPTER 3

1. (a) Wu, F.; Foley, S. R.; Burns, C. T.; Jordan, R. F. *J. Am. Chem. Soc.* **2005**, *127*, 1841. (b) Groux, L. F.; Weiss, T.; Reddy, D. N.; Chase, P. A.; Piers, W. E.; Ziegler, T.; Parvez, M.; Benet-Bucholz, J. *J. Am. Chem. Soc.* **2005**, *127*, 1854.
2. (a) Albano, V. G.; Castellari, C.; Cucciolito, M. E.; Panunzi, A.; Vitagliano, A. *Organometallics*, **1990**, *9*, 1269. (b) del Río, I. D.; Gossage, R. A.; Hannu, M. S.; Lutz, M.; Spek, A. L.; van Koten, G. *Organometallics*, **1999**, *18*, 1097.
3. Johnson, L. K.; Killian, C. M.; Brookhart, M. *J. Am. Chem. Soc.* **1995**, *117*, 6414.
4. (a) Deubel, D. V.; Ziegler, T. *Organometallics*, **2002**, *21*, 1603. (b) Deubel, D. V.; Ziegler, T. *Organometallics*, **2002**, *21*, 4432. (c) Ziegler, T. private communication. (d) Szabo, M. J.; Jordan, R. F.; Michalak, A.; Piers, W. E.; Weiss, T.; Yang, S.-Y.; Ziegler, T. *Organometallics*, **2004**, *23*, 5565. (e) Yang, S.-Y.; Szabo, M. J.; Michalak, A.; Weiss, T.; Piers, W. E.; Jordan, R. F.; Ziegler, T. *Organometallics*, **2005**, *24*, 1242.
5. (a) Nakamoto, K *Infrared and Raman Spectra of Inorganic and Coordination Compounds*, 4th ed.; Wiley and Sons: New York, 1986; p 280. (b) Bovey, F. A. *Nuclear Magnetic Resonance Spectroscopy*; Academic Press: New York, 1969; pp 64-71.
6. (a) Gerdes, G.; Chen, P. *Organometallics*, **2003**, *22*, 2217. (b) Baratta, W.; Stoccoro, S.; Doppiu, A.; Herdtweck, E.; Zucca, A.; Rigo, P. *Angew. Chem., Int. Ed. Engl.* **2003**, *42*, 105. (c) Yang, P.; Chan, B. C. K.; Baird, M. C. *Organometallics*, **2004**, *23*, 2752.
7. Guan, Z.; Ma, X.S.; Chen, G. *J. Am. Chem. Soc.* **2003**, *125*, 6697.

8. (a) Carballeira, N.M; Miranda, C. *Chem. Phys. Lipids,* **2003**, *124*, 63-67. (b) Prugh, J. D.; Rooney, C. S.; Deana, A. A.; Ramijit, H. G. *J. Org. Chem.* **1986**, *51*, 648. (c) Silverstein, R. M.; Webster, F. X. *Spectrometric Identification of Organic Compounds*, 6th ed.; John Wiley and Sons: New York, 1998; Chapters 4 and 5.

9. (a) Azizi, N. Saidi, M. R. *Organometallics*, **2004**, *23*, 1457. (b) See for example,(i) Lalonde, M. Chan, T. H. *Synthesis* **1985**, 817.; (ii) Firouzabadi, H.; Iranpoor, N.; Amani, F. Nowrouzi, F. *J. Chem. Soc., Perkin Trans.* **2002**, *1*, 2601. (c) Clayden, J.; Greeves, N.; Warren, S.; Wothers, P. *Organic Chemistry*; Oxford University Press: Oxford, 2001; p 1289.

10. (a) Blackwell, J. M.; Foster, K. L.; Beck, V. H.; Piers, W. E. *J. Org. Chem.,* **1999**, 64, 4887. (b) Parks, D. J.; Piers, W. E *J. Am. Chem. Soc.* **1996**, *118*, 9440. (c) Parks, D. J. *Ph. D. Dissertation*, University of Calgary, **1998**.

11. (a) Sivak, A. J.; Cullo, L. A. Ziegler-Natta polymerization of siloxy group-containing alkenes in preparation of polymers containing functional groups. PCT Int. Appl. **1988**, 59 pp. CODEN: PIXXD2 WO 8808856 A1 19881117. (b) Sivak, A. J.; Cullo, L.A. Alkene-alkenylsilane copolymers with high stereoregularity. (Aristech Chemical Corp., USA). Eur. Pat. Appl. (1990), 38 pp. CODEN: EPXXDW EP 363990 A2 19900418.

12. For chemical shifts, see website http://riodb01.ibase.aist.go.jp/sdbs/cgi-bin/direct_frame_top.cgi. (accessed 09/20/2004).

13. Chen, E. Y-X.; Marks, T. J. *Chem. Rev.* **2000**, *100*, 1391.

14. (a) Hakala, K.; Lofgren, B.; Helaja, T. *Eur. Polym. J.* **1998**, *34*, 1093. (b) See references within Yanjarappa, M. J.; Sivaram, S. *Prog. Poly. Sci.* **2002**, *27*, 1347.

15. (a) Quijada, R., Galland, G.B., Mauler, R.S. *Macromol.Chem.Phys.* **1996**, *197*, 3091. (b) Chien, J. C. W., He, D. *J. Polym. Sci., Part A: Polym. Chem.* **1991**, *29*, 1585. (c) Kaminsky, W., Bark, A., Armdt, M. *Makromol. Chem., Macromol. Symp.***1991**, *47*, 83.

16. (a) Vanka, K.; Ziegler, T. *Organometallics*, **2001**, *20*, 905. (b) Zurek, E.; Ziegler, T. *Prog. Poly. Sci*. **2004**, *29*, 107.

17. (a) Escher, F.F.; Fernanda, F. N.; Gallard, G. B.; Ferreira, M. *J. Polym. Sci., Part A: Polym. Chem.* **2003**, *41*, 2531. (b) Hakala, K.; Helaja, T.; Löfgren, B. *J. Polym. Sci., Part A: Polym. Chem.* **2000**, *38*, 1966.

18. T_m for HDPE see for example, Odian, G. G. *Principles of Polymerization*, 4th Ed.; Wiley-Interscience: Hoboken, NJ, 2004; p 696.

19. (a) Reference for ^{1}H NMR of *i*-PP see for example, Cheng, H. N.; Lee, G. H. *Polymer Bulletin*, **1985**, *13*, 549. (b) i) Imuta, J.-I.; Toda, Y.; Kashiwa, N. *Chem. Lett.* **2001**, 710. ii) Kashiwa, N.; Matsugi, T.; Kojoh, S.; Kaneko, H.; Kawahara, N.; Matsuo, S.; Nobori, T.; Imuta, J. *J. Polym. Sci., Part A: Polym. Chem.* **2003**, *41*, 3657.

20. (a) i) Aaltonen, P.; Fink, G.; Löfgren, B.; Seppälä, J. *Macromolecules* **1996**, *29*, 5255. ii) Tonelli, A. E.; Schilling, F. C. *Acc. Chem. Res.* **1981**, *14*, 233. (b) Resconi, L.; Camurati, I.; Sudmeijer, O. *Top. Catal.* **1999**, *7*, 145-163.

21. Silverstein, R. M.; Webster, F. X. *Spectrometric Identification of Organic Compounds*, 6th ed.; John Wiley and Sons: New York, 1998; pp 83-84.

22. Rieger, B.; Mu, X.; Mallen, D. T.; Rausch, M. D.; Chien, J. C. W. *Macromolecules*, **1990**, *23*, 3559.

23. For example, (a) Aaltonen, P.; Löfgren, B. *Macromolecules* **1995**, *28*, 5357. (b) Aaltonen, P.; Löfgren, B. *Eur. Polym. J.* **1997**, *33*, 1187. (c) Wilén, C.-E.; Näsman, J. H. *Macromolecules* **1994**, *27*, 4051. (d) Wilén, C.-E.; Luttikhedde, H.; Hjertberg, T.; Näsman, J. H. *Macromolecules* **1996**, *29*, 8569. (e) Jiang, G. J.; Chiu, H.-W. *Polymer Preprints* **1998**, *39*, 318. (f) Hwu, J. M.; Jiang, G. J. *Polymer Preprints* **1999**, *40*, 177.

24. Kissin, Y. V.; Brandolini, A. J. *Macromolecules*, **1991**, *24*, 2632.

25. For example, see (a) Hakala, K.; Helaja, T.; Löfgren, B. *J. Polym. Sci., Part A: Polym. Chem.* **2000**, *38*, 1966. (b) Paavola, S.; Löfgren, B.; Seppaela, J. V. *Eur. Polym. J.* **2005**, *41*, 2861.

26. For example, see (a) Kawahara, N.; Kojoh, S.; Matsuo, S.; Kaneko, H.; Matsugi, T.; Kashiwa, N. *J. Mol. Catal. A: Chem.* **2005**, *241*, 156. (b) Hagihara, H.; Tsuchihara, K.; Sugiyama, J.; Takeuchi, K.; Shiono, T. *Macromolecules* **2004**, *37*, 5145.

27. (a) Tritto, I.; Mealares, C.; Sacchi, M. C.; Locatelli, P. *Macromol. Chem. Phys.* **1997**, *198*, 3963. (b) Stellbrink, J.; Niu, A.; Allgaier, J.; Richer, D.; Koenig, B. W.; Hartmann, R.; Coates, G. W.; Fetters, L. J. *Macromolecules* **2007**, *40*, 4972. (c) Panchenkov, V. N.; Zakharov, V. A.; Danilova, I. G.; Paukshtis, E. A.; Zakharov, I. I.; Goncharov, V. G.; Suknev, A. P. *J. Mol. Catal. A: Chem.* **2001** *174*, 107. (d) Novokspnova, L. A.; Koveleva, N. Y.; Ushakova, T. M.; Meshkova, I. N.; Krasheninnikov, V. G.; Ladygina, T. A.; Leipunskii, I. O.; Zhigach, A. N. Kuskov, M.L. *Kinet. Catal.* **2005**, *46*, 853.

28. (a) Hagihara, H.; Murata, M.; Uozumi, T. *Macromol. Rapid Comm*. **2001**, *22*, 353. (b) Marques, M. M.; Correia, S. G.; Ascenso, J. R.; Ribeiro, A. F. G.; Gomes, P. T.; Dias, A. R.; Foster, P.; Rausch, M. D.; Chien, J. C. W. *J. Poly. Sci. Part A: Poly. Chem*. **1999**, *37*, 2457. (c) Hagihara, H.; Tsuchihara, K.; Takeuchi, K.; Murata, M.; Ozaki, H.; Shiono, T. *J. Polym. Sci., Part A: Polym. Chem*. **2004**, *42*, 52.

29. Chien, J. C. W.; Tsai, W-M.; Rausch, M. D. *J. Am. Chem. Soc.* **1991**. *113*, 8570.

CHAPTER 4

SUMMARY AND CONCLUSIONS

4.0 Part 1

Brookhart's diimine catalyst $[Pd(N\text{-}N)Me(Et_2O)]^+$ (**1**) (N-N = (2,6-(i-Pr)$_2$C$_6$H$_3$)-N=CH$_2$CH$_2$=N-(2,6-(i-Pr)$_2$C$_6$H$_3$)) was synthesized and reacted with acrylonitrile to generate the N-bonded species $[Pd(N\text{-}N)Me(AN)]^+$ (**2**), which exists as two equilibrating rotamers (**2a** and **2b**). Complex [(N-N)PdMeAN][BAr$^f_4$] (**2**) was successfully characterized by elemental analysis, ^{1}H NMR and electrospray mass spectrometry. On heating, $[Pd(N\text{-}N)Me(AN)]^+$ (**2**) does undergo 2,1-insertion, presumably via an unobserved η^2-isomer, to give the new complex, $[Pd(N\text{-}N)(CH(CN)CH_2CH_3)(AN)]^+$ (**3**). It has been demonstrated that, while nitrogen-coordination of acrylonitrile in the diimine palladium complex **2** is preferred, η^2-coordination followed by slow migratory insertion into the Pd-Me bond occurs based on NMR and mass spectrometry results. Although $[Pd(N\text{-}N)Me(AN)]^+$ (**2**) does behave as a typical Brookhart ethylene polymerization catalyst, it does not catalyze AN polymerization and added AN suppresses ethylene polymerization. The trace amounts of polyacrylonitrile formed in this study may result from coordination or, more likely, conventional free radical polymerization, but $[Pd(N\text{-}N)Me(AN)]^+$ (**2**) does not copolymerize ethylene and acrylonitrile.

Future work in this area would possibly involve investigating different ligand systems around the palladium metal center (i.e. fine tune the electronics and sterics) to favour insertion with the η^2-bond acrylonitrile instead of the N-bond acrylonitrile. The N-bonded acrylonitrile does not promote insertion reactions (as shown in this thesis), unless harsh conditions are imposed (e.g. heating).

4.1 Part 2

The investigation into copolymerizing olefins (such as ethylene and propylene) with protected functional monomers **A** – **D** was achieved in this study. Functional monomer **E** gave no detectable incorporation. Incorporation of up to 2.0 mol % of the protected polar monomer into polypropylene and up to 1.2 mol % into polyethylene was achieved using the catalyst system *rac*-$C_2H_4(Ind)_2ZrCl_2$/methylaluminoxane (MAO). All materials were characterized by ^1H and ^{13}C NMR spectroscopy, differential scanning calorimetry (DSC) and infrared spectroscopy (IR). It was found that increasing the bulkiness of the protecting group (i.e. from Me (**A**) to Ph_3C (**C**) or Ph_3Si(**E**)) actually did not increase the amount of polar monomer within the new copolymers obtained. In fact, the smallest protecting group comonomer **A** (R = Me) gave the best incorporation (up to 2.0 mol %). A possible rationale for this effect was that the small monomer is able to maneuver into the spaces in between the bulky MAO-based counteranions and the catalytic site on zirconium, and eventually bind weakly to the latter. Once anion-cation separation has been achieved, the olefinic ether can exchange ends such that the C=C bond coordinates and migratory insertion can occur. Such a process may be less available to the non-polar 1-hexene and to the much bulkier phenyl-containing ethers. Propylene-1-hexene copolymerizations, using the same catalyst system as above, gave incorporations of up to 2.9 mol % of 1-hexene. This result was quite comparable to that of the highest incorporated polar monomer (2.0 mol %) using similar reaction conditions.

The ^1H NMR monitoring reactions of the homopolymerization of these vinyl and silyl ethers (**A** – **E**) with the zwitterionic compound $[Cp_2ZrMe][MeB(C_6F_5)_3]$ (**J**) showed the protecting groups were effective in preventing the functional group from poisioning the metal center. This observation was made based upon the disappearance of the vinyl

region in the ^{1}H NMR spectra over time, indicating that monomer insertion was occurring.

The effects of 'aging' MAO on the incorporation of polar monomers into polyolefins were found to decrease the incorporation amounts under the modifying procedures used. Pretreatments such as heating MAO, removing residual TMA and water content all showed a decreasing effect on polar monomer incorporations into polyolefins, whereas added oxygen content to MAO showed little effect on polar monomer incorporations.

In light of the result found here, current and future work in this area should involve screening new monomers with small to intermediate protecting groups (i.e. R = Me, Et). This would allow for protected monomers to access the active metal center and allow for insertion reactions to occur. The exploration of late metal systems (such as nickel and palladium) is another viable research area, since late metals are more functional group tolerant than early metal systems.